A *Very Oil Yellow1* modifier of the *Oil Yellow1-N1989* allele uncovers a cryptic phenotypic impact of cis-regulatory variation in maize

Rajdeep S. Khangura[†], Sandeep Marla[†1], Bala P. Venkata[†2], Nicholas J. Heller[†3], Gurmukh S. Johal[†‡], Brian P. Dilkes[§‡4]

[†]Department of Botany and Plant Pathology, Purdue University, West Lafayette, Indiana 47907
[‡]Center for Plant Biology, Purdue University, West Lafayette, Indiana 47907
[§]Department of Biochemistry, Purdue University, West Lafayette, Indiana 47907

Current address
[1]Department of Agronomy, Kansas State University, Manhattan, Kansas 66506
[2]Donald Danforth Plant Science Center, St. Louis, Missouri 63132
[3]Department of Crop Sciences, University of Illinois, Urbana, IL 61801

[4]Corresponding Author
Brian Dilkes, 170 S University Ave, Purdue University, West Lafayette, Indiana 47907, phone: (765) 494 2584, Email: bdilkes@purdue.edu

Abstract

Forward genetics determines the function of genes underlying trait variation by identifying the change in DNA responsible for changes in phenotype. Detecting phenotypically-relevant variation outside protein coding sequences and distinguishing this from neutral variants is not trivial; partly because the mechanisms by which DNA polymorphisms in the intergenic regions affect gene regulation are poorly understood. Here we utilized a dominant genetic marker with a convenient phenotype to investigate the effect of cis and trans-acting regulatory variation. We performed a forward genetic screen for natural variation that suppress or enhance the semi-dominant mutant allele *Oy1-N1989,* encoding the magnesium chelatase subunit I of maize. This mutant permits rapid phenotyping of leaf color as a reporter for chlorophyll accumulation, and mapping of natural variation in maize affecting chlorophyll metabolism. We identified a single modifier locus segregating between B73 and Mo17 that was linked to the reporter gene itself, which we call *very oil yellow1*. Based on the variation in OY1 transcript abundance and genome-wide association data, *vey1* is predicted to consist of multiple cis-acting regulatory sequence polymorphisms encoded at the wild-type *oy1* alleles. The *vey1* allele appears to be a common polymorphism in the maize germplasm that alters the expression level of a key gene in chlorophyll biosynthesis. These *vey1* alleles have no discernable impact on leaf chlorophyll in the absence of the *Oy1-N1989* reporter. Thus, use of a mutant as a simple and efficient reporter for magnesium chelatase activity resulted in the detection of expression-level polymorphisms not readily visible in the laboratory.

KEYWORDS chlorophyll biosynthesis; cryptic variation; cis-acting; complex traits; epistasis

Introduction

Genetic variation in the coding or regulatory sequences causes differences between genotypes and is fundamental to crop improvement (Springer and Stupar 2007). Gene function discovery via mutant analyses focuses on linking phenotype alterations to gene variants. As a result, forward genetics has been of great value to understand biological systems but is predominantly useful for determining functions for genes with alleles that cause large phenotypic impacts. Natural variants, including those that encode alleles of relevance to adaptation and fitness of the organism, are often of small effect (Fisher 1930; Orr 1998, 2005). Mutant alleles with conditional impacts on phenotypes, through genetic interactions or modifiers, as well as alleles of small individual effect are difficult to study. Further, even if we identify loci that have not been previously associated with a biological process, it can be difficult to validate and associate such natural variants with physiological and biochemical mechanisms.

A forward genetics approach that uses a mutant phenotype as a reporter for genetic interactions can be used to detect modifiers in natural populations and expose cryptic variation affecting traits of interest (Johal *et al*. 2008). This Mutant-Assisted Gene Identification and Characterization (MAGIC) approach is particularly efficient in species where outcrossing is easy, such as maize (*Zea mays*). It can be applied to any mutant with any quantifiable phenotype to expand our understanding of the process disrupted by mutation. This approach is convenient when a dominant mutant allele is used as a reporter because natural variants that encode enhancers or suppressors of a given mutant phenotype can be detected in F_1 crosses. Thus, it enables easy detection of dominant enhancers and suppressors. Any germplasm collection, diversity panel, or line-cross population that can serve as the variable parents in these crosses, can be utilized to detect and map loci that alter mutant phenotype expression. Natural variants discovered this way have an experimental link (genetic modifiers) of the processes affected by the mutant reporter allele (induced variation). Thus, this approach speeds the assignment of mechanism(s) to natural variation in the germplasm. Indeed, one can consider this as a screen for epistatic or contingent gene action. MAGIC screens have identified loci from maize involved in the hypersensitive response (Chintamanani *et al*. 2010; Penning, Johal, and McMullen 2004; Olukolu *et al*. 2013, 2014, 2016) and plant development (Buescher *et al*. 2014), among

others. In each case, in the absence of a mutant allele, no phenotype was previously associated to the modifier loci demonstrating the remarkable efficiency of this genetic screen to detect epistatic interactions between mutant and modifier alleles. Thus, this approach is a powerful way to both characterize cryptic variation in genomes and construct genetic pathways affecting phenotypes of interest.

The easy visual scoring and simplicity of quantifying chlorophyll make chlorophyll biosynthetic mutants an excellent reporter for MAGIC screens. Chlorophyll is a major component of central metabolism in plants, which can produce phototoxic intermediates during both synthesis (Hu *et al.* 1998; Huang *et al.* 2009) and breakdown (Gray *et al*. 1997; Gray *et al*. 2002; Mach *et al*. 2001; Yang et al. 2004), and its levels are carefully regulated in plants (Meskauskiene *et al.* 2001). Enzymatic conversion of protoporphyrin IX into magnesium protoporphyrin IX by Magnesium Chelatase (MgChl) is the first committed step in chlorophyll biosynthesis (Wettstein *et al.* 1995). MgChl is a hetero-oligomeric enzyme consisting of three subunits (I, D, and H) that are conserved from prokaryotes to plants. The MgChl subunit I is encoded by the *oil yellow1* (*oy1*; GRMZM2G419806) gene in maize and encodes the AAA^{+}-type ATPase subunit that energizes the complex (Fodje *et al.* 2001). Weak loss-of-function alleles of *oy1* result in recessive yellow-green plants while complete loss-of-function alleles result in a recessive yellow seedling-lethal phenotype (Sawers *et al.* 2006). The semi-dominant *Oy1-N1989* allele carries a leucine (L) to phenylalanine (F) change at amino acid position 176 (L176F) that hinders the formation of a functional complex between the OY1 protein and other subunits of MgChl. Heterozygous plants carrying one *Oy1-N1989* allele and one wild-type allele are oil-yellow, but homozygous *Oy1-N1989* plants lack any MgChl activity, resulting in a recessive yellow seedling-lethal phenotype with no chlorophyll accumulation (Sawers *et al.* 2006). Consistent with the conservation of this protein complex, the orthologous L->F mutation (encoded by *Oy1-N1989*) was identified in barley (L161F) and also results in a recessive yellow seedling-lethal phenotype with no detectable chlorophyll in homozygous condition and a pale-green phenotype as a heterozygote (Hansson *et al.* 1999). The biochemical basis of this semi-dominant mutant allele was studied by creating a mutant MgChl subunit I in *Rhodobacter* (BCHI), with the orthologous amino acid change at position 111 of wild-type BCHI (Hansson *et al*. 2002). The L111F mutation converted BCHI into a competitive

inhibitor of MgChl that reduced enzyme activity by 4-fold when mixed 1:1 with wild-type BCHI (Hansson *et al*. 2002; Lundqvist *et al*. 2013). This conserved leucine residue is between the ATP-binding fold of MgChl subunit I created by the Walker A and B motifs (Hansson *et al*. 2002; Sawers *et al*. 2006; Lundqvist *et al*. 2013), and its substitution with phenylalanine was deleterious to dephosphorylation activity. The ATPase activity of wild-type MgChl complex is directly proportional to the magnesium chelation reaction. However, complexes assembled from MgChl subunit I with the L->F change exhibit reduced ATPase activity and no ability to chelate Mg^{2+} ions into protoporphyrin IX (Hansson *et al*. 1999, 2002; Sawers *et al*. 2006). The absence of MgChl activity displayed by the mutant BCHI carrying L111F substitution ($BCHI^{L111F}$) demonstrates that this amino acid change results in a dominant-negative subunit which disrupts the coupling of ATPase activity to magnesium chelation (Hansson *et al*. 2002; Lundqvist *et al*. 2013).

We screened maize germplasm for cryptic variation using the *Oy1-N1989* mutant as a dominant reporter for chlorophyll biosynthesis. We hypothesized that alteration in the quantity of biochemically active MgChl complex should read out as a change in chlorophyll content and plant color in heterozygous *Oy1-N1989* mutants. For instance, in a population of heterozygous *Oy1-N1989/oy1* F_1 plants, an amino acid change in the wild-type OY1 protein that alters the dissociation constant (k_D) of OY1 for the other protein subunits of MgChl should contribute to variance in chlorophyll biogenesis. Similarly, a cis-acting expression QTL (eQTL) that increases expression of the wild-type *oy1* allele should result in assembly of more active MgChl complexes and increase chlorophyll content in F_1 mutant plants. Thus, chlorophyll content of *Oy1-N1989* mutants should be modulated by the stoichiometry of both the wild-type and mutant OY1 proteins present in the MgChl complex in heterozygous *Oy1-N1989/oy1* plants either by protein structure or abundance changes.

We introgressed the maize *Oy1-N1989* mutant allele into the B73 inbred background and maintained it as a heterozygote (*Oy1-N1989*/*oy1*:B73). While crossing this mutant to multiple backgrounds, we detected genetic variation in the *Oy1-N1989/oy1* mutant phenotype expression between the maize inbred lines B73 and Mo17. The phenotype of the *Oy1-N1989* mutant heterozygotes was suppressed in the B73 background. However, F_1 hybrids with Mo17 dramatically enhanced it. In an attempt to determine the

genetic basis of this modification, we carried out genetic mapping experiments using five F_1 populations. In each of these mapping experiments, the *Oy1-N1989/oy1*:B73 parents were crossed with (1) the intermated B73 x Mo17 recombinant inbred lines (IBM), (2) B73 x Mo17 doubled haploid lines (Syn10), (3) Mo17 x B73 F_1 hybrids, (4) B73 x Mo17 near-isogenic lines (BM-NILs), and (5) a genome-wide association mapping panel of diverse maize inbred lines (MDL). In each case, we identified a quantitative trait locus (QTL) of large effect on chromosome 10 linked to the *oy1* locus itself. In each of the B73 x Mo17 line-cross populations, the B73 wild-type allele at *oy1* suppressed the *Oy1-N1989/oy1* mutant phenotype. This QTL, which we call *very oil yellow1* (*vey1*), was not associated with changes in protein sequence at *oy1* and did not correlate with the chlorophyll content of the wild-type mapping parents. However, a cis-acting eQTL causing higher expression of the B73 allele of *oy1* in the IBM lines was consistent with the observed phenotypic variation in the mutant siblings. Consistently, the allele-specific expression at *oy1* in the mutant heterozygotes was biased towards the *Oy1-N1989* allele in the hybrids comprising wild-type *oy1* allele from Mo17. The inheritance of the traits, proposed allele expression bias at *oy1* due to a putative cis-acting regulatory element, implications of the discovered cryptic variation, and the utility of this study in general are discussed.

Materials and Methods

Plant materials

The *Oy1-N1989* mutant allele was acquired from the Maize Genetics Cooperation Stock Center (University of Illinois, Urbana-Champaign, IL). The original allele of the *Oy1-N1989* mutation was isolated from a *r1 c1* colorless synthetic stock of mixed parentage (G. Neuffer, personal communication). This allele was introgressed into B73 for eight generations by repeated backcrossing of B73 ear-parents with *Oy1-N1989/oy1* pollen-parents and is maintained as a heterozygote (*Oy1-N1989*/*oy1*:B73) by crossing to wild-type siblings.

Line-cross QTL mapping: For these experiments, *Oy1-N1989*/*oy1*:B73 plants were crossed as pollen-parents to 216 Intermated B73 x Mo17 recombinant inbred lines (IBM; Lee *et al*, 2002) and 251 Syn10 doubled haploid lines (Syn10; Hussain *et al*, 2007). The

QTL validation was done using F_1 progenies derived from the cross of 35 B73-Mo17 Near-Isogenic lines (BM-NILs) ears with pollen from *Oy1-N1989*/*oy1*:B73. These BM-NILs consisted of 22 B73-like NILs and 13 Mo17-like NILs with introgression of the reciprocal parental genome (B73 or Mo17) and were developed by three repeated backcrosses into recurrent parent followed by four to six generations of self-pollination (Eichten *et al.* 2011).

Genome-wide association (GWA) mapping: For this experiment, *Oy1-N1989*/*oy1*:B73 plants were crossed to 343 inbred lines that included 249 inbreds from maize association panel (Flint-Garcia *et al.* 2005), and 94 inbred lines that included 82 Expired Plant Variety Protections (ExPVP) lines from the Ames panel (Romay *et al.* 2013). Pollen from *Oy1-N1989*/*oy1*:B73 plants were used for these crosses except for the popcorn lines in the maize association panel, where *Oy1-N1989*/*oy1*:B73 plants were used as an ear-parent to avoid the crossing barrier affected by gametophytic factor GA1-S (first described by Correns in 1902; Mangelsdorf and Jones 1926; Lauter *et al.* 2017). This panel of 343 inbred lines is referred to as maize diversity lines (MDL). The full list of IBM, Syn10, BM-NILs, and MDL used to develop F_1 hybrid populations are provided in **Tables S1-S4**.

Field trials

All field experiments were performed at the Purdue Agronomy Center for Research and Education (ACRE) in West Lafayette, Indiana. All F_1 populations described below were planted as a single plot of 12-16 plants that segregated for both mutant and wild-type siblings. Plots were sown in a 3.84 m long row with the inter-row spacing of 0.79 meters and an alley space of 0.79 meters. No irrigation was applied during the entire crop season as rainfalls were uniformly distributed for satisfactory plant growth. Conventional fertilizer, pest and weed control practices for growing field maize in Indiana were followed. Progenies of *Oy1-N1989*/*oy1*:B73 pollen-parents crossed with B73 and Mo17 were planted as parental checks in each block of every experiment. The testcross F_1 populations with IBM were evaluated in a single replication in the summer of 2013 with each range treated as a block. In 2016, the testcross F_1 populations with Syn10 lines were evaluated as two replications in a randomized complete block design (RCBD) with each range divided into two blocks. The testcross F_1 progenies with BM-NILs and parents (B73 and Mo17) were

155 planted in a RCBD with five replications in 2016. In the same year, F_1 populations with
156 MDL were also evaluated with three replications planted in a RCBD. Each replication of
157 MDL F_1 population was divided into ten blocks of the same size, and parental checks were
158 randomized within each block.
159
160 **Phenotyping and data collection**
161 Maize seedlings used for destructive chlorophyll quantification were grown under
162 greenhouse conditions using mogul base high-pressure sodium lamps (1000 Watts) as the
163 supplemental light source for L:D cycle of 16:8 and temperature around 28ºC (day-time)
164 and 20ºC (night-time). Destructive chlorophyll measurements were performed on the fresh
165 weight basis in 80% acetone solution using a UV-VIS spectroscopic method described in
166 Lichtenthaler & Buschmann, 2001.
167 For the field-grown experiments, mutant siblings in the suppressing genetic
168 backgrounds were tagged at knee height stage with plastic tags so that they can be easily
169 distinguished from the wild-type siblings for trait measurements at later developmental
170 stages in the season. All the F_1 families segregated for the mutant (*Oy1-N1989*/*oy1*) and
171 wild-type (*oy1*/*oy1*) siblings in approximately 1:1 fashion. For each F_1 family, two to four
172 plants of each phenotypic class were picked at random for trait measurements. Non-
173 destructive chlorophyll content in the maize leaves was approximated using a chlorophyll
174 content meter model CCM-200 plus (Opti-Sciences, Inc., Hudson, NH) and the
175 measurements were expressed as chlorophyll content index (CCM). Measurements were
176 taken on the leaf lamina of the top fully expanded leaf at two time points. First CCM
177 measurements were taken at 25-30 days after sowing (expressed as CCMI) and the second
178 at 45-50 days after sowing (expressed as CCMII). For each trait, measurements were
179 performed on both mutant (reported with a prefix MT) and wild-type (reported with a
180 prefix WT) siblings. Besides using primary trait measurements of CCMI and CCMII on
181 mutant and wild-type siblings, indirect CCM measurements were also calculated and
182 expressed as ratios (MT/WT) and differences (WT-MT) of CCMI and CCMII. Phenotypic
183 data of all the CCM traits in the F_1 populations with both bi-parental populations, BM-
184 NILs and MDL are provided in **Tables S1-S4**.
185

Public/open-access genotypic and gene expression data

Public marker data for the IBM was obtained from www.maizegdb.org (Sen *et al.* 2010). A total of 2,178 retrieved markers were reduced to 2,156 after the removal of markers with the duplicate assessment. Approximately 13.3% of the marker data were missing. The reads per kilobase of transcript per million mapped reads (RPKM) for the *oy1* locus were obtained from a public repository of the National Science Foundation grant (GEPR: Genomic Analyses of shoot meristem function in maize; NSF DBI-0820610; https://ftp.maizegdb.org/MaizeGDB/FTP/shoot_apical_meristem_data_scanlon_lab/). These data consist of normalized read counts (expressed as RPKM) of the maize genes from the transcriptome of shoot apex of 14 days old IBM seedlings.

Marker data for Syn10 lines was obtained from Liu *et al*. 2015. The Syn10 lines were genotyped at 6611 positions (B73 RefGenv2) with SNP markers covering all ten chromosomes of maize. The entire set of markers were used for linkage analysis as there was no missing data. All B73-Mo17 NILs in both the B73 and Mo17 recurrent backgrounds that had introgression of the critical region from the opposite parent were selected for QTL validation. Genotyping data of the BM-NILs to choose informative lines and perform QTL validation was obtained from Eichten *et al*. 2011.

Genotypes for the MDL used in this study to perform GWA were obtained from third generation maize haplotypes (HapMap3) described in Bukowski *et al.* 2018. We identified 305 common inbred lines that were part of HapMap3. Briefly, HapMap3 consists of over 83 million variant sites across ten chromosomes of maize that are anchored to B73 version 3 assembly. After obtaining the genotypic data of 305 common inbred lines, variant sites were filtered for ≤10 percent missing data and minor allele frequency of ≥0.05 using VCFtools (Danecek *et al.* 2011). The filtered SNP dataset was used for GWA analyses. A summary of variant sites before and after the filtering procedure are listed in **Table S5.** A reduced set of genotypes for the same set of 305 accessions were obtained from the maize inbred lines described in Romay *et al*. 2013. These genotypes consist of 681 257 SNPs (physical positions from B73 RefGenv2) obtained using a GBS protocol (Elshire *et al.* 2011) covering all ten chromosomes of maize. This marker dataset was filtered for ≤10 percent missing data and minor allele frequency of ≥0.05 using TASSEL (Bradbury *et al.* 2007), reducing the marker number to 150 920 SNPs. This genotypic dataset was solely

used to compute principal components (PC) and a kinship matrix to control for population structure and familial relatedness in a unified mixed linear model, respectively (Yu *et al.* 2006). GWA analyses using the reduced marker dataset (Romay *et al*. 2013) on the full set of MDL found similar results to the one by the larger marker dataset (HapMap3) on the reduced set of MDL (data not shown). To test for cis-eQTL at the *oy1* locus in the maize diversity lines used for GWA mapping, normalized count of OY1 expression derived from the germinating seedling shoots was obtained from http://www.cyverse.org (Kremling *et al.* 2018).

Statistical analyses

QTL mapping: Line-cross phenotypes and markers were used to detect and localize QTL using the R/QTL package version 1.40-8 (Broman *et al*. 2003). Trait means were used for the QTL analyses. Single interval mapping (SIM) was used for all traits, although composite interval mapping (CIM) was carried out with remarkably similar results (data not shown). Statistical thresholds were computed by 1000 permutations (Churchill and Doerge 1994) of each trait in both bi-parental F_1 populations.

Genome-wide association study (GWAS): Preliminary data analysis was done using JMP 13.0 (SAS Institute Inc. 2016). Statistical corrections on the raw phenotypic data were performed by determining the most significant terms in the model using analysis of variance (Fisher 1921). Genotype and replication were used as a random effect in a linear mixed-effects model built in the lme4 package (Bates *et al*. 2015) implemented in R (R core team, 2014) to calculate the best linear unbiased predictor (BLUP) for each trait. Broad-sense heritability (line mean basis) were calculated using BLUP values, using the method described by Lin and Allaire 1977. BLUP estimates for each trait were used to perform GWAS. GWAS was done using a compressed mixed linear model implemented in R package GAPIT (Lipka *et al*. 2012; Zhang *et al*. 2010). HapMap3 SNPs were used to calculate genotype to phenotype associations. As explained before, kinship and population structure estimates were obtained for the same population using the second subset of 150 920 SNPs to correct for spurious associations. The Bonferroni correction and false discovery rate (FDR) adjustments were used to compute a statistical threshold for the

positive association to further control for false positive assessment of associations (Holm 1979; Benjamini and Hochberg 1995).

Molecular Analyses

Genotyping: The recombinants in selected Syn10 lines and the BC_1F_1 population were detected using three PCR-based markers. Two markers detecting insertion polymorphisms flanking the *oy1* locus and one dCAPS marker at *oy1* locus were designed for this purpose. Genotyping at insertion-deletion (indel) marker *ftcl1* (flanking an indel polymorphism in intron 4 of *ftcl1*; GRMZM2G001904) was performed with forward primer 5'- GCAGAGCTGGAATATGGAATGC-3' and reverse primer 5'- GATGACCTGAGTAGGGGTGC -3'. Genotyping at indel marker *gfa2* (flanking an indel polymorphism in the intron of *gfa2*; GRMZM2G118316) was performed with forward primer 5'- ACGGCTCCAAAAGTCGTGTA -3' and reverse primer 5'- ATGGATGGGGTCAGGAAAGC -3'. A polymorphic SNP in the second intron at *oy1* was used to design a dCAPS forward primer 5'- CGCCCCCGTTCTCCAATCCTGC -3' and a gene-specific reverse primer 5'- GACCTCGGGGCCCATGACCT -3' (http://helix.wustl.edu/dcaps/dcaps.html; Neff *et al*. 2002). The PCR products from polymerization reactions with the dCAPS oligonucleotide at *oy1* were digested by *Pst*I restriction endonuclease (New England Biolabs, MA, USA) and resolved on 3.5% agarose gel.

Allele-specific expression analyses: Allelic bias at transcriptional level was quantified using the third leaf of maize seedlings at the V3 developmental stage. Total RNA was extracted using a modified Phenol/Lithium chloride protocol (Eggermont *et al*. 1996). The modification involved grinding of plant tissue in pestle and mortar into a fine powder using liquid nitrogen, instead of quartz sand and glass beads in the original protocol. Total RNA was subjected to DNase I treatment using Invitrogen Turbo DNA-free kit (Catalog#AM1907, Life Technologies, Carlsbad, CA) and 1 µg of DNase treated RNA from each sample was converted to cDNA using oligo dT primers and a recombinant M-MLV reverse transcriptase provided in iScript™ Select cDNA synthesis kit (catalog#170-8896, Bio-Rad, Hercules, CA) according to the manufacturer's recommendations. Besides the cDNA samples, genomic DNA samples were also prepared

as a control to test the sensitivity of the assay. Genomic DNA controls included a 1:1 (F_1 hybrid), 1:2, and 2:1 mixture of B73 and Mo17. PCR was conducted using gene-specific forward primer 5'- CAACGTCATCGACCCCAAGA -3' and reverse primer 5'- GGTTACCAGAGCCGATGAGG -3' for 30 cycles (94˚ for 30s, 56˚ for 30s, 72 ˚ for 30s and final extension for 2 minutes) to amplify the OY1 gene product. These primers flank SNP252 (C->T), which is the causative mutation of *Oy1-N1989*, and SNP317 (C->T) which is polymorphic between B73 and Mo17 but monomorphic between the B73 and *Oy1-N1989* genetic backgrounds. Corresponding PCR products were used to generate sequencing libraries using transposon-mediated library construction with the Illumina Nextera® DNA library preparation kit, and sequence data were generated on a MiSeq instrument (Illumina, San Diego, CA) at the Purdue Genomics Core Facility. The SNP variation and read counts were decoded from the sequenced PCR amplicons by alignment of the quality controlled reads to the *oy1* reference allele from B73 using the BBMap (Bushnell 2014) and the GATK packages (DePristo *et al.* 2011). Additional analysis was performed using IGV (Robinson *et al.* 2011) to manually quality-check the alignments and SNP calls. Read counts at polymorphic sites obtained from GATK was used to calculate allele-specific expression. Genomic DNA control samples showed bias in the read counts in a dosage-dependent manner. DNA from F_1 hybrids between B73 and Mo17 resulted in 1:1 reads at *oy1* demonstrating no bias in the assay to quantify expression.

OY1 sequencing: The coding sequence of the *oy1* locus from B73, Mo17, W22, and *Oy1-N1989* homozygous seedlings was obtained from the genomic DNA using PCR amplification. For the rest of the maize inbred lines, the *oy1* locus was amplified from cDNA synthesized from total RNA derived from the shoot tissue of 14 days old maize seedlings. PCR amplification of *oy1* locus from genomic DNA was performed using four primer pairs: (a) forward primer Oy1-FP1 5'- GCAAGCATGTTGGGCACAGCG -3' and reverse primer Oy1-RP12 5'- GGGCGGCGGGATTGGAGAAC -3', (b) forward primer Oy1-FP5 5'- GGTGGAGAGGGAGGGTATCT -3' and reverse primer Oy1-RP6 5'- GGACCGAGGAAATACTTCCG -3', (c) forward primer Oy1-F8 5'- ATGCCCCTTCTTCCTCTCCT -3' and reverse primer Oy1-R8 5'- CGCCTTCTCGATGTCAATGG -3', (d) forward primer Oy1-F9 5'- GGCACCATTGACATCGAGAA -3' and reverse primer Oy1-R9 5'-

GCTGTCCCTTCCTTTCAACG -3'. PCR amplification of OY1 transcripts from cDNA was performed using all primer pairs except Oy1-FP1/RP12. The PCR products from these samples were sequenced either using Sanger or Illumina sequencing. For Sanger sequencing, amplified PCR products were cleaned using homemade filters with sterile cotton plug and Bio-Gel® P-30 gel (Bio-Rad, Hercules, CA) to remove unused dNTPs and primers. Cleaned PCR products were used to perform a cycle reaction using Big Dye version 3.1 chemistry (Applied Biosystems, Waltham, MA) and run on ABI 3730XL sequencer by Purdue genomics core facility. Read with high-quality base pairs from Sanger sequencing were aligned using ClustalW (Thompson *et al*. 1994). Illumina sequencing was performed as described above except in this case paired-end reads were aligned to the B73 reference of *oy1* gene using bwa version 0.7.12 (Li and Durbin 2009) and variant calling was done using Samtools (Li *et al*. 2009).

Results

Mo17 encodes an enhancer of the semi-dominant mutant allele *Oy1-N1989* of maize

The *Oy1-N1989* allele was recovered from a nitrosoguanidine mutant population in mixed genetic background. The molecular nature of the mutation is a single non-synonymous base pair change (Sawers *et al.* 2006). Heterozygous *Oy1-N1989* plants have the eponymous oil-yellow color but are reasonably vigorous and produce both ears and tassels. During introgression of the semi-dominant *Oy1-N1989* allele into B73 and Mo17 inbred backgrounds, we observed a dramatic suppression of the mutant phenotype in F_1 crosses of the mutant stock (obtained from Maize COOP) to the B73 background. In contrast, crosses to Mo17 enhanced the mutant phenotype. The difference in phenotype expression was stable and persisted in both genetic backgrounds through all six backcross generations observed to date. To further explore and quantify this suppression, B73, Mo17, as well as *Oy1-N1989/oy1*:B73, crossed with each of these inbred lines were grown to the V3 stage in the greenhouse. To improve upon our visual assessment of leaf color and provide quantitation, optical absorbance was measured using a Chlorophyll Content Meter-200 plus (CCM; Opti-Sciences, Inc), a hand-held LED-based instrument. CCM is predicted to strongly correlate with chlorophyll and carotenoid contents. To confirm that our rapid

phenotyping with the CCM would accurately assess chlorophyll levels, we measured these pigments using a UV-VIS spectrophotometer following destructive sampling of the same leaves used for CCM measurements. The non-destructive CCM measurements and destructive pigment quantification using UV-VIS protocol displayed a strong positive correlation with an R^2 value of 0.94 for chl*a*, chl*b*, and total chlorophyll (**Figure S1**). Given this high correlation of maize leaf greenness between the rapid measurement using CCM-200 plus instrument and absolute pigment contents quantified using UV-VIS spectrophotometer (destructive sampling), we performed all chlorophyll measurements of *Oy1-N1989* enhancement discussed in later results using CCM values.

In the greenhouse grown seedlings, we observed no visible chlorophyll accumulation in the *Oy1-N1989* homozygotes using CCM or spectrophotometric method. In wild-type plants, CCM measurements were slightly higher in B73 than Mo17, but the spectrophotometric method did not identify any significant difference in the amount of chlorophyll *a* (chl*a*), chlorophyll *b* (chl*b*), total chlorophyll, or carotenoids between these two genotypes (**Table S6**). We detected a mild parent-of-origin-effect for both CCM and absolute amounts of chl*a*, chl*b*, total chlorophyll, and carotenoids in the wild-type siblings of our F_1 crosses. These plants had slightly higher chlorophyll accumulation when B73 was used as the pollen parent (**Table S6**). However, no such effect of parent-of-origin was observed for the mutant heterozygotes (*Oy1-N1989/oy1*) and reciprocal hybrid combinations of crosses between *Oy1-N1989/oy1*:B73 and Mo17 were indistinguishable. Further, both CCM and absolute chlorophyll contents were higher in the *Oy1-N1989/oy1*:B73 plants compared to the mutants in B73 x Mo17 hybrid background. Thus, there was a strong effect of genetics on chlorophyll pigment variation in mutants, that went opposite to predictions for hybrid vigor.

Heterozygous maize plants encoding the *Oy1-N1989* allele display reduced chlorophyll pigment abundance compared to the wild-type siblings, resulting in a yellow-green whole plant phenotype due to reduced MgChl and ATPase activity (Sawers *et al.* 2006). We tested the progenies from the crosses of *Oy1-N1989/oy1*:B73 with B73 and Mo17 inbred lines in the field. Consistent with our previous observation, B73 inbred background resulted in substantially greener mutant heterozygotes (*Oy1-N1989*/*oy1*) than mutant siblings in the Mo17 x B73 F_1 hybrid background (**Figure 1, Table S7**). The

increased severity of *Oy1-N1989* heterozygotes in the Mo17 genetic background was observed even after six backcrosses (**Figure S2**). No suppressed mutant plants were observed during any generation of backcrossing into Mo17 (data not shown). Thus, these results demonstrate the profound negative impact of the *Oy1-N1989* allele on chlorophyll pigment accumulation and the dramatic differential suppression response of this allele by B73 and Mo17 genetic backgrounds.

vey1 maps to a single locus that co-segregates with the _oy1_ allele of Mo17 in DH, RIL, BC_1F_1 and NIL families derived from B73 and Mo17

To identify the genetic basis of the suppression of heterozygotes with the *Oy1-N1989* allele in B73, we performed a series of crosses to four mapping populations. In each case, we crossed a B73 line into which we have introgressed *Oy1-N1989* allele in heterozygous condition (*Oy1-N1989*/*oy1*:B73) as a pollen-parent to a population of recombinant lines as ear-parent (**Figure 2**). We chose two public populations to map all modifiers altering the severity of the *Oy1-N1989* phenotypes. The IBM is a publicly available RIL population that has been extensively used by the maize community for a variety of mapping experiments (Lee *et al*. 2002). A second intermated B73 x Mo17 population Syn10 is derived from ten rounds of intermating followed by fixing alleles using double haploid process (Hussain *et al*. 2007). IBM and Syn10 differ in the number of rounds of intermating, and therefore vary in the number of recombinants captured and genetic resolution of trait localization. Each F_1 progeny of the testcross with *Oy1-N1989/oy1*:B73 pollen-parent segregated approximately 1:1 for wild-type (*oy1*/*oy1*) and mutant heterozygote (*Oy1-N1989*/*oy1*) in the hybrid genetic background with B73. In the mutant heterozygote siblings of both (IBM and Syn10) F_1 populations, chlorophyll approximation using CCM measured at an early (CCMI) and late (CCMII) developmental stages displayed bimodal trait distributions (**Figures 3a and 3b; Figures S3 and S4**), and there was no overlap between the wild-type and mutant CCM distribution (**Figures S5a and S5b**). Moreover, mutant siblings alone in these F_1 populations with IBM and Syn10 displayed bimodality for CCM measurements, suggesting segregation of a single, effectively Mendelian, suppressor locus (**Figures 3a and 3b**). We name this suppressor locus *very oil yellow1* (*vey1*). CCM values collected at two different times (CCMI and

CCMII) in the wild-type F_1 siblings show positive correlations in both F_1 populations (**Tables S8 and S9; Figures S3 and S4**). Similar trend was also observed for the CCMI and CCMII in the mutant F_1 siblings. However, CCM measurements in the wild-type and mutant displayed statistically insignificant correlations with each other. This suggests that higher chlorophyll accumulation in the mutant siblings is not predicted by the amount of chlorophyll accumulation in the wild-type siblings. To control for variation in CCM observed due to the genetic potential of each line that was independent of the *Oy1-N1989* modification, we divided the mutant CCM trait values by the congenic wild-type sibling CCM values to derive ratio for both time points. We also calculated differences between congenic wild-type and mutant CCM values. Each of the direct measurements, as well as the ratio-metric and difference values, were used as phenotypes to detect and localize QTL.

QTL mapping was carried out on all traits using single interval mapping by the EM algorithm as implemented in R/qtl (Broman *et al.* 2003). Summary of the peak positions of all QTLs passing a permutation computed threshold are presented in **Table S10** for the IBM F_1 populations and **Table S11** for the Syn10 F_1 populations. All mutant CCM traits, all mutant to wild-type CCM ratios, and all differences between mutant and wild-type CCM measurements identified *vey1* as a QTL of large effect on chromosome 10. A plot of the $\log_{10}$ of odds (LOD) score and permutation calculated threshold for CCMII from the mutant siblings in the Syn10 F_1 population is plotted in **Figures 3c and 3d**. Other mutant-related traits in Syn10 and IBM F_1 populations produced similar plots (data not shown). The magnitude of the effects of *vey1* genetic position on all of the traits in the mutant siblings, particularly the effects on CCMI and CCMII, were consistent with the prediction of a single Mendelian locus controlling the majority of the phenotypic variance in these traits based on trait distributions (**Figure 3a and 3b**). Only one additional minor effect QTL was identified that influenced the wild-type CCMI. This QTL was only found in the IBM F_1 population (**Table S10**). No QTL affecting the chlorophyll accumulation of wild-type siblings were detected at the position of *vey1,* or anywhere else in the genome. Interestingly, *vey1* mapped to the same genetic position as *oy1* locus itself (**Figures 3e and 3f**). These analyses indicate that the *vey1* QTL encodes a single locus with an effect contingent upon the allelic status at *oy1* responsible for the suppression of *Oy1-N1989* in these populations.

The identification of the *vey1* modifier as a single Mendelian locus of large effect in the presence of the *Oy1-N1989* allele suggested that we could take a similar approach to localization as for a previous metabolic QTL (Li *et al*. 2014). Thus, we classified each F_1 mutant hybrid in Syn10 F_1 population as high or low CCMII by using the bimodal distribution to assign lines into phenotypic categories. We then compared the marker genotypes at each marker under *vey1* with the phenotypic categories. **Table S12** shows the mutant trait values, marker genotypes, and phenotypic categories for the nine F_1 Syn10 lines with recombinants within the *vey1* region (between the flanking markers 10.90.5 and 10.95.5). Because of the high penetrance of the CCM trait, we interpret a discordance between the marker genotype and F_1 mutant phenotype for high and low CCMII categorization as recombination between *vey1* and that marker. A summary of the recombinant data across the *vey1* flanking markers and additional markers with the physical position of each marker annotated by the number of instances of discordance between the markers and the phenotypic class is presented in **Figures 3e and 3f**. Genotypes at marker 10.93 perfectly predicted CCMII trait expression in Syn10 F_1 mutant siblings. Recombinants separated the trait outcome from the marker genotype in one Syn10 line at marker 10.94.5 and two Syn10 lines at 10.90.5, indicating that the QTL resides in ~227kb interval between markers 10.94.5 and 10.90.5 (**Figure 3e**). This physical position includes the *oy1* locus itself, suggesting that *vey1* may be encoded by the Mo17 allele of *oy1* which enhances the impact of the *Oy1-N1989* allele. In the three Syn10 lines that contained recombination within this critical region, the genotype at *oy1* matched mutant CCM trait values perfectly. To improve the resolution of *vey1* localization we developed additional markers in the region. The genotypes at polymorphic indel markers were determined for the Syn10 recombinants. One marker was encoded by the *ftcl1* locus, two genes towards the telomere from *oy1* and the second, was encoded by *gfa2*, one gene towards the centromere. No recombinants were detected between an indel marker in the proximal end of the *gfa2* gene and *vey1*, although marker 10.94.5 from the Syn10 population is at the distal end of the *gfa2* gene and did show one recombinant (**Figure 3e**). Three recombinants were identified that separated the *ftcl1* marker from the *vey1* QTL. As a result, *vey1* could be encoded by the genomic region between *ftcl1* and *gfa2*. This region includes *oy1*, *ereb28*

(GRMZM2G544539), the small regions of *gfa2* (from marker 10.94.5), and *ftcl1* proximate to *oy1*.

A similar fine mapping approach was adopted for the data from the F_1 crosses to the IBM. Mutant CCMII readings were used to bin IBM F_1 population into suppressed and enhanced categories. The number of cases of discordance between each marker genotype in the *vey1* region and the F_1 mutant phenotypic class is summarized in **Figure 3f**. For all IBM with unambiguous genotypes, the *Oy1-N1989* suppression or enhancement phenotype was correctly predicted by marker genotypes at isu085b. A single recombinant between phenotype and genotype was identified for the flanking marker phi059 which is ~372 kb from the *oy1* locus (towards the telomere). Twenty-seven recombinants between the phenotype and genotype were noted for the marker umc2069 which is ~3.14 Mb from *oy1* (towards the centromere). This analysis identified an ~3.51 Mbp window in IBM containing *vey1* on chromosome 10 providing a confirmation of the Syn10 results with no additional resolution. We attempted to generate additional recombinants by generating a population of ~1100 BC_1F_1 plants from (B73 x Mo17) x *Oy1-N1989/oy1*:B73 crosses. All the mutant siblings from this population (n=576) were separated into suppressed and enhanced phenotype categories by CCM readings and genotyped at *ftcl1*, *oy1*, and *gfa2*. In a sample of 576 mutants, we identified three recombinants between *vey1* and *ftcl1* indel marker, whereas, no recombinant at *oy1* and *gfa2* were detected (**Figure 3e**). Thus, we could not further narrow down this QTL interval.

To validate the *vey1* locus, we made crosses between *Oy1-N1989/oy1* in the B73 background and a series of BM-NILs that contained the *vey1* QTL region introgressed into a homogeneous background of either B73 or Mo17. These BM-NILs also displayed the bimodal effect observed in the QTL experiment, but now without additional segregating B73 and Mo17 alleles. This bimodality was still visible in crosses of *Oy1-N1989* mutant to NILs that used B73 as the recurrent parent to test the *vey1* QTL in an otherwise inbred B73 background demonstrating that a hybrid background was not necessary for *vey1* expression (**Figure S6 and Table S3**). We also observed an increase in the mutant CCM in F_1 hybrids of *Oy1-N1989/oy1*:B73 with NILs that used Mo17 as a recurrent parent but had B73 introgression at *vey1* locus. Thus, our NIL data confirm the expectation of the QTL mapping and validates the existence of the *vey1* modifier. The recombinants in the BM-

NILs were sufficient to identify an ~3.01 Mb region that must contain the *vey1* QTL, but this did not further narrow the region from the four gene window which included the *oy1* locus itself, identified in the Syn10 F_1 population.

Thus, the formal list of candidate genes for the *vey1* QTL is the *oy1* gene itself and the three most closely linked loci. Locus *ftcl1* is annotated as a 5-formyl tetrahydrofolate cyclo-ligase1, which is involved in folate metabolism. The ortholog of *Zmftcl1* (~62% protein identity) from *Arabidopsis thaliana* has been shown to be localized in the chloroplast and T-DNA insertion knockouts are embryo lethal (Pribat *et al.* 2011). The maize gene *gfa2* is uncharacterized, but mutation of the *Arabidopsis* ortholog caused defects in megagametogenesis including failures of polar nuclear fusion in the female gametophyte and synergid cell-death at fertilization (Christensen *et al*. 2002; Christensen, Subramanian, and Drews 1998). The third linked gene, *ereb28* (Apetela2-Ethylene Responsive Element Binding Protein-transcription factor 28) exhibits poor homology to other plant species but has a highly conserved AP2/EREB domain. This gene has a very low expression level and is localized only to the root tissue of maize (https://www.maizegdb.org/gene_center/gene?id=GRMZM2G544539#rnaseq).

Controlling for the *vey1* QTL neither detected additional epistatic interactions with *vey1* nor *Oy1-N1989* phenotype expression

The non-normality of some of the trait distributions and apparent thresholds prompted us to explore additional QTL models. No additional QTL were recovered by implementing two-part threshold models (Broman *et al.* 2003) for any of the traits (data not shown). This observation is consistent with a single major QTL affecting the non-normality in the phenotypic data and normal distribution of residuals remaining after single marker regressions (data not shown). Similarly, two-way scans of the genome also failed to detect any statistically significant genetic interactions. It is worth noting that in both the IBM and the Syn10, the region encoding *vey1* exhibited substantial segregation distortion with the B73:Mo17 alleles present at 120:72 in the IBM and 175:76 in the Syn10 population. This uneven sample size will reduce the power to detect epistasis with *vey1* but would not limit the detection of additional unlinked epistatic modifiers of *Oy1-N1989*.

We used the top marker at *vey1* as a covariate to control for the contribution of this allele to phenotypic variation and performed a one-dimensional scan of the genome (Broman *et al.* 2003). In our previous naïve one-dimensional scans, the large effect of *vey1* partitioned into the error term and might reduce our power to detect additional unlinked QTL(s). By adding a marker linked to *vey1* as a covariate, this term will capture the variance explained by *vey1* and should improve detection of additional QTL(s) of presumably smaller effect. Use of *vey1* linked marker as a covariate, in both IBM and Syn10 F_1 populations, did not identify any additional QTL for any trait (data not shown). Thus, modification of the *Oy1-N1989* phenotype by *vey1* was inherited as a single QTL, acting alone.

GWAS for chlorophyll content in maize diversity lines and *Oy1-N1989*/*oy1* F_1 genotypes identifies *vey1*

We undertook GWA mapping of *Oy1-N1989* severity to search for additional loci and potentially identify recombinants at *vey1*. A population of 343 lines including members of the maize association panel (Flint-Garcia *et al.* 2005) and the Ames panel including ExPVPs (Romay *et al.* 2013) were crossed to *Oy1-N1989/oy1*:B73. This procedure generated MDL x *Oy1-N1989/oy1*:B73 F_1 populations segregating 1:1 for mutant and wild-type siblings in hybrid genetic background. There was total separation between mutant and wild-type siblings in the MDL F_1 populations for the CCMI and CCMII traits (**Figure S5c**). Additionally, dramatically enhanced mutant F_1 families, similar to the F_1 progeny of Mo17 x *Oy1-N1989*/*oy1*:B73, were present within the MDL F_1 populations (**Figure S7**). Pairwise correlations of the CCM trait measurements at two-time points (CCMI and CCMII) in the wild-type siblings displayed statistically significant positive relationship (**Table S13**). CCM traits were much more strongly correlated in the mutant F_1 siblings, similar to the B73 x Mo17 F_1 populations. However, weak positive correlations were also observed between mutant and wild-type CCM measurements in the MDL F_1 populations. Broad-sense heritability estimates were also calculated in the MDL F_1 population. The chlorophyll estimates of the leaves (CCMI and CCMII) showed very high heritability for the mutant and ratio traits, whereas wild-type siblings had much lower repeatability (**Table S14**).

GWA was performed using the HapMap3 SNP data set (Bukowski *et al.* 2018). Although 343 inbred maize lines were crossed to *Oy1-N1989*/*oy1*:B73, only 305 inbred lines were genotyped as part of HapMap3 and were subsequently used for GWAS. The variation in mutant plant's CCMI, CCMII, and their ratios identified a single locus that passed a multiple test correction (see Methods) on chromosome 10 at the site of the *oy1* gene. Just like the detection of the *vey1* QTL in the B73 x Mo17 RIL, no other loci modifying these traits were identified in the GWA analysis. No statistically significant peak was detected for the wild-type CCM traits. The Manhattan plot showing the negative $\log_{10}$ of the p-values from GWA tests for all the SNPs for MT_CCMII trait is graphed in **Figure 4a**. A closer view of the SNPs within the region encoding the *vey1* locus on chromosome 10 are plotted in **Figure 4c**. A summary of the GWAS results for mutant CCM and ratio traits is presented in **Table S15**. The top association for the mutant CCM traits was a SNP at position 9161643 on chromosome 10 located just 3' of the *oy1* locus (a gene on the reverse strand). This SNP displays high allelic frequency in our population (f=0.49). Thus, it appears that the *oy1* locus can be responsible for the suppression of the *Oy1-N1989* mutant allele in the diverse panel of maize inbred lines analyzed in this experiment. Analysis of the LD between S10_9161643 and the other variants in this region identified no other variants with r^2 greater than 0.5 despite the relatively strong associations between many SNPs and the CCM traits (**Figure 4e**). LD was substantially higher for SNPs encoded towards the telomere from *oy1* than towards the centromere, with a strong discontinuity of LD at the 3'-end of *oy1*. Given the relatively low p-values calculated for multiple SNPs in the area, this raises the possibility that multiple alleles could contribute to the suppression of the *Oy1-N1989* phenotype. To test for multiple genetic effects at this locus, the genotypes at SNP S10_9161643 were used as a covariate, and the genetic associations were recalculated. If SNPs segregate independently of S10_9161643 and contribute to *Oy1-N1989* suppression, the p-values of association test statistics for such variants should decrease in this analysis (become more significant). On the contrary, those SNPs that have relatively low p-values due to linkage with S10_9161643 should become less significant in the covariate model. When these analyses were done, low-frequency variants at the 5' end of the *oy1* locus were identified as the most significant SNPs and passed a chromosome-wide multiple test correction (**Figure 4b and 4d**). This result suggests that

585 there are multiple alleles capable of modifying the *Oy1-N1989* mutant phenotype in the
586 MDL panel. The top SNP on chromosome 10 in the covariate model of MLM was detected
587 at position 9179932 and the allele associated with *Oy1-N1989* suppression is a relatively
588 rare variant (f=0.08). It remains formally possible that the SNP S10_9179932 is not
589 causative and merely in LD with a causative polymorphism, and the second locus is
590 fortuitously present in recombinant haplotypes. Analysis of LD of S10_9179932 with other
591 SNPs in ~500 kb window detected multiple SNPs of low allelic frequency that were in high
592 LD (r^2 ~0.85) towards the 5' end of *oy1* (**Figure 4f**). Consistent with the strong
593 discontinuity of LD at 3' end of *oy1* with S10_9161643, we observed discontinuity of LD
594 with S10_9179932 at 5' end of the *oy1* locus. The LD analyses suggest that S10_9161643
595 and S10_9179932 are not in LD with each other and can act independently. These two
596 SNPs account for ~27 percent of the mutant CCMII variation in the MDL x *Oy1-*
597 *N1989/oy1*:B73 F_1 population (**Table S15**).
598 Given that the MLM model using S10_9161643 as a covariate detected
599 S10_9179932 as the most significant association, we tested the phenotypic outcome of the
600 four possible haplotypes at these two SNPs in the MDL F_1 population. We observed that
601 the four haplotypes at these two SNPs varied only for mutant CCM traits, with haplotypes
602 AG and CA being the most favorable (highest CCM mean) and least favorable (lowest
603 CCM mean), respectively (**Table S16**). Alleles at these two SNPs affected CCMI and
604 CCMII in the mutant plants, consistent with additive inheritance for two polymorphisms.
605 The additive impacts of the SNPs make mechanistic predictions about the suppression of
606 *Oy1-N1989*. This additivity is consistent with independent alleles acting in cis at *oy1* to
607 modify the *Oy1-N1989* mutant phenotype. Consistent with the strong enhancement caused
608 by crossing Mo17 to *Oy1-N1989/oy1*:B73, the Mo17 *oy1* locus encodes the most severe,
609 and relatively rare, CA allele combination, and B73 encodes the most suppressing AG
610 allele combination (**Table S16**). Thus, the line-cross mapping was performed with inbred
611 lines that carry the most phenotypically extreme allele combinations of these two SNPs in
612 the vicinity of the *oy1* locus.
613

_Oy1-N1989_ is a semi-dominant chlorophyll mutant and enhanced by reduced function at _oy1_

If alleles of *oy1* encode the suppression of *Oy1-N1989*, then the phenotype of heterozygous *Oy1-N1989* should be strongly responsive to other mutant alleles at *oy1*. Maize seedlings that are heterozygotes between *Oy1-N1989* and hypomorphic *oy1* alleles are more severe than isogenic *Oy1-N1989*/*oy1* siblings (Sawers *et al.* 2006). To confirm that the reduced *oy1* function could determine the differential sensitivity to *Oy1-N1989*, we crossed dominant and recessive mutant alleles of *oy1* to each other. The recessive weak hypomorphic allele *oy1-yg* was obtained from the Maize COOP in the unknown genetic background. The homozygous *oy1-yg* plants were crossed as a pollen-parent with both B73 and Mo17 to develop F_1 material that would segregate the mutation. The F_1 plants were then crossed to *Oy1-N1989/oy1:*B73 as well as backcrossed to the *oy1-yg* homozygotes in the original mixed background. These crosses allowed us to recover plants that had *Oy1-N1989* in combination with the wild-type $oy1^{B73}$, wild-type $oy1^{Mo17}$, and mutant *oy1-yg* alleles. Chlorophyll contents were determined using CCM at 21 and 40 days after sowing in the field. The *Oy1-N1989* allele was substantially enhanced when combined with the *oy1-yg* allele, demonstrating that reduced function of the *oy1* allele in Mo17 could be the genetic basis of *vey1* QTL (**Figures 5a and 5b**). A summary of these data is presented in **Table S17**. This result is similar to the one described by Sawers *et al.* 2006, where a reduction in chlorophyll content was observed when *Oy1-N1989* mutant allele was combined with a recessive allele of *oy1* (*chlI-MTM1*). We also noticed a similar drop in chlorophyll accumulation in the *oy1-yg* homozygotes as oppose to *oy1-yg* heterozygotes with wild-type *oy1* allele from both B73 and Mo17 in the BC_1F_1 progenies (**Figure 5c and Table S17**). However, we did not observe any significant difference in the *oy1-yg* heterozygotes with B73 and Mo17 wild-type *oy1* allele. Selfed progeny from *Oy1-N1989* heterozygotes segregated for yellow-seedling lethal *Oy1-N1989* homozygotes with no detectable chlorophyll by either CCM or spectrophotometer quantification (**Table S6**). Therefore, consistent with previous work (Hansson *et al.* 2002; Sawers *et al.* 2006), the *Oy1-N1989* is a dominant-negative neomorphic mutant allele with no evident MgChl activity under the tested conditions. Based on these genetic data, any QTL resulting in

644 decreased expression of *oy1* or an increased proportion of mutant to wild-type gene product
645 in the *Oy1-N1989*/*oy1* heterozygotes can increase the severity of the mutant phenotype.
646
647 **No coding sequence difference in OY1 accounts for *vey1* inheritance**
648 Our reliance on SNP variation leaves us open to the problem that linked, but the
649 unknown non-SNP variation can be responsible for *vey1*. Given that reduced *oy1* activity
650 enhanced the phenotype of *Oy1-N1989*, we sequenced the *oy1* locus from Mo17 and B73
651 to determine if coding sequence differences could encode the *vey1* modifier. The only non-
652 synonymous changes that distinguish these two alleles is at the site of the previously
653 reported in-frame 6 bp insertion (Sawers *et al.* 2006), which adds alanine (A) and threonine
654 (T) amino acid residues to the OY1 protein. PCR amplification of *oy1* locus in 18 maize
655 inbred lines, as well as the *Oy1-N1989* allele, was performed. Sequencing of the
656 amplification products confirmed the absence of the 6 bp insertion in *Oy1-N1989* allele
657 reported by Sawers *et al.* 2006. In addition, multiple inbred lines including B73, CML103,
658 and CML322 also carried this 6 bp in-frame deletion. A polymorphism within the 6 bp
659 insertion was also found that resulted in an alternative in-frame insertion encoding an
660 alanine and serine (S) codon in Mo17 and five other inbred lines. Thus, three alleles at this
661 site were found to be a common variant in OY1 gene product. These allelic states of *oy1*
662 did not explain the phenotypic severity of CCM trait value in the F_1 mutant siblings (**Figure**
663 **6**). The allelic state of *oy1* at this polymorphic site in 18 maize inbred lines and the average
664 CCM trait values in the wild-type and mutant siblings of their respective F_1 progenies with
665 *Oy1-N1989/oy1*:B73 are summarized in **Table S18.** Five inbred lines, including Mo17,
666 resulted in dramatic enhancement of the CCMI and ratio of CCMI phenotypes of F_1 plants
667 crossed to *Oy1-N1989/oy1*:B73. These enhanced genotypes encoded all three possible
668 alleles at *oy1*. In addition, the suppressing inbred lines also encoded all three possible
669 alleles. Besides this 6 bp indel, three inbred lines had few more variants in OY1 protein.
670 An enhancing inbred line CML322 had two missense mutations that lead to amino acid
671 change at position 321 (D->E), and 374 (S->I). A suppressing inbred line NC358 had one
672 amino acid change at position 336 (D->G) and the enhancing inbred Tzi8 had a 15 bp in-
673 frame deletion leading to the removal of five amino acids (VMGPE) in the third exon of
674 the coding sequence. Even considering the additional alleles at *oy1* found in few maize

675 inbred lines, these results suggest that the only coding sequence polymorphism at *oy1*
676 between B73 and Mo17 could not be genetic basis of *vey1*. This result leaves the two
677 additive top SNPs in cis with *oy1* as the most likely cause of cis-acting regulatory variation.
678
679 **Expression level polymorphism at *oy1* co-segregates with suppression of *Oy1-N1989***
680 Measurements of mRNA accumulation from *oy1* in the IBM was available in a
681 previously published study (Li *et al*. 2013, 2018). The normalized transcript abundance
682 (expressed as RPKM) of OY1 from the shoot apex of 14 days old maize seedlings from
683 IBM were obtained from MaizeGDB (Sen *et al.* 2010). Out of 105 IBM lines that were
684 assessed for expression level, 74 were among those tested for chlorophyll accumulation in
685 *Oy1-N1989* F_1 hybrid populations. Using the genetic marker isu085b that is linked to *oy1*
686 locus, we determined that a cis-acting eQTL controlled the accumulation of OY1
687 transcripts in IBM shoot apex **(Figure 7)**. A summary of these data is presented in **Table**
688 **S19**. This cis-acting eQTL conditioned greater expression of the B73 allele and explained
689 19 percent of the variation ($p < 0.0001$) in OY1 transcript abundance in the IBM. Given
690 the enhancement of *Oy1-N1989* by the *oy1-yg* allele, a lower expression of the wild-type
691 *oy1* allele from Mo17 is expected to enhance the phenotype of *Oy1-N1989* (**Figure 5**). In
692 addition, OY1 RPKM values obtained from the shoot apex of IBM were able to predict the
693 CCM trait values in the mutant but not the wild-type siblings in IBM F_1 population with
694 *Oy1-N1989/oy1*:B73 (**Figure 7**). This result suggests that inbred lines with increased
695 MgChl subunit I transcripts available for protein production and MgChl complex assembly
696 could overcome chlorophyll accumulation defects caused by the *Oy1-N1989/oy1* genotype
697 in IBM F_1 hybrids. Consistent with this, full linear regression model that included both the
698 isu085b marker (cis-eQTL) genotypes and the residual variation in RPKM at OY1 did a
699 better job in predicting CCMI and CCMII in the IBM mutant F_1 hybrids than the isu085b
700 marker by itself. If the cis-eQTL at *oy1*, which results in differential accumulation of OY1
701 transcripts in the IBM inbred lines can affect allele-specific expression in the F_1 hybrids, it
702 could explain the better performance of the IBM mutant F_1 hybrids with the B73 allele at
703 *vey1*.
704 A previous study of allele-specific expression in the F_1 hybrid maize seedlings
705 identified expression bias at *oy1* towards B73 in the hybrid combinations of B73 inbred

line with PH207 and Mo17 but not Oh43 (Waters *et al.* 2017). We used two SNP positions, SNP_252 and SNP_317, to explore the allele-specific expression of OY1 in our materials. SNP_252 is the causative polymorphism for the *Oy1-N1989* missense allele while SNP_317 is polymorphic between B73 and Mo17, but monomorphic between *Oy1-N1989* and B73. As the original allele of the *Oy1-N1989* mutation was isolated from a *r1 c1* colorless synthetic stock of mixed parentage (G. Neuffer, personal communication), this raises the possibility that the same cis-acting regulatory variation that lowered expression of OY1 from PH207 and Mo17 when combined with the B73 allele might also be present in the *oy1* allele that was the progenitor of *Oy1-N1989*. We tested this possibility by using the SNPs that distinguish B73, Mo17, and the *Oy1-N1989* alleles to measure allele-specific expression in each of the hybrids. Consistent with the previous data (Waters *et al.* 2017), we observed biased expression at *oy1* towards the B73 allele in the B73 x Mo17 F_1 wild-type hybrids (**Table 1**). Extended data from this experiment is provided in **Table S20**. In the B73 isogenic crosses, transcripts from the *Oy1-N1989* and B73 wild-type alleles accumulated to equal levels in the heterozygotes, indicating that the suppressed phenotype of the mutants in B73 background was not due to a lowered expression of *Oy1-N1989* relative to the wild-type allele. Remarkably, mutant siblings from the reciprocal crosses between *Oy1-N1989/oy1*:B73 and Mo17 resulted in greater expression from the *Oy1-N1989* allele than the wild-type *oy1* allele of Mo17. Allele-specific bias at *oy1* was significantly higher towards the *Oy1-N1989* allele in the *Oy1-N1989* mutant heterozygotes in the B73 x Mo17 hybrid background compared to B73 isogenic material. Thus, in mutant hybrids, overexpression of *Oy1-N1989* relative to the wild-type *oy1* allele in Mo17 could account for increased phenotypic severity.

If *vey1* is encoded by an eQTL, then PH207 should encode an enhancing allele and Oh43 should encode a suppressing allele of *vey1*. We tested this genetically by producing F_1 progenies in crosses of PH207 and Oh43 by *Oy1-N1989/oy1*:B73 pollen. Oh43 was evaluated in our initial screening and also as part of the MDL panel used for GWAS. In both experiments, the F_1 hybrids between Oh43 and *Oy1-N1989/oy1*:B73 suppressed the mutant phenotype, suggesting that Oh43 is a suppressing inbred line (CCM values in **Tables S4 and S18**). B73 x PH207 F_1 hybrids were missing from our previous datasets. We crossed PH207 ears with pollen from *Oy1-N1989/oy1*:B73 plants. The F_1 hybrids from

this cross were analyzed in the greenhouse at seedlings stage along with F_1 hybrids of B73 x *Oy1-N1989/oy1*:B73 and Mo17 x *Oy1-N1989/oy1*:B73 F_1 progenies as controls. PH207 was an enhancing inbred genotype as mutant heterozygotes in a PH207 x B73 F_1 genetic background accumulated less chlorophyll than mutants in the B73 isogenic background (**Figure S8 and Table S21**).

We further leveraged the normalized expression data of OY1 in the emerging shoot tissue of the maize diversity lines (Kremling *et al.* 2018) and used the top two additive SNPs (S10_9161643 and S10_9179932) at *vey1* from GWAS to test if these cis-variants of *oy1* affect its expression. When tested, plants carrying alleles A and G at marker S10_9161643 and S10_9179932, respectively, showed highest OY1 abundance in the emerging shoots of diverse maize inbred lines, whereas, plants with alleles C and A at S10_9161643 and S10_9179932, respectively, showed lowest OY1 count (**Table S22**). Alleles that suppress *Oy1-N1989* linked to either SNP were associated with the greater abundance of OY1 transcripts. This observation is consistent with the hypothesis that increased OY1 abundance can overcome the negative effect of the *Oy1-N1989* allele. Consistent with the additive suppression of leaf greenness in *Oy1-N1989* mutants by the alleles at S10_9161643 and S10_9179932 discussed previously (**Table S16**), these alleles were also additive for their impacts on OY1 transcript abundance (**Table S22**). Thus, it is likely that multiple phenotypically affective polymorphisms linked to these top unlinked SNPs underlie cis-acting regulatory variation at *oy1*.

The effect sizes of the gene expression changes observed in the IBM, diverse maize inbred lines, and allele-specific expression in hybrids are quite modest, resulting in ~10% of differences in *oy1* accumulation. If these changes in wild-type OY1 transcript accumulation are responsible for suppression of *Oy1-N1989*, then the severity of the mutant phenotype (as indicated by CCM) in the MDL F_1 population should correlate with OY1 expression level. As expected, we observed a statistically significant positive correlation between the mutant derived CCM traits and OY1 counts (**Table S23**). Wild-type CCM in the MDL F_1 population did not show any significant correlation with OY1 abundance in the emerging shoot tissue of maize inbred lines. These correlations are in agreement with the lack of any QTL at this locus controlling wild-type chlorophyll levels, and the epistatic relationship between *vey1* and *Oy1-N1989*.

Discussion

The semi-dominant mutant allele *Oy1-N1989* encodes a dominant-negative allele at the *oy1* locus, which compromises MgChl enzyme activity (Sawers *et al.* 2006). In a heterozygous condition, the strength of the negative effect of this allele on the MgChl enzyme complex depends on the wild-type *oy1* allele. B73 and Mo17 show differential suppression response in mutant heterozygotes resulting in suppressed and severe mutant phenotype, respectively. Thus, the *Oy1-N1989* mutant allele can sensitize maize plants to variation in MgChl and expose a phenotypic consequence for genetic variants that are otherwise invisible. Similar methodology has been adopted previously in maize to gain the genetic understanding of various traits (Chintamanani *et al.* 2010; Olukolu *et al.* 2013, 2014; Buescher *et al.* 2014). Employing a mutant allele as a reporter to screen for effects of natural variants is a simple and efficient technique to detect standing variation in a specific biological process. Although *vey1* polymorphisms are phenotypically consequential in the presence of *Oy1-N1989* allele, no QTL was detected in the absence of *Oy1-N1989* allele. These cryptic genetic variants, or contingent QTL, result from epistasis of *Oy1-N1989* and permits the discovery and re-classification of DNA sequence variants that might otherwise be hypothesized to be neutral or non-functional in plant adaptation. Thus, genetic screens based upon semi-dominant mutant alleles as reporters offer a cost-effective and robust approach to map QTL(s) for metabolic pathways of interest by leveraging the publicly available genetic resources such as bi-parental mapping populations and maize diversity lines.

Alleles with modest fitness consequences may not be visible to researchers working with population sizes even in the thousands, such as in GWAS. By contrast, evolutionarily-relevant segregating variation may have minimal phenotypic effects. One of the possible uses of MAGIC is in boosting the relative contribution of natural variants to phenotypic variance in the trait of interest. This can both uncover cryptic variation affecting a biochemical pathway of interest and assist in improving the mapping resolution of a detected QTL. Not all of the cryptic variation observed by these mutant-contingent QTL approaches need be fitness-affecting, and interpreting mutant-conditioned phenotypes as non-neutral variation would be a mistake. It is, of course, possible that neutral variants may

result in increased severity of a mutant phenotype due to changes not physiologically relevant for all alleles of that reporter gene present in a species. Nevertheless, it can identify new pathway member and inform us about the allelic variation in the species and pathway topology via gene discovery.

In the current study, use of bi-parental mapping populations derived from the same inbred lines but developed using different intercross and inbreeding schemes provided the opportunity to compare the effect of additional rounds of random interbreeding in the development of mapping population on the genetic resolution. The comparative fine mapping of *vey1* in the Syn10 population, that employed ten rounds of random mating, provided far better localization of the *vey1* QTL than the IBM populations that was derived from four rounds of random mating. This observation demonstrates the benefits of increased recombination during random intermating of early generations in QTL localization. Based on these results, as future RILs are generated, we recommend increased intermating in the early generations followed by DH induction rather than relying on further recombination during the self-pollination cycles of RIL development.

As expected, GWAS provided a fine-scale genetic resolution and corroborated the mapping of *vey1*. The distance between the best marker and the *oy1* gene was substantially less in the GWA experiments. GWAS identified two SNPs, one in the 5' and another in the 3' intergenic DNA, proximate to *oy1* that represent candidate quantitative trait nucleotides (QTN). The architecture of this region included four haplotypes with every combination of alleles at these two SNPs. The signal detection by multiple unlinked SNPs in GWAS may indicate a complex set of phenotypically affective alleles at the *oy1* locus. Alternatively, it could very well be an artifact of missing the causative polymorphism within our genetic data resulting in strong associations with markers that are tightly linked to the causative variation but unlinked or in repulsion to each other. For example, indel variation is not captured by the approaches used in the GWA analysis. Consistent with two QTN, rather than fortuitous linkage of tag SNPs with a single causative polymorphism, alleles at the two SNPs additively influenced chlorophyll contents in the mutant siblings. Future work to identify the nucleotide changes responsible for the differences between B73, Mo17, and other inbred lines that encode *vey1* will be required to test these possibilities definitively.

Together, this study illustrates the complementary nature of line-cross QTL mapping and GWAS to explore the genetics of the trait under investigation.

We used *Oy1-N1989* together with a non-destructive, inexpensive, and rapid phenotyping method to measure leaf chlorophyll. Rapid and robust phenotyping is critical and contributed to the strong correlation between the absolute trait measurement and the estimated phenotypes like CCM. Previous studies have highlighted the importance of benchmarking indirect measurements or proxies for traits of interest. For instance, near infrared reflectance spectroscopy (NIRS) that estimates major and total carotenoids in maize kernels could replace sensitive, accurate, cumbersome, expensive, slow, and destructive measurements by HPLC (Berardo *et al.* 2004). Comparisons of HPLC and NIRS measurements resulted in a correlation of 0.85 for total carotenoids (Berardo *et al.* 2004). A subjective visual score for yellow color in maize kernels was not adequate, yielding a correlation of 0.12 with HPLC measurements of total carotenoids (Harjes *et al.* 2008). Thus, using mutant alleles as reporters to develop methodologies that rely on non-invasive multispectral or hyperspectral data as proxies for specific biochemical compounds will accelerate studies on gene function and allele discovery. This approach can enable genetic studies that are currently deemed unfeasible due to the arduous task of phenotyping large populations for traits only visible in the laboratory.

How could a 10% change in wild-type OY1 expression affect chlorophyll biosynthesis in the *Oy1-N1989*/*oy1* mutant heterozygotes?

Magnesium chelatase (MgChl) is formed by a trimer of dimers of MgChl subunit I interacting with the other subunits of MgChl complex. A previous study found that addition of mutant or wild-type BCHI protein to pre-assembled MgChl complexes resulted in altered reaction rates due to differences in subunit turnover, which occurred on a minutes time-scale (Lundqvist *et al.* 2013). This subunit turnover and reformation of the complex dynamically exchange mutant and wild-type BCHI subunits over time. Therefore, any net increase in the amount of wild-type OY1 in the reaction pool, for instance, due to higher transcription of wild-type *oy1* allele will allow a higher rate of magnesium chelatase activity and result in more chlorophyll biosynthesis. The observation of stronger affinity and greater dissociation rate of $BCHI^{L111F}$ subunits (orthologous to the L176F change

encoded by *Oy1-N1989*) for the wild-type subunits (Hansson *et al*. 2002) suggests that exchange of BCHI monomeric units in the magnesium chelatase complex might also differ based on the structure of BCHI protein (Lundqvist *et al.* 2013). In the AAA^+ protein family, the ATP-binding site is located at the interface of two neighboring subunits in the oligomeric complex (Vale 2000). Since a dimer of functional MgChl subunit I proteins are required for the complex to carry out MgChl activity (Lundqvist *et al.* 2013), approximately 1 in 3 dimers of assembled MgChl subunit I will be active in a 1:1 mixture of wild-type and $BCHI^{L111F}$. Indeed, complexes made from reaction mixtures with equal proportions of wild-type and $BCHI^{L111F}$ subunits resulted in ~26% of the enzyme activity of an equivalent all-wildtype mix (Lundqvist *et al.* 2013). Therefore, we expect that decreasing expression of the wild-type *oy1* subunit by 10% and creating a 0.9:1.1 mixture of wild-type OY1 and mutant OY1-N1989 protein, respectively, would result in ~21% activity compared to the activity of all-wildtype mixture. Likewise, increasing the wild-type *oy1* expression by 10% would result in ~30% activity of MgChl compared to the all-wildtype mixture. This dosage-sensitivity is a general feature of protein complexes (Birchler and Veitia 2012; Veitia 2003; Grossniklaus, Madhusudhan, and Nanjundiah 1996; Birchler and Newton 1981), and the semi-dominant nature of *Oy1-N1989* is dosage sensitive. Taking these observations and proposed models on the dynamics of molecular interaction between the wild-type and mutant BCHI protein subunits (especially $BCHI^{L111F}$) into account, it is formally possible that a small change in the expression of wild-type OY1 can have a significant impact on the magnesium chelatase activity of heterozygous *Oy1-N1989*/*oy1* plants. The increase in magnesium chelatase activity due to the even small relative increase in the proportion of wild-type OY1 transcripts over the mutant OY1-N1989 transcripts will read out as a proportional, presumably non-linear, increase in chlorophyll accumulation.

What is *vey1*?

Variation at the *vey1* locus appears to be the result of allelic diversity linked to the *oy1* locus. The only remaining possibilities are regulatory polymorphisms within the cis-acting control regions of *oy1*. Previous studies have utilized reciprocal test-crosses to loss-of-function alleles in multiple genetic backgrounds to provide single-locus tests of additive

QTL alleles in an otherwise identical hybrid background (Dilkes *et al.* 2008). Protein-null alleles of *oy1* isolated directly from the B73 and Mo17 backgrounds could be used to carry out a similar test. The intergenic genomic region in maize is spanned by transposable elements and can be highly divergent between different inbred lines due to large insertions/deletions polymorphisms (SanMiguel and Bennetzen 1998). Consistent with this, inbreds B73 and Mo17 are polymorphic at the region between *oy1* and *gfa2*. These two maize inbred lines share ~12 kb of sequence interspersed with numerous large insertions and deletions that add ~139 kb of DNA sequence to Mo17 as compared to B73 (data not shown). However, we did not find any conserved non-coding sequence (CNS) in this region (data not shown). It is conceivable that recombinants at *oy1* between B73 and Mo17 themselves could be identified and used to test the effects of upstream or downstream regulatory sequences. The recombinant haplotypes encoding all four possible alleles at the top two SNPs identified in the GWAS indicate that Mo17 may be a strong enhancer due to more than one causative polymorphism.

In the absence of such recombinants, we can only consider what mechanisms might be consistent with the observed suppression of the chlorophyll biosynthesis defects such as cis-acting effects on OY1 transcript abundance, and allele-specific gene expression. Genotype at *vey1* in wild-type plants accounted for only 19 percent of the variation in OY1 abundance in the shoot apices of the IBM. This QTL accounted for more than 80 percent of the variation in chlorophyll content in mutants. If transcript accumulation is insensitive to the presence of *Oy1-N1989* allele, then the remaining ~80 percent of the variation in OY1 abundance observed as not *vey1*-dependent in the wild-type IBM might be expected to account for a greater change in phenotype. However, trans-acting effects or environmental effects that would equally affect both alleles at the *oy1* locus would be expected to have a lesser impact on suppression of the deleterious *Oy1-N1989* allele. The effect of cis-acting eQTL on *oy1* expression would eventually result in a greater or lesser proportion of wild-type OY1 protein accumulation. These allele-specific differences will alter the mutant to wild-type subunit stoichiometry which should have a greater impact on chlorophyll content than changes in absolute RPKM, due to the competitive inhibition of MgChl complex activity by *Oy1-N1989* (Sawers *et al.* 2006; Lundqvist *et al.* 2013), as detailed above.

The reciprocal crosses between *Oy1-N1989*/*oy1*:B73 and Mo17 did not result in different phenotypes. Thus, *vey1* does not exhibit imprinting. Allele-specific expression at *oy1* locus in the *Oy1-N1989* heterozygous mutants demonstrated the existence of functional cis-acting regulatory polymorphism between *Oy1-N1989* and both wild-type *oy1* alleles in B73 and Mo17. In addition, *oy1* is affected by a cis-eQTL in the IBM and MDL. Together with our other data, the allele-specific expression at OY1 that was visible when we re-analyzed the data from Waters *et al.* 2017, we propose that *vey1* is encoded by cis-acting regulatory DNA sequence variation (**Figure S9**). Ultimately, transgenic testing of *oy1* cis-acting regulatory polymorphisms identified from assembled maize genomes is required to determine the causative variant(s) encoding *vey1*. Sequence comparisons outside the protein coding sequence of the gene can be quite challenging, especially in maize, as it exhibits limited to poor sequence conservation between different inbred lines (SanMiguel *et al.* 1996). Thus, distinguishing phenotypically affective polymorphisms from the neutral variants is not trivial. As a result, biochemical and *in vitro* studies are the best tool for functional validation of these polymorphisms (Wray *et al.* 2003). Similar experiments have been done to characterize the role of DNA sequence polymorphisms in cis on the expression of downstream genes in case of *flowering locus T* in *Arabidopsis* and *teosinte branched1* in maize (Adrian *et al.* 2010; Studer *et al.* 2011).

Relevance to research on transcriptional regulation

Since their discovery, the role of regulatory elements in gene function has been recognized as vital to our understanding of biological systems (McClintock 1950, 1956a, 1956b, 1961; Peterson 1953; Jacob and Monod 1961). Gene regulation and gene product dosage are at the forefront of evolutionary theories about sources of novelty and diversification (Ohno 1972; King and Wilson 1975). Transcriptional regulation of a gene can be as important as the protein coding sequence (Wray *et al.* 2003). For instance, complete knock-down of expression of a gene by a regulatory polymorphism will have the same phenotypic consequence as the non-sense mediated decay of a transcript harboring an early stop codon (Willing *et al.* 1996). But we do not have a set of rules, analogous to codon tables, for functional polymorphisms outside the coding sequence of a gene.

Detecting expression variation and tying it to phenotypic consequence, especially in the absence of CNS, remains a challenge to this day.

Several eQTL studies ranging from unicellular to multicellular eukaryotic organisms have found abundant cis and trans-acting genomic regions that affect gene expression (Brem *et al*. 2002; West *et al*. 2007; Li *et al*. 2013, 2018). The proportion of cis-acting eQTLs from the total eQTLs detected in various studies including yeast, mouse, rat, humans, eucalyptus, and maize range from 19-92% (Gibson and Weir 2005; Li *et al*. 2013, 2018). Expression polymorphisms are a potential source of variation in some phenotypic traits (Gibson and Weir 2005), and multiple studies detected expression polymorphisms co-segregating with phenotypic variation, including contributions to species domestication (Clark *et al.* 2006; Salvi *et al.* 2007; Schwartz *et al.* 2009; Lemmon *et al.* 2014). But a majority of the cis-eQTLs only exhibit a moderate difference in the gene expression. Detecting such variants and linking them to visible phenotypes may require detailed study using approaches focused on the specific biological process affected by the gene product. We do not yet have a standardized experimental tool for these purposes. As such, we cannot simultaneously identify and characterize the phenotypic impact of most cis-acting eQTLs.

The *vey1* polymorphism detected in the current study co-segregates with a cis-eQTL at *oy1* in IBM (Li *et al*. 2013, 2018) and diverse maize inbred lines (Kremling *et al.* 2018). Using *Oy1-N1989* allele to expose the consequences of these cis-eQTLs allowed chlorophyll approximation using CCM to substitute for expensive, cumbersome, highly sensitive gene expression assays or metabolite measurements. The high heritability of this alternative and direct phenotype, allowed us to scan large populations at a rapid rate to identify the genomic regions underlying the cis-acting regulatory elements and study allelic diversity in the natural population of maize. We propose that the approach we have taken is not likely to be unique to *oy1*. Therefore, we propose that all semi-dominant mutant alleles can be used as reporters to not only detect novel cis-acting gene regulatory elements but also functionally validate previously-detected cis-eQTL(s) from genome-wide eQTL studies.

Acknowledgements

Authors acknowledge the help of the staff at Purdue ACRE farm for assistance with planting and crop management of all the field experiments described in this study. R.S.K was supported by USAID Feed the Future CGIAR-US Initiative grant "Heat stress resilient maize for South Asia through a public-private partnership" to G.S.J.. This work was supported by NSF grant 1444503 awarded to G.S.J. and B.P.D. We especially thank the Muehlbauer lab for making their data open to the public, and the USDA for the MaizeGDB website, which allowed us to reanalyze the eQTL data.

Tables

Table 1. The allele-specific expression at *oy1* in the top fully-expanded leaf at the V3 developmental stage of B73 x Mo17 F_1 wild-type and *Oy1-N1989*/*oy1* mutant siblings, and inbred *Oy1-N1989*/*oy1:B73* mutants.

Figures

Figure 1. The chlorophyll pigment accumulation differs in severity for *Oy1-N1989/oy1* heterozygotes in the B73 and B73 x Mo17 hybrid backgrounds.
Figure 2. The crossing scheme used to map *Oy1-N1989* enhancer/suppressor loci in IBM and Syn10 populations.
Figure 3. The phenotypic distribution, QTL analysis, and fine mapping results of MT_CCMII trait.
Figure 4. The Manhattan plots of SNPs associations with MT_CCMII trait in MDL x *Oy1-N1989/oy1*:B73 F_1 populations.
Figure 5. The single locus test of *oy1* showing the interaction between wild-type alleles of *oy1* from B73 and Mo17 with semi-dominant and recessive mutant alleles *Oy1-N1989* and *oy1-yg*, respectively.
Figure 6. The distributions of CCM trait measurements in the F_1 progenies of a sub-set of maize inbred lines crossed with *Oy1-N1989/oy1*:B73 at three allelic variants in the *oy1* coding sequence identified in respective inbred lines.
Figure 7. Expression of OY1 in the shoot apices of 14 days old IBM seedlings co-segregates with *vey1*.

Supplemental tables

Table S1. The trait mean values of the CCM traits for the wild-type (WT) and mutant (MT) siblings of the F_1 hybrids of *Oy1-N1989*/*oy1*:B73 (pollen-parent) with respective IBM lines.
Table S2. The trait mean values of the CCM traits for the wild-type (WT) and mutant (MT) siblings of F_1 hybrids of *Oy1-N1989*/*oy1*:B73 (pollen-parent) with respective Syn10 line.
Table S3. The average values of the CCM traits in wild-type (WT) and mutant (MT) siblings of the F_1 hybrids between *Oy1-N1989/oy1*:B73 (as a pollen-parent) with respective BM-NILs. Data is derived from the field-grown plants with five replications planted in a RCBD. Parental (B73 and Mo17) F_1 crosses were planted as checks in each replication. Multiple plants (2-3) were measured for each genotype (wild-type or mutant) in each replication.
Table S4. The BLUP values of the wild-type (WT) and mutant (MT) siblings of the F_1 hybrids of *Oy1-N1989*/*oy1*:B73 with respective maize diversity lines (MDL). Information on the inbred lines from maize association panel (referred to as 302) was adapted from Flint-Garcia *et al.* 2005.
Table S5. The summary of the HapMap3 variants before and after filtering to remove SNPs with minor allele frequency < 0.05 (5%) and missing > 0.1 (10%).

Table S6. The chlorophyll accumulation in the third fully-expanded leaf at the V3 stage of greenhouse-grown maize seedlings.
Table S7. Means and standard deviation of pigment absorbance (index) from mutant (*Oy1-N1989/oy1*) and wild-type plants grown at the Purdue Agronomy Farm.
Table S8. The trait correlations among the CCM traits in IBM x *Oy1-N1989/oy1*:B73 F_1 hybrid populations.
Table S9. The trait Correlations among the CCM traits in Syn10 x *Oy1-N1989/oy1*:B73 F_1 hybrid populations.
Table S10. The summary of the QTL detected for CCM traits in IBM x *Oy1-N1989/oy1*:B73 F_1 hybrid populations.
Table S11. The summary of the QTL detected from CCM traits in Syn10 x *Oy1-N1989/oy1*:B73 F_1 hybrid populations.
Table S12. Recombinants within the *vey1* region derived from Syn10 x *Oy1-N1989/oy1*:B73 F_1 populations.
Table S13. The trait correlations of various CCM traits using mean values of MDL x *Oy1-N1989/oy1*:B73 F_1 hybrid populations.
Table S14. The broad sense heritability and variance estimates of CCM traits measured in MDL x *Oy1-N1989/oy1*:B73 F_1 hybrid populations.
Table S15. The summary of the top four statistically significant SNP markers associated with CCM traits by GWAS and top SNP following the addition of S10_9161643 as a covariate for each trait.
Table S16. Haplotypes at two SNPs at *vey1* locus associated with *Oy1-N1989* suppression and its effect on CCM traits in MDL x *Oy1-N1989*/*oy1*:B73 F_1 populations.
Table S17. The chlorophyll quantification of plants segregating for the allelic interaction between *Oy1-N1989* and *oy1-yg* alleles at *oy1*.
Table S18. The summary of the average CCM value of the F_1 hybrids of inbred lines crossed with *Oy1-N1989/oy1*:B73, and allelic state at the 6 bp (two amino acids) indel in the coding sequence of OY1 transcript in the respective parental inbred line.
Table S19. The linear regression of the top *vey1* linked marker (isu085b) and CCM traits from wild-type and mutant siblings of IBM x *Oy1-N1989/oy1*:B73 F_1 populations on to OY1 expression (RPKM values) of the respective IBM line (n=74).
Table S20. The allele expression bias at *oy1* in leaf tissue from the top fully-expanded leaf at the V3 stage.
Table S21. The chlorophyll approximation (using CCM) from the middle of the third leaf at the V3 stage on greenhouse-grown maize seedlings from a cross of B73, Mo17, and PH207 inbred lines (ear-parents) with *Oy1-N1989/oy1*:B73 plants (pollen-parent).
Table S22. The distribution of normalized OY1 expression in the emerging shoot tissue of maize diversity lines (Kremling *et al.* 2018) at two SNPs associated with suppression of *Oy1-N1989* phenotype in MDL x *Oy1-N1989*/*oy1*:B73 F_1 populations.
Table S23. The pairwise trait correlations between OY1 transcript abundance in the emerging shoots of maize inbred lines and the CCM traits of corresponding F_1 hybrids with *Oy1-N1989*/*oy1*:B73 for the 198 inbred lines common between the current study and Kremling *et al*. 2018.

Supplemental figures

Figure S1. The linear regression of the chlorophyll pigment measurements using non-destructive CCM-200 plus meter (expressed as CCM index) and absolute chlorophyll pigment quantification using the spectrophotometric method from the same leaf.
Figure S2. The CCM quantification of the (a) mutant (*Oy1-N1989/oy1*), and (b) wild-type (*oy1/oy1*) siblings in B73, Mo17 x B73, and Mo17 (BC_6 generation) genetic background at 30 days after planting.
Figure S3. The pairwise scatter plot of primary trait measurements in IBM x *Oy1-N1989/oy1*:B73 F_1 populations.
Figure S4. The pairwise scatter plot of primary trait measurements in Syn10 x *Oy1-N1989/oy1*:B73 F_1 populations.
Figure S5. The CCMI and CCMII distribution in the wild-type (WT) and mutant (MT) siblings of (a) IBM x *Oy1-N1989/oy1*:B73 F_1 populations, (b) Syn10 x *Oy1-N1989/oy1*:B73 F_1 populations, and (c) MDL x *Oy1-N1989/oy1*:B73 F_1 populations.
Figure S6. The cartoon showing *vey1* validation in BM-NILs x *Oy1-N1989/oy1*:B73 F_1 populations.
Figure S7. The pairwise scatter plot of primary trait measurements in MDL x *Oy1-N1989/oy1*:B73 F_1 populations.
Figure S8. The chlorophyll approximation (using CCM) from the middle of the third leaf in the greenhouse grown F_1 maize seedlings from a cross of B73, Mo17, and PH207 inbred lines (ear-parents) with *Oy1-N1989/oy1*:B73 plants (pollen-parent) at the V3 developmental stage.
Figure S9. The proposed model for cis-acting regulatory variation as the basis of *vey1*.

Supplemental files

1. S1_IBM_F1_Rqtl_input: CSV file with average CCM values and genotypic data of IBM x *Oy1-N1989/oy1*:B73 F_1 population formatted for R/qtl.
2. S2_Syn10_F1_Rqtl_input: CSV file with BLUP value of CCM traits and genotypic data of Syn10 x *Oy1-N1989/oy1*:B73 F_1 population formatted for R/qtl.

Literature cited

Adrian, J., S. Farrona, J. J. Reimer, M. C. Albani, G. Coupland *et al.*, 2010 Cis-Regulatory Elements and Chromatin State Coordinately Control Temporal and Spatial Expression of FLOWERING LOCUS T in Arabidopsis. Plant Cell 22: 1425–1440.

Bates, D. M., M. Machler, B. M. Bolker, and S. C. Walker, 2015 Fitting Linear Mixed-Effects Models using lme4. J. Stat. Softw. 67: 1–48.

Benjamini, Y., and Y. Hochberg, 1995 Controlling the False Discovery Rate: A Practical and Powerful Approach to Multiple Testing. J. R. Stat. Soc. Ser. B 57: 289–300.

Berardo, N., O. V. Brenna, A. Amato, P. Valoti, V. Pisacane *et al.*, 2004 Carotenoids concentration among maize genotypes measured by near infrared reflectance spectroscopy (NIRS). Innov. Food Sci. Emerg. Technol. 5: 393–398.

Birchler, J. A., and K. J. Newton, 1981 Modulation of protein levels in chromosomal dosage series of maize: the biochemical basis of aneuploid syndromes. Genetics 99: 247–266.

Birchler, J. A., and R. A. Veitia, 2012 Gene balance hypothesis: Connecting issues of dosage sensitivity across biological disciplines. Proc. Natl. Acad. Sci. 109: 14746–14753.

Bradbury, P. J., Z. Zhang, D. E. Kroon, T. M. Casstevens, Y. Ramdoss *et al.*, 2007 TASSEL: software for association mapping of complex traits in diverse samples. Bioinformatics 23: 2633–5.

Brem, R. B., G. Yvert, R. Clinton, and L. Kruglyak, 2002 Genetic dissection of transcriptional regulation in budding yeast. Science. 296: 752–755.

Broman, K. W., H. Wu, S. Sen, and G. a. Churchill, 2003 R/qtl: QTL mapping in experimental crosses. Bioinformatics 19: 889–890.

Buescher, E. M., J. Moon, A. Runkel, S. Hake, and B. P. Dilkes, 2014 Natural Variation at sympathy for the ligule Controls Penetrance of the Semidominant Liguleless narrow-R Mutation in Zea mays. G3 4: 2297–2306.

Bukowski, R., X. Guo, Y. Lu, C. Zou, B. He *et al.*, 2018 Construction of the third generation Zea mays haplotype map. Gigascience 7: 1–12.

Bushnell, B., 2014 BBMap: A Fast, Accurate, Splice-Aware Aligner.:

Chintamanani, S., S. H. Hulbert, G. S. Johal, and P. J. Balint-Kurti, 2010 Identification of a maize locus that modulates the hypersensitive defense response, using mutant-assisted gene identification and characterization. Genetics 184: 813–25.

Christensen, C. A., S. W. Gorsich, R. H. Brown, L. G. Jones, J. Brown *et al.*, 2002 Mitochondrial GFA2 Is Required for Synergid Cell Death in Arabidopsis. Plant Cell 14: 2215–2232.

Christensen, C. A., S. Subramanian, and G. N. Drews, 1998 Identification of Gametophytic Mutations Affecting Female Gametophyte Development in Arabidopsis. Dev. Biol. 202: 136–151.

Churchill, G. A., and R. W. Doerge, 1994 Empirical threshold values for quantitative trait mapping. Genetics 138: 963–71.

Clark, R. M., T. N. Wagler, P. Quijada, and J. Doebley, 2006 A distant upstream enhancer at the maize domestication gene tb1 has pleiotropic effects on plant and inflorescent architecture. Nat. Genet. 38: 594–7.

Danecek, P., A. Auton, G. Abecasis, C. A. Albers, E. Banks *et al.*, 2011 The variant call format and VCFtools. Bioinformatics 27: 2156–2158.

DePristo, M. A., E. Banks, R. Poplin, K. V Garimella, J. R. Maguire *et al.*, 2011 A framework for variation discovery and genotyping using next-generation DNA sequencing data. Nat. Genet. 43: 491–498.

Dilkes, B. P., M. Spielman, R. Weizbauer, B. Watson, D. Burkart-Waco *et al.*, 2008 The Maternally Expressed WRKY Transcription Factor TTG2 Controls Lethality in Interploidy Crosses of Arabidopsis. PLoS Biol. 6: 2707–2720.

Eggermont, K., I. J. Goderis, and W. F. Broekaert, 1996 High-throughput RNA Extraction from Plant Samples Based on Homogenisation by Reciprocal Shaking in the Presence of a Mixture of Sand and Glass Beads. Plant Mol. Biol. Report. 14: 273–279.

Eichten, S. R., J. M. Foerster, N. de Leon, Y. Kai, C.-T. Yeh *et al.*, 2011 B73-Mo17 near-isogenic lines demonstrate dispersed structural variation in maize. Plant Physiol. 156: 1679–90.

Elshire, R. J., J. C. Glaubitz, Q. Sun, J. a Poland, K. Kawamoto *et al.*, 2011 A robust, simple genotyping-by-sequencing (GBS) approach for high diversity species. PLoS One 6(5): e19379.

Fisher, R. ., 1921 On the "probable error" of a coefficient of correlation deduced from a small sample. Metron 1: 3–32.

Fisher, R. A., 1930 *The genetical theory of natural selection.* Oxford, UK: Oxford University Press.

Flint-Garcia, S. a, A.-C. Thuillet, J. Yu, G. Pressoir, S. M. Romero *et al.*, 2005 Maize association population: a high-resolution platform for quantitative trait locus dissection. Plant J. 44: 1054–1064.

Fodje, M. N., A. Hansson, M. Hansson, J. G. Olsen, S. Gough *et al.*, 2001 Interplay between an AAA module and an integrin I domain may regulate the function of magnesium chelatase. J. Mol. Biol. 311: 111–122.

Gibson, G., and B. Weir, 2005 The quantitative genetics of transcription. Trends Genet. 21: 616–623.

Gray, J., P. S. Close, S. P. Briggs, and G. S. Johal, 1997 A novel suppressor of cell death in plants encoded by the Lls1 gene of maize. Cell 89: 25–31.

Gray, J., D. Janick-Buckner, B. Buckner, P. S. Close, and G. S. Johal, 2002 Light-dependent death of maize lls1 cells is mediated by mature chloroplasts. Plant Physiol. 130: 1894–1907.

Grossniklaus, U., M. S. Madhusudhan, and V. Nanjundiah, 1996 Nonlinear Enzyme Kinetics Can Lead to High Metabolic Flux Control Coefficients: Implications for the Evolution of Dominance. J. Theor. Biol. 182: 299–302.

Hansson, A., C. G. Kannangara, D. V Wettstein, and M. Hansson, 1999 Molecular basis for semidominance of missense mutations in the XANTHA-H (42-kDa) subunit of magnesium chelatase. Proc. Natl. Acad. Sci. U. S. A. 96: 1744–1749.

Hansson, A., R. D. Willows, T. H. Roberts, and M. Hansson, 2002 Three semidominant barley mutants with single amino acid substitutions in the smallest magnesium chelatase subunit form defective AAA+ hexamers. Proc. Natl. Acad. Sci. U. S. A. 99: 13944–13949.

Harjes, C. E., T. R. Rocheford, L. Bai, T. P. Brutnell, C. B. Kandianis *et al.*, 2008 Natural

Genetic Variation in Lycopene Epsilon Cyclase Tapped for Maize Biofortification. Science. 319: 330–333.

Holm, S., 1979 A simple sequentially rejective multiple test procedure. Scand. J. Stat. 6: 65–70.

Huang, M., T. L. Slewinski, R. F. Baker, D. Janick-Buckner, B. Buckner *et al.*, 2009 Camouflage patterning in maize leaves results from a defect in porphobilinogen deaminase. Mol. Plant 2: 773–89.

Hu, G., N. Yalpani, S. P. Briggs, and G. S. Johal, 1998 A porphyrin pathway impairment is responsible for the phenotype of a dominant disease lesion mimic mutant of maize. Plant Cell 10: 1095–1105.

Hussain, T., P. Tausend, G. Graham, and J. Ho, 2007 Registration of IBM2 SYN10 Doubled Haploid Mapping Population of Maize. J. Plant Regist. 1: 81.

Jacob, F., and J. Monod, 1961 Genetic regulatory mechanisms in the synthesis of proteins. J. Mol. Biol. 3: 318–356.

Johal, G. S., P. Balint-Kurti, and C. F. Weil, 2008 Mining and Harnessing Natural Variation: A Little MAGIC. Crop Sci. 48: 2066.

King, M.-C., and A. C. Wilson, 1975 Evolution at two levels in Humans and Chimpanzees. Science. 108: 107–116.

Kremling, K. A. G., S.-Y. Chen, M.-H. Su, N. K. Lepak, M. C. Romay *et al.*, 2018 Dysregulation of expression correlates with rare-allele burden and fitness loss in maize. Nature. 55: 520–523.

Lauter, A. N. M., M. G. Muszynski, R. D. Huffman, and M. P. Scott, 2017 A Pectin Metethylesterase ZmPme3 Is Expressed in Gametophyte factor1-s (Ga1-s) Silks and Maps to that Locus in Maize (Zea mays L.). Front. Plant Sci. 8: 1–11.

Lee, M., N. Sharopova, W. D. Beavis, D. Grant, M. Katt *et al.*, 2002 Expanding the genetic map of maize with the intermated B73 x Mo17 (IBM) population. Plant Mol. Biol. 48: 453–61.

Lemmon, Z. H., R. Bukowski, Q. Sun, and J. F. Doebley, 2014 The Role of cis Regulatory Evolution in Maize Domestication. PLoS Genet. 10:.

Li, H., and R. Durbin, 2009 Fast and accurate short read alignment with Burrows-Wheeler transform. Bioinformatics 25: 1754–1760.

Li, H., B. Handsaker, A. Wysoker, T. Fennell, J. Ruan *et al.*, 2009 The Sequence Alignment/Map format and SAMtools. Bioinformatics 25: 2078–2079.

Li, L., K. Petsch, R. Shimizu, S. Liu, W. W. Xu *et al.*, 2018 Correction: Mendelian and Non-Mendelian Regulation of Gene Expression in Maize. PLoS Genet. 1–4.

Li, L., K. Petsch, R. Shimizu, S. Liu, W. W. Xu *et al.*, 2013 Mendelian and non-Mendelian regulation of gene expression in maize. PLoS Genet. 9: e1003202.

Li, X., E. Svedin, H. Mo, S. Atwell, B. P. Dilkes *et al.*, 2014 Exploiting natural variation of secondary metabolism identifies a gene controlling the glycosylation diversity of dihydroxybenzoic acids in Arabidopsis thaliana. Genetics 198: 1267–1276.

Lichtenthaler, H. K., and C. Buschmann, 2001 Chlorophylls and Carotenoids: measurement and characterization by UV-VIS spectroscopy. Curr. Protoc. Food Anal. Chem. F4.3.1-F4.3.8.

Lin, C. Y., and F. R. Allaire, 1977 Heritability of a linear combination of traits. Theor. Appl. Genet. 51: 1–3.

Lipka, A. E., F. Tian, Q. Wang, J. Peiffer, M. Li *et al.*, 2012 GAPIT: genome association

and prediction integrated tool. Bioinformatics 28: 2397–9.

Liu, H., Y. Niu, P. J. Gonzalez-Portilla, H. Zhou, L. Wang *et al.*, 2015 An ultra-high-density map as a community resource for discerning the genetic basis of quantitative traits in maize. BMC Genomics 16: 1078.

Lundqvist, J., I. Braumann, M. Kurowska, A. H. Müller, and M. Hansson, 2013 Catalytic turnover triggers exchange of subunits of the magnesium chelatase AAA+ motor unit. J. Biol. Chem. 288: 24012–24019.

Mach, J. M., A. R. Castillo, R. Hoogstraten, and J. T. Greenberg, 2001 The Arabidopsis-accelerated cell death gene ACD2 encodes red chlorophyll catabolite reductase and suppresses the spread of disease symptoms. Proc. Natl. Acad. Sci. 98: 771–776.

Mangelsdorf, P. ., and D. . Jones, 1926 The expression of mendelian factors in the gametophyte of maize. Genetics 11: 423–455.

McClintock, B., 1956a Controlling elements and the gene. Cold Spring Harb. Symp. Quant. Biol. 21: 197–216.

McClintock, B., 1956b Intranuclear systems controlling gene action and mutation. Brookhaven Symp. Biol. 8: 58–74.

McClintock, B., 1961 Some Parallels Between Gene Control Systems in Maize and in Bacteria. Am. Nat. 95: 265–277.

McClintock, B., 1950 The origin and behavior of mutable loci in maize. PNAS 36: 344–355.

Meskauskiene, R., M. Nater, D. Goslings, F. Kessler, R. op den Camp *et al.*, 2001 FLU: A negative regulator of chlorophyll biosynthesis in Arabidopsis thaliana. Proc. Natl. Acad. Sci. 98: 12826–12831.

Neff, M. M., E. Turk, and M. Kalishman, 2002 Web-based primer design for single nucleotide polymorphism analysis. Trends Genet. 18: 613–615.

Ohno, S., 1972 An argument for the genetic simplicity of man and other mammals. J. Hum. Evol. 1: 651–662.

Olukolu, B. A., Y. Bian, B. De Vries, W. F. Tracy, R. J. Wisser *et al.*, 2016 The Genetics of Leaf Flecking in Maize and Its Relationship to Plant Defense and Disease Resistance. Plant Physiol. 172: 1787–1803.

Olukolu, B. A., A. Negeri, R. Dhawan, B. P. Venkata, P. Sharma *et al.*, 2013 A connected set of genes associated with programmed cell death implicated in controlling the hypersensitive response in maize. Genetics 193: 609–620.

Olukolu, B. A., G.-F. Wang, V. Vontimitta, B. P. Venkata, S. Marla *et al.*, 2014 A genome-wide association study of the maize hypersensitive defense response identifies genes that cluster in related pathways. PLoS Genet. 10: 1–15.

Orr, H. A., 2005 The genetic theory of adaptation: A brief history. Nat. Rev. Genet. 6: 119–127.

Orr, H. A., 1998 The Population Genetics of Adaptation: The Distribution of Factors Fixed during Adaptive Evolution. Evolution (N. Y). 52: 935–949.

Penning, B. W., G. S. Johal, and M. D. Mcmullen, 2004 A major suppressor of cell death, slm1, modifies the expression of the maize (Zea mays L .) lesion mimic mutation les23. Genome 47: 961–969.

Peterson, P. A., 1953 A study of a mutable pale green locus in maize: University of Illinois. Ph.D. Dissertation.

Pribat, A., I. K. Blaby, A. Lara-Núñez, L. Jeanguenin, R. Fouquet *et al.*, 2011 A 5-

formyltetrahydrofolate cycloligase paralog from all domains of life: Comparative genomic and experimental evidence for a cryptic role in thiamin metabolism. Funct. Integr. Genomics 11: 467–478.

Robinson, J. T., H. Thorvaldsdóttir, W. Winckler, M. Guttman, E. S. Lander *et al.*, 2011 Integrative Genome Viewer. Nat. Biotechnol. 29: 24–6.

Romay, M. C., M. J. Millard, J. C. Glaubitz, J. a Peiffer, K. L. Swarts *et al.*, 2013 Comprehensive genotyping of the USA national maize inbred seed bank. Genome Biol. 14: R55.

Salvi, S., G. Sponza, M. Morgante, D. Tomes, X. Niu *et al.*, 2007 Conserved noncoding genomic sequences associated with a flowering-time quantitative trait locus in maize. Proc. Natl. Acad. Sci. U. S. A. 104: 11376–11381.

SanMiguel, P., and J. L. Bennetzen, 1998 Evidence that a Recent Increase in Maize Genome Size was Caused by the Massive Amplification of Intergene Retrotransposons. Ann. Bot. 82: 37–44.

SanMiguel, P., A. Tikhonov, Y.-K. Jin, N. Motchoulskaia, D. Zakharov *et al.*, 1996 Nested Retrotransposons in the Intergenic regions of the maize genome. Science. 274: 765–768.

Sawers, R. J. H., J. Viney, P. R. Farmer, R. R. Bussey, G. Olsefski *et al.*, 2006 The maize Oil yellow1 (Oy1) gene encodes the I subunit of magnesium chelatase. Plant Mol. Biol. 60: 95–106.

Schwartz, C., S. Balasubramanian, N. Warthmann, T. P. Michael, J. Lempe *et al.*, 2009 Cis-regulatory changes at Flowering Locus T mediate natural variation in flowering responses of Arabidopsis thaliana. Genetics 183: 723–732.

Sen, T. Z., L. C. Harper, M. L. Schaeffer, C. M. Andorf, T. E. Seigfried *et al.*, 2010 Choosing a genome browser for a Model Organism Database: surveying the Maize community. Database 2010: 1–9.

Springer, N. M., and R. M. Stupar, 2007 Allelic variation and heterosis in maize: how do two halves make more than a whole? Genome Res. 17: 264–75.

Studer, A., Q. Zhao, J. Ross-Ibarra, and J. Doebley, 2011 Identification of a functional transposon insertion in the maize domestication gene tb1. Nat. Genet. 43: 1160–1163.

Thimijan, R. W., and R. D. Heins, 1983 Photometric, radiometric, and quantum light units of measure: a review of procedures for interconversion. HortScience 18: 818–822.

Thompson, J. D., D. G. Higgins, and T. J. Gibson, 1994 ClustalW: improving the sensitivity of progressive multiple sequence alignment through sequence weighting, position specific gap penalties and weight matrix choice. Nucleic Acids Res. Acids Res 22: 4673–4680.

Vale, R. D., 2000 AAA proteins: Lords of the ring. J. Cell Biol. 150: 13–19.

Veitia, R. A., 2003 Nonlinear effects in macromolecular assembly and dosage sensitivity. J. Theor. Biol. 220: 19–25.

Waters, A. J., I. Makarevitch, J. Noshay, L. T. Burghardt, C. N. Hirsch *et al.*, 2017 Natural variation for gene expression responses to abiotic stress in maize. Plant J. 89: 706–717.

West, M. A. L., K. Kim, D. J. Kliebenstein, H. Van Leeuwen, R. W. Michelmore *et al.*, 2007 Global eQTL mapping reveals the complex genetic architecture of transcript-

level variation in Arabidopsis. Genetics 175: 1441–1450.

Wettstein, D. von, S. Gough, and C. G. Kannangara, 1995 Chlorophyll Biosynthesis. Plant Cell 7: 1039–1057.

Willing, M. C., S. P. Deschenes, R. L. Slayton, and E. J. Roberts, 1996 Premature chain termination is a unifying mechanism for COL1A1 null alleles in osteogenesis imperfecta type I cell strains. Am. J. Hum. Genet. 59: 799–809.

Wray, G. A., M. W. Hahn, E. Abouheif, J. P. Balhoff, M. Pizer *et al.*, 2003 The evolution of transcriptional regulation in eukaryotes. Mol. Biol. Evol. 20: 1377–1419.

Yang, M., E. Wardzala, G. S. Johal, and J. Gray, 2004 The wound-inducible Lls1 gene from maize is an orthologue of the Arabidopsis Acd1 gene, and the LLS1 protein is present in non-photosynthetic tissues. Plant Mol. Biol. 0: 1–17.

Yu, J., G. Pressoir, W. H. Briggs, I. Vroh Bi, M. Yamasaki *et al.*, 2006 A unified mixed-model method for association mapping that accounts for multiple levels of relatedness. Nat. Genet. 38: 203–8.

Zhang, Z., E. Ersoz, C.-Q. Lai, R. J. Todhunter, H. K. Tiwari *et al.*, 2010 Mixed linear model approach adapted for genome-wide association studies. Nat. Genet. 42: 355–60.

Tables

A *Very Oil Yellow1* modifier of the *Oil Yellow1-N1989* allele uncovers a cryptic phenotypic impact of cis-regulatory variation in maize

Rajdeep S. Khangura, Sandeep Marla, Bala P. Venkata, Nicholas J. Heller, Gurmukh S. Johal, Brian P. Dilkes

Table 1. The allele-specific expression at *oy1* in the top fully-expanded leaf at the V3 developmental stage of B73 x Mo17 F_1 wild-type and *Oy1-N1989/oy1* mutant siblings, and inbred *Oy1-N1989/oy1*:B73 mutants.

Genotype[1]	SNP_252	SNP_317	Ratio_SNP252	Ratio_SNP317	Average
oy1/*oy1*:B/M[&]	.	.	.	.	1.19±0.07
oy1/*oy1*:B/M	C/C	C/T	.	1.08±0.01[a]	1.08±0.01[a]
Oy1-N1989/*oy1*:M/B	C/T	C/T	1.12±0.01[a]	1.10±0.02[a]	1.11±0.01[a]
Oy1-N1989/*oy1*:B/M	C/T	C/T	1.15±0.03[a]	1.10±0.01[a]	1.13±0.02[a]
Oy1-N1989/*oy1*:B	C/T	C/C	1.01±0.02[b]	.	1.01±0.02[b]

[1]B73 is denoted as B, Mo17 is denoted as M, B/M denotes B73 x Mo17 cross direction and M/B is vice-versa. The mean ± standard deviation of the ratios of the read count from the reference/alternate allele at SNP_252, SNP_317, and the average of the ratios at SNP position 252 and 317. The connecting letter report for each trait indicates the statistical significance calculated using ANOVA with post-hoc analysis using Tukey's HSD with $p<0.01$.

[&]Data obtained from Waters et al. 2017.

Supplemental Tables

Table S1. The trait mean values of the CCM traits for the wild-type (WT) and mutant (MT) siblings of the F_1 hybrids of *Oy1-N1989*/*oy1*:B73 (pollen-parent) with respective IBM lines.

IBM_ID	WT_CCMI	MT_CCMI	Ratio_CCMI	Diff_CCMI	WT_CCMII	MT_CCMII	Ratio_CCMII	Diff_CCMII
M0001	45.3	6.3	0.139	39	49.6	17.5	0.353	32.1
M0003	35.5	8.3	0.234	27.2	37.3	16.2	0.434	21.1
M0007	46.8	4	0.085	42.8	54.8	5.8	0.106	49
M0008	47.4	10.3	0.217	37.1	51.9	16.1	0.31	35.8
M0010	48.2	11.4	0.237	36.8	42.9	18.6	0.434	24.3
M0013	33.7	8.7	0.258	25	47.7	16.3	0.342	31.4
M0014	54.6	3.5	0.064	51.1	47.3	5.1	0.108	42.2
M0016	52.3	3.2	0.061	49.1	43.9	6.2	0.141	37.7
M0017	54.3	9.3	0.171	45	67.9	21.4	0.315	46.5
M0018	34.3	8	0.233	26.3	51.2	18.2	0.355	33
M0019	36.9	8.4	0.228	28.5	40.9	14.5	0.355	26.4
M0021	50.1	3.6	0.072	46.5	65.4	5.4	0.083	60
M0022	46.3	8.6	0.186	37.7	45.7	15.8	0.346	29.9
M0023	47.9	3.1	0.065	44.8	55.2	3.8	0.069	51.4
M0024	47.1	8.6	0.183	38.5	50.3	19.2	0.382	31.1
M0025	49.6	3.6	0.073	46	57.9	6.9	0.119	51
M0028	35	4.3	0.123	30.7	52.5	5.5	0.105	47
M0029	47.8	11.8	0.247	36	41.9	19.6	0.468	22.3
M0031	41.9	3.2	0.076	38.7	54.9	5.2	0.095	49.7
M0032	57.9	4	0.069	53.9	52.3	7.1	0.136	45.2
M0033	46.5	12	0.258	34.5	52.9	19.5	0.369	33.4
M0036	39	3.3	0.085	35.7	54	4.6	0.085	49.4
M0039	52.6	4.1	0.078	48.5	52.4	5.7	0.109	46.7
M0040	42.2	11	0.261	31.2	62.9	22.5	0.358	40.4
M0042	53	10	0.189	43	47.4	18.6	0.392	28.8
M0044	42.8	2.8	0.065	40	52.7	4.4	0.083	48.3

IBM_ID	WT_CCMI	MT_CCMI	Ratio_CCMI	Diff_CCMI	WT_CCMII	MT_CCMII	Ratio_CCMII	Diff_CCMII
M0045	41.8	6.9	0.165	34.9	42.4	12.6	0.297	29.8
M0047	35.7	4	0.112	31.7	36.7	8.1	0.221	28.6
M0048	30.3	6.4	0.211	23.9	35.5	18.2	0.513	17.3
M0051	40.2	4	0.1	36.2	45.6	7.3	0.16	38.3
M0052	53.1	10.7	0.202	42.4	56.3	15.5	0.275	40.8
M0054	50.6	8.4	0.166	42.2	43.7	13.9	0.318	29.8
M0055	38.6	16.9	0.438	21.7	37.7	24.5	0.65	13.2
M0056	41.6	8.8	0.212	32.8	44.9	18	0.401	26.9
M0057	47.9	9.2	0.192	38.7	45.4	19.6	0.432	25.8
M0060	44.3	3.7	0.084	40.6	54.9	6	0.109	48.9
M0061	43.3	11.2	0.259	32.1	64.7	29.3	0.453	35.4
M0062	43	11.4	0.265	31.6	62	20.6	0.332	41.4
M0063	55.5	11.6	0.209	43.9	55.2	20.5	0.371	34.7
M0066	47.9	9.1	0.19	38.8	50.4	21.5	0.427	28.9
M0067	41.3	8.6	0.208	32.7	44.9	13.6	0.303	31.3
M0074	48.5	3.7	0.076	44.8	48.5	4.9	0.101	43.6
M0076	56	3.9	0.07	52.1	64	6.5	0.102	57.5
M0077	49.1	3.1	0.063	46	44	6.7	0.152	37.3
M0079	42.9	9.9	0.231	33	46.4	18.3	0.394	28.1
M0080	39.2	6.1	0.156	33.1	52.6	15.4	0.293	37.2
M0081	41	3.3	0.08	37.7	58.3	5.4	0.093	52.9
M0082	45.5	3.2	0.07	42.3	58	4.9	0.084	53.1
M0083	49.2	9.9	0.201	39.3	54.7	22.8	0.417	31.9
M0085	41.7	3.8	0.091	37.9	36.3	3.7	0.102	32.6
M0086	58.4	9.5	0.163	48.9	65.2	24.8	0.38	40.4
M0088	48.2	11.4	0.237	36.8	53.8	27	0.502	26.8
M0092	53.7	10.4	0.194	43.3	60.5	27.5	0.455	33
M0093	51.4	6.7	0.13	44.7	51.9	12.6	0.243	39.3

IBM_ID	WT_CCMI	MT_CCMI	Ratio_CCMI	Diff_CCMI	WT_CCMII	MT_CCMII	Ratio_CCMII	Diff_CCMII
M0097	48	4.9	0.102	43.1	56.9	7.4	0.13	49.5
M0098	49.5	7.4	0.149	42.1	64.9	17.5	0.27	47.4
M0099	59.8	3.1	0.052	56.7	55	6	0.109	49
M0101	41.8	8.4	0.201	33.4	50.1	22.7	0.453	27.4
M0106	44.1	5.5	0.125	38.6	51	16.8	0.329	34.2
M0109	43.1	7.3	0.169	35.8	52.9	18.4	0.348	34.5
M0110	43.9	4	0.091	39.9	46.5	7.1	0.153	39.4
M0113	53.8	10.1	0.188	43.7	59.4	24.5	0.412	34.9
M0114	36.3	7.4	0.204	28.9	52.3	20.8	0.398	31.5
M0116	46.6	8.7	0.187	37.9	50.2	16.5	0.329	33.7
M0118	43.2	10.1	0.234	33.1	39.8	18.7	0.47	21.1
M0119	42.7	4.3	0.101	38.4	46.5	6.4	0.138	40.1
M0121	51.8	10	0.193	41.8	43.7	19.5	0.446	24.2
M0124	35.8	8	0.223	27.8	39.4	18	0.457	21.4
M0125	39.6	10.6	0.268	29	40.1	16	0.399	24.1
M0127	57.4	7	0.122	50.4	49.6	24.1	0.486	25.5
M0129	49.4	3.6	0.073	45.8	41.5	6	0.145	35.5
M0130	45.7	8.1	0.177	37.6	51.5	23.3	0.452	28.2
M0131	39.5	10	0.253	29.5	62.2	26	0.418	36.2
M0133	43.2	2.8	0.065	40.4	56.3	4.7	0.083	51.6
M0134	43.2	6.3	0.146	36.9	42.9	11.2	0.261	31.7
M0138	50.3	9.8	0.195	40.5	47.9	24.7	0.516	23.2
M0141	37.5	2	0.053	35.5	41.8	3.7	0.089	38.1
M0142	45.3	8.4	0.185	36.9	62.3	15.5	0.249	46.8
M0146	48.8	9.8	0.201	39	52.3	15.9	0.304	36.4
M0147	44.8	3.5	0.078	41.3	46.3	6.7	0.145	39.6
M0153	52.1	9.7	0.186	42.4	47.3	14.5	0.307	32.8
M0154	49	3.3	0.067	45.7	55.6	6	0.108	49.6

IBM_ID	WT_CCMI	MT_CCMI	Ratio_CCMI	Diff_CCMI	WT_CCMII	MT_CCMII	Ratio_CCMII	Diff_CCMII
M0156	51.4	10.3	0.2	41.1	74.1	16	0.216	58.1
M0157	49.4	9.7	0.196	39.7	61.3	20.7	0.338	40.6
M0159	47	10.2	0.217	36.8	50	12.3	0.246	37.7
M0160	36.3	4.2	0.116	32.1	57	7.5	0.132	49.5
M0161	44.8	3.3	0.074	41.5	53.9	7.4	0.137	46.5
M0162	54	3.8	0.07	50.2	56.7	5.6	0.099	51.1
M0165	51.3	3.2	0.062	48.1	51	6	0.118	45
M0168	46.4	4.1	0.088	42.3	45.9	8.4	0.183	37.5
M0169	44.8	11.7	0.261	33.1	49.1	21	0.428	28.1
M0170	43.1	8.1	0.188	35	46.1	25	0.542	21.1
M0171	45.9	8.5	0.185	37.4	48.7	26.7	0.548	22
M0174	54	3.5	0.065	50.5	60.9	8.7	0.143	52.2
M0176	30.1	3.5	0.116	26.6	49.1	5.1	0.104	44
M0177	40.6	3.5	0.086	37.1	53.1	5.2	0.098	47.9
M0178	45.9	8.8	0.192	37.1	55.1	23.4	0.425	31.7
M0180	45	8.1	0.18	36.9	52.5	17.9	0.341	34.6
M0181	38.7	8.3	0.214	30.4	72.7	17	0.234	55.7
M0182	37.1	3.5	0.094	33.6	48.6	7	0.144	41.6
M0183	42	7.5	0.179	34.5	44.3	16.5	0.372	27.8
M0184	55	4.7	0.085	50.3	56.4	8.6	0.152	47.8
M0185	35.7	6.6	0.185	29.1	38.6	12	0.311	26.6
M0186	25	2.5	0.1	22.5	51.7	3.8	0.074	47.9
M0189	50.1	13	0.259	37.1	50.8	17.3	0.341	33.5
M0191	50.2	3.8	0.076	46.4	55.4	6	0.108	49.4
M0192	42.5	2.6	0.061	39.9	46.2	3.9	0.084	42.3
M0194	48.2	12.4	0.257	35.8	51.8	17.8	0.344	34
M0195	43	8.6	0.2	34.4	43.5	18.3	0.421	25.2
M0196	46.1	10.5	0.228	35.6	62.5	26.3	0.421	36.2

IBM_ID	WT_CCMI	MT_CCMI	Ratio_CCMI	Diff_CCMI	WT_CCMII	MT_CCMII	Ratio_CCMII	Diff_CCMII
M0197	52.8	8.3	0.157	44.5	60.5	22.2	0.367	38.3
M0198	55.4	8.9	0.161	46.5	65.5	21.9	0.334	43.6
M0199	49.7	9.2	0.185	40.5	50.4	21.4	0.425	29
M0200	41.4	9.1	0.22	32.3	45.4	19.1	0.421	26.3
M0201	40.6	3.4	0.084	37.2	40.1	5.7	0.142	34.4
M0204	35.9	3.8	0.106	32.1	38.9	5.9	0.152	33
M0205	39.4	5.7	0.145	33.7	41.8	13.6	0.325	28.2
M0206	53.2	9.7	0.182	43.5	45.3	18	0.397	27.3
M0208	54.7	10.1	0.185	44.6	53.2	18.6	0.35	34.6
M0209	54.7	10.9	0.199	43.8	52.2	18.8	0.36	33.4
M0214	51.1	9.5	0.186	41.6	59.8	19.8	0.331	40
M0215	45	4	0.089	41	60.2	6.2	0.103	54
M0216	42.2	10.3	0.244	31.9	51.4	23	0.447	28.4
M0218	52.1	3.3	0.063	48.8	56.1	5.4	0.096	50.7
M0219	43.4	10.2	0.235	33.2	53.5	14.1	0.264	39.4
M0220	42.7	8.3	0.194	34.4	51.1	18.2	0.356	32.9
M0222	49	11.2	0.229	37.8	42.6	21.9	0.514	20.7
M0223	47.7	7.7	0.161	40	67	18.4	0.275	48.6
M0224	50	8.7	0.174	41.3	58.5	28.6	0.489	29.9
M0225	44.2	3.6	0.081	40.6	45.1	5.5	0.122	39.6
M0228	36.6	9.9	0.27	26.7	38.8	15.5	0.399	23.3
M0229	45.7	10.9	0.239	34.8	45.9	20.1	0.438	25.8
M0232	42.6	9.9	0.232	32.7	45.4	17.5	0.385	27.9
M0233	39.9	6.7	0.168	33.2	48.6	15.1	0.311	33.5
M0237	59.3	3.5	0.059	55.8	47	6.6	0.14	40.4
M0240	57.3	3.2	0.056	54.1	57.6	6.7	0.116	50.9
M0241	42.7	8.9	0.208	33.8	49	15.3	0.312	33.7
M0244	54.6	4.1	0.075	50.5	51.8	5.3	0.102	46.5

IBM_ID	WT_CCMI	MT_CCMI	Ratio_CCMI	Diff_CCMI	WT_CCMII	MT_CCMII	Ratio_CCMII	Diff_CCMII
M0248	44.3	10.6	0.239	33.7	66.4	22.3	0.336	44.1
M0250	44.3	3	0.068	41.3	61.5	3.8	0.062	57.7
M0253	47.3	2.9	0.061	44.4	41.5	4.6	0.111	36.9
M0255	39.9	3.1	0.078	36.8	44.8	4.8	0.107	40
M0256	48.8	3.2	0.066	45.6	57.7	5.4	0.094	52.3
M0258	41.9	6.6	0.158	35.3	54.2	24.8	0.458	29.4
M0262	48.8	3.7	0.076	45.1	56	5	0.089	51
M0263	40.9	3.2	0.078	37.7	63.2	4.5	0.071	58.7
M0264	50.2	3.7	0.074	46.5	50.7	5.5	0.108	45.2
M0265	43.1	7.4	0.172	35.7	56.8	15.5	0.273	41.3
M0266	44.1	9	0.204	35.1	52.2	17.5	0.335	34.7
M0267	47.9	7.6	0.159	40.3	45.7	13.7	0.3	32
M0269	44	8.6	0.195	35.4	50.1	18.6	0.371	31.5
M0270	66.2	12.3	0.186	53.9	56.5	23.6	0.418	32.9
M0271	47.4	12.7	0.268	34.7	51.4	21.8	0.424	29.6
M0272	43.6	4	0.092	39.6	55.5	4.8	0.086	50.7
M0274	43.1	8.9	0.206	34.2	46.5	23.5	0.505	23
M0275	52.9	5.9	0.112	47	47.1	13.7	0.291	33.4
M0276	50.6	7	0.138	43.6	57.2	14.6	0.255	42.6
M0277	47.4	9.1	0.192	38.3	52.3	27.8	0.532	24.5
M0279	38.8	3.5	0.09	35.3	40	6.1	0.153	33.9
M0280	43.6	9	0.206	34.6	36.2	15.8	0.436	20.4
M0282	44.8	3.2	0.071	41.6	42.6	5.9	0.138	36.7
M0286	61.7	3.1	0.05	58.6	48.4	5.1	0.105	43.3
M0287	47.4	3.4	0.072	44	46.2	5.5	0.119	40.7
M0292	46.6	3.7	0.079	42.9	42	6.2	0.148	35.8
M0295	53.5	9.1	0.17	44.4	51	18.1	0.355	32.9
M0296	56.7	3.2	0.056	53.5	58	7.2	0.124	50.8

IBM_ID	WT_CCMI	MT_CCMI	Ratio_CCMI	Diff_CCMI	WT_CCMII	MT_CCMII	Ratio_CCMII	Diff_CCMII
M0297	44.9	8.8	0.196	36.1	53.7	13.8	0.257	39.9
M0298	50.3	8.4	0.167	41.9	48.5	22.4	0.462	26.1
M0300	43.5	6	0.138	37.5	46.7	19.8	0.424	26.9
M0301	45.6	8.4	0.184	37.2	45.4	17.2	0.379	28.2
M0304	45.7	3.5	0.077	42.2	53.8	5.4	0.1	48.4
M0305	43.3	6.9	0.159	36.4	42.3	17.7	0.418	24.6
M0307	27.9	2.9	0.104	25	40.2	3.4	0.085	36.8
M0311	37.9	8.1	0.214	29.8	52.3	18.6	0.356	33.7
M0313	43.3	3.4	0.079	39.9	50.7	5.6	0.11	45.1
M0314	39	9.5	0.244	29.5	42	18.4	0.438	23.6
M0318	44.3	3.9	0.088	40.4	56.9	6.2	0.109	50.7
M0321	59.3	3.4	0.057	55.9	55.1	4.6	0.083	50.5
M0322	41.7	8.2	0.197	33.5	38.9	18.5	0.476	20.4
M0325	44.8	7.2	0.161	37.6	58	19	0.328	39
M0326	58.5	4.1	0.07	54.4	56.1	8.5	0.152	47.6
M0328	45.4	3	0.066	42.4	48.7	4.5	0.092	44.2
M0331	44.4	6.2	0.14	38.2	49.3	11.2	0.227	38.1
M0334	50.7	8.8	0.174	41.9	60.3	18.5	0.307	41.8
M0335	36.2	6.5	0.18	29.7	44.4	11.5	0.259	32.9
M0337	46.7	10.7	0.229	36	48.4	25.2	0.521	23.2
M0340	49	10	0.204	39	54.6	22.4	0.41	32.2
M0341	45.3	3.2	0.071	42.1	48.6	4.1	0.084	44.5
M0344	51.7	3.8	0.074	47.9	45.6	5.8	0.127	39.8
M0345	42.7	9.3	0.218	33.4	49	16.2	0.331	32.8
M0346	46.2	10.1	0.219	36.1	48.4	19.8	0.409	28.6
M0347	53.5	4.2	0.079	49.3	60.1	8.8	0.146	51.3
M0349	52.8	4.3	0.081	48.5	59.2	6.9	0.117	52.3
M0351	34.4	7.3	0.212	27.1	59.8	25.5	0.426	34.3

IBM_ID	WT_CCMI	MT_CCMI	Ratio_CCMI	Diff_CCMI	WT_CCMII	MT_CCMII	Ratio_CCMII	Diff_CCMII
M0352	40.9	11.5	0.281	29.4	52.3	24.1	0.461	28.2
M0353	52.9	10.1	0.191	42.8	60.1	23.4	0.389	36.7
M0354	45.4	3.4	0.075	42	56.2	5.6	0.1	50.6
M0355	48.4	9.5	0.196	38.9	58.5	20.1	0.344	38.4
M0356	49.7	4.5	0.091	45.2	59.7	7	0.117	52.7
M0357	53.4	10.6	0.199	42.8	46.2	18	0.39	28.2
M0358	44.5	7.2	0.162	37.3	50.4	17.2	0.341	33.2
M0360	39.1	11.4	0.292	27.7	52.3	18.9	0.361	33.4
M0361	29.7	3.5	0.118	26.2	41.8	4.9	0.117	36.9
M0362	36.8	8.9	0.242	27.9	56.4	15.1	0.268	41.3
M0364	46.2	11.4	0.247	34.8	60.2	17.8	0.296	42.4
M0368	51.1	6.9	0.135	44.2	55.3	19.8	0.358	35.5
M0369	48.7	10.2	0.209	38.5	49.4	17.3	0.35	32.1
M0372	44.3	3.7	0.084	40.6	42.7	6.3	0.148	36.4
M0373	49.4	3.6	0.073	45.8	59.2	4.9	0.083	54.3
M0378	53.4	7.4	0.139	46	64.5	16.2	0.251	48.3
M0379	42.6	3	0.07	39.6	52.7	3.8	0.072	48.9
M0380	49.7	12.2	0.245	37.5	70.3	30.4	0.432	39.9
M0381	40	9.5	0.238	30.5	43.6	28.9	0.663	14.7
M0382	48.7	8.6	0.177	40.1	57.2	20.6	0.36	36.6
M0383	55.7	2.7	0.048	53	50.1	4.9	0.098	45.2
M0384	27.3	2.5	0.092	24.8	46.8	4.2	0.09	42.6

Table S2. The trait mean values of the CCM traits for the wild-type (WT) and mutant (MT) siblings of F_1 hybrids of *Oy1-N1989*/*oy1*:B73 (pollen-parent) with respective Syn10 line.

Syn10_ID	Liu et.al-ID	WT_CCMI	MT_CCMI	Ratio_CCMI	Diff_CCMI	WT_CCMII	MT_CCMII	Ratio_CCMII	Diff_CCMII
M0001	IBM_1	61.60	2.48	0.04	59.12	88.70	6.48	0.07	82.22
M0002	IBM_2	63.63	6.95	0.11	56.68	63.52	31.85	0.50	31.67
M0009	IBM_5	43.13	7.93	0.19	35.20	77.85	28.33	0.38	49.52
M0010	IBM_6	62.70	3.02	0.05	59.68	78.75	8.97	0.11	69.78
M0011	IBM_7	41.67	6.12	0.15	35.55	70.70	25.72	0.37	44.98
M0012	IBM_8	51.43	7.13	0.14	44.30	67.83	30.13	0.45	37.70
M0015	IBM_9	43.57	6.50	0.15	37.07	64.53	25.20	0.39	39.33
M0019	IBM_11	53.63	1.87	0.04	51.77	77.97	5.27	0.07	72.70
M0020	IBM_12	56.82	2.03	0.04	54.78	73.58	6.05	0.08	67.53
M0023	IBM_13	55.87	7.20	0.13	48.67	75.42	27.42	0.36	48.00
M0024	IBM_14	47.42	8.05	0.17	39.37	63.79	29.90	0.47	33.89
M0025	IBM_15	51.28	9.50	0.19	41.78	69.18	25.88	0.37	43.30
M0027	IBM_16	42.02	2.10	0.05	39.92	70.55	6.00	0.09	64.55
M0029	IBM_17	55.58	6.52	0.12	49.07	63.40	25.62	0.40	37.78
M0030	IBM_18	54.60	5.95	0.11	48.65	69.72	22.88	0.33	46.83
M0032	IBM_19	54.28	7.90	0.15	46.38	68.08	33.97	0.51	34.12
M0034	IBM_20	58.70	6.80	0.12	51.90	78.75	33.10	0.42	45.65
M0036	IBM_21	56.42	2.27	0.04	54.15	89.33	8.30	0.09	81.03
M0038	IBM_22	51.83	10.80	0.23	41.03	64.40	34.07	0.53	30.33
M0041	IBM_23	50.20	4.72	0.10	45.48	57.35	25.40	0.44	31.95
M0042	IBM_24	47.48	6.48	0.14	41.00	73.33	34.02	0.47	39.32
M0043	IBM_25	46.65	7.57	0.16	39.08	67.40	30.68	0.46	36.72
M0047	IBM_26	53.45	2.75	0.05	50.70	59.08	6.85	0.12	52.23
M0049	IBM_27	41.42	2.40	0.06	39.02	72.32	7.62	0.11	64.70
M0050	IBM_28	56.25	8.95	0.16	47.30	75.12	33.12	0.44	42.00
M0053	IBM_30	47.47	7.65	0.16	39.82	76.62	30.73	0.40	45.88

Syn10_ID	Liu et.al-ID	WT_CCMI	MT_CCMI	Ratio_CCMI	Diff_CCMI	WT_CCMII	MT_CCMII	Ratio_CCMII	Diff_CCMII
M0054	IBM_31	52.93	6.98	0.13	45.95	72.35	33.18	0.46	39.17
M0055	IBM_32	57.95	2.75	0.05	55.20	74.55	6.08	0.08	68.47
M0056	IBM_33	54.38	5.38	0.10	49.00	73.98	26.03	0.36	47.95
M0057	IBM_34	43.82	6.00	0.14	37.82	70.92	26.43	0.37	44.48
M0061	IBM_35	45.27	1.57	0.03	43.70	64.03	4.67	0.07	59.37
M0062	IBM_36	56.05	5.82	0.10	50.23	73.72	21.98	0.30	51.73
M0068	IBM_39	56.32	1.72	0.03	54.60	70.68	5.55	0.08	65.13
M0069	IBM_40	48.58	13.27	0.27	35.32	74.30	32.48	0.44	41.82
M0070	IBM_41	48.43	2.30	0.05	46.13	73.15	6.97	0.10	66.18
M0074	IBM_42	53.02	1.82	0.04	51.20	76.63	6.42	0.08	70.22
M0076	IBM_43	46.47	2.58	0.06	43.88	74.67	7.85	0.11	66.82
M0078	IBM_44	57.53	6.85	0.12	50.68	74.27	27.07	0.36	47.20
M0084	IBM_48	52.07	1.75	0.03	50.32	80.42	4.33	0.05	76.08
M0090	IBM_49	49.07	7.13	0.15	41.93	67.05	30.32	0.45	36.73
M0091	IBM_50	38.28	7.72	0.20	30.57	72.65	31.47	0.44	41.18
M0092	IBM_51	48.08	8.28	0.18	39.80	66.43	45.65	0.69	20.78
M0093	IBM_52	55.40	7.07	0.13	48.33	68.63	32.85	0.48	35.78
M0095	IBM_53	53.27	6.13	0.11	47.13	70.05	27.83	0.40	42.22
M0105	IBM_55	60.37	6.47	0.11	53.90	61.80	33.78	0.55	28.02
M0108	IBM_56	40.58	7.47	0.19	33.12	64.13	29.22	0.47	34.92
M0109	IBM_57	50.32	5.77	0.12	44.55	62.47	25.20	0.40	37.27
M0111	IBM_59	45.63	7.33	0.16	38.30	82.28	31.27	0.38	51.02
M0116	IBM_62	48.72	6.35	0.13	42.37	72.90	25.85	0.35	47.05
M0118	IBM_63	52.32	7.85	0.15	44.47	63.05	31.90	0.51	31.15
M0119	IBM_64	50.62	6.68	0.13	43.93	70.95	30.12	0.43	40.83
M0120	IBM_65	49.90	6.75	0.14	43.15	69.55	33.57	0.49	35.98
M0126	IBM_67	47.63	5.70	0.12	41.93	70.72	32.02	0.45	38.70
M0130	IBM_69	51.00	.	.	.	71.08	.	.	.

Syn10_ID	Liu et.al-ID	WT_CCMI	MT_CCMI	Ratio_CCMI	Diff_CCMI	WT_CCMII	MT_CCMII	Ratio_CCMII	Diff_CCMII
M0136	IBM_70	49.98	6.73	0.14	43.25	74.30	28.55	0.38	45.75
M0317	IBM_151	52.90	8.10	0.16	44.80	79.77	28.58	0.36	51.18
M0316	IBM_150	47.23	5.35	0.11	41.88	71.78	25.22	0.35	46.57
M0315	IBM_149	60.88	1.65	0.03	59.23	65.95	5.67	0.09	60.28
M0312	IBM_147	48.80	7.48	0.15	41.32	70.07	23.83	0.34	46.23
M0305	IBM_144	50.60	1.68	0.03	48.92	76.28	5.60	0.07	70.68
M0298	IBM_142	44.60	6.25	0.14	38.35	70.28	28.63	0.41	41.65
M0296	IBM_141	47.62	7.18	0.15	40.43	69.92	25.70	0.37	44.22
M0295	IBM_140	57.23	9.92	0.17	47.32	75.47	31.70	0.42	43.77
M0293	IBM_139	50.68	2.38	0.05	48.30	69.17	7.75	0.11	61.42
M0290	IBM_138	46.50	8.70	0.19	37.80	64.85	28.65	0.44	36.20
M0285	IBM_136	47.28	5.52	0.12	41.77	70.60	26.97	0.38	43.63
M0272	IBM_134	53.27	6.82	0.13	46.45	63.68	29.03	0.45	34.65
M0267	IBM_133	45.87	8.60	0.19	37.27	71.52	31.93	0.44	39.58
M0266	IBM_132	55.32	2.10	0.04	53.22	73.52	4.48	0.06	69.03
M0264	IBM_131	56.15	6.17	0.11	49.98	75.85	29.72	0.40	46.13
M0262	IBM_130	47.27	6.37	0.13	40.90	69.78	35.73	0.52	34.05
M0258	IBM_127	47.32	6.10	0.13	41.22	63.32	22.58	0.36	40.73
M0256	IBM_126	44.07	5.60	0.13	38.47	68.58	23.98	0.35	44.60
M0253	IBM_125	48.80	6.07	0.12	42.73	71.77	21.50	0.30	50.27
M0252	IBM_124	36.88	6.03	0.16	30.85	70.33	33.90	0.48	36.43
M0250	IBM_123	51.53	2.27	0.04	49.27	75.92	6.67	0.09	69.25
M0249	IBM_122	44.30	1.87	0.04	42.43	60.27	4.72	0.08	55.55
M0245	IBM_121	51.08	8.55	0.17	42.53	70.38	32.10	0.46	38.28
M0243	IBM_119	44.28	7.90	0.18	36.38	73.25	33.73	0.46	39.52
M0240	IBM_117	36.15	2.02	0.06	34.13	76.32	6.57	0.09	69.75
M0237	IBM_115	44.67	6.83	0.16	37.83	67.78	28.33	0.42	39.45
M0234	IBM_114	48.87	8.12	0.17	40.75	75.62	24.95	0.33	50.67

Syn10_ID	Liu et.al-ID	WT_CCMI	MT_CCMI	Ratio_CCMI	Diff_CCMI	WT_CCMII	MT_CCMII	Ratio_CCMII	Diff_CCMII
M0231	IBM_113	54.68	2.88	0.05	51.80	83.48	6.00	0.07	77.48
M0230	IBM_112	52.75	6.33	0.12	46.42	74.83	28.87	0.39	45.97
M0227	IBM_111	43.10	1.85	0.04	41.25	70.48	5.58	0.08	64.90
M0223	IBM_110	41.03	2.33	0.06	38.70	68.05	7.30	0.11	60.75
M0221	IBM_109	49.03	7.90	0.16	41.13	66.18	26.78	0.40	39.40
M0218	IBM_108	43.58	7.63	0.18	35.95	64.90	35.08	0.54	29.82
M0217	IBM_107	48.13	9.65	0.20	38.48	71.27	30.12	0.42	41.15
M0215	IBM_106	47.88	9.38	0.20	38.50	60.53	35.68	0.60	24.85
M0212	IBM_104	54.03	8.73	0.16	45.30	78.37	33.65	0.43	44.72
M0210	IBM_103	43.23	5.53	0.13	37.70	68.23	26.13	0.38	42.10
M0209	IBM_102	57.28	7.55	0.13	49.73	73.48	37.03	0.50	36.45
M0208	IBM_101	56.32	7.42	0.13	48.90	66.25	28.10	0.42	38.15
M0206	IBM_100	47.27	6.17	0.13	41.10	70.88	26.03	0.37	44.85
M0202	IBM_98	51.02	2.15	0.04	48.87	72.88	7.50	0.10	65.38
M0198	IBM_97	51.87	5.98	0.12	45.88	77.87	35.22	0.45	42.65
M0196	IBM_96	50.05	10.48	0.23	39.57	67.02	39.60	0.59	27.42
M0195	IBM_95	70.67	8.12	0.12	62.55	85.57	26.82	0.31	58.75
M0193	IBM_94	44.08	6.98	0.16	37.09	66.80	31.60	0.47	35.20
M0189	IBM_93	64.22	8.82	0.14	55.40	75.55	29.77	0.39	45.78
M0188	IBM_92	45.37	8.08	0.19	37.28	69.07	22.22	0.32	46.85
M0184	IBM_91	57.68	7.43	0.13	50.25	69.73	36.22	0.52	33.52
M0179	IBM_90	51.85	9.25	0.18	42.60	80.60	34.78	0.43	45.82
M0178	IBM_89	46.08	6.40	0.14	39.68	78.50	36.05	0.46	42.45
M0175	IBM_87	53.80	7.90	0.15	45.90	79.70	40.65	0.51	39.05
M0173	IBM_86	50.12	5.15	0.10	44.97	64.60	28.38	0.44	36.22
M0172	IBM_85	40.22	3.00	0.08	37.22	68.17	6.92	0.10	61.25
M0171	IBM_84	53.13	2.63	0.05	50.50	72.98	7.03	0.10	65.95
M0169	IBM_83	49.82	2.08	0.04	47.73	67.88	7.08	0.10	60.80

Syn10_ID	Liu et.al-ID	WT_CCMI	MT_CCMI	Ratio_CCMI	Diff_CCMI	WT_CCMII	MT_CCMII	Ratio_CCMII	Diff_CCMII
M0166	IBM_81	53.28	5.27	0.10	48.02	82.12	24.98	0.30	57.13
M0162	IBM_79	46.07	8.60	0.19	37.47	57.95	26.57	0.46	31.38
M0159	IBM_78	41.42	2.03	0.05	39.38	67.48	5.05	0.07	62.43
M0156	IBM_76	35.48	2.27	0.06	33.22	59.70	7.23	0.12	52.48
M0155	IBM_75	52.38	6.88	0.13	45.50	71.03	34.25	0.49	36.78
M0152	IBM_74	39.67	2.00	0.05	37.67	69.10	4.42	0.06	64.68
M0145	IBM_72	52.87	2.17	0.04	50.70	67.30	7.12	0.11	60.18
M0138	IBM_71	60.95	8.98	0.15	51.97	72.48	37.67	0.52	34.82
M0319	IBM_152	47.40	7.65	0.16	39.75	71.78	31.78	0.45	40.00
M0324	IBM_154	44.90	7.67	0.18	37.23	76.93	30.53	0.40	46.40
M0328	IBM_155	40.57	2.50	0.06	38.07	68.15	6.97	0.10	61.18
M0330	IBM_156	51.43	2.80	0.06	48.63	66.87	9.32	0.14	57.55
M0332	IBM_157	55.77	7.72	0.14	48.05	74.23	34.78	0.47	39.45
M0335	IBM_158	45.13	6.30	0.14	38.83	66.22	29.42	0.44	36.80
M0336	IBM_159	54.95	5.62	0.10	49.33	66.20	24.33	0.36	41.87
M0340	IBM_160	50.07	6.42	0.13	43.65	70.92	32.45	0.46	38.47
M0341	IBM_161	45.77	5.88	0.13	39.88	66.17	29.02	0.44	37.15
M0345	IBM_163	39.53	2.00	0.05	37.53	66.82	5.43	0.08	61.38
M0347	IBM_165	47.03	6.58	0.14	40.45	78.90	26.65	0.34	52.25
M0349	IBM_166	48.20	7.65	0.16	40.55	80.10	33.42	0.42	46.68
M0356	IBM_167	51.57	1.57	0.03	50.00	75.72	5.28	0.07	70.43
M0357	IBM_168	44.47	5.68	0.13	38.78	69.68	23.17	0.33	46.52
M0358	IBM_169	67.85	5.88	0.09	61.97	82.13	34.42	0.42	47.72
M0366	IBM_170	55.93	2.47	0.04	53.47	73.63	6.35	0.09	67.28
M0372	IBM_171	51.37	9.13	0.18	42.23	77.35	34.88	0.45	42.47
M0373	IBM_172	37.92	1.78	0.05	36.13	72.35	4.80	0.07	67.55
M0374	IBM_173	41.17	1.80	0.05	39.37	66.05	5.58	0.09	60.47
M0375	IBM_174	46.17	6.23	0.14	39.93	67.58	29.42	0.44	38.16

Syn10_ID	Liu et.al-ID	WT_CCMI	MT_CCMI	Ratio_CCMI	Diff_CCMI	WT_CCMII	MT_CCMII	Ratio_CCMII	Diff_CCMII
M0376	IBM_175	58.53	2.32	0.04	56.22	74.37	8.18	0.11	66.18
M0381	IBM_178	50.28	2.27	0.04	48.02	57.35	6.95	0.12	50.40
M0382	IBM_179	52.32	4.85	0.09	47.47	77.27	21.68	0.29	55.58
M0385	IBM_180	34.77	5.25	0.15	29.52	71.38	24.52	0.34	46.87
M0388	IBM_181	60.67	6.83	0.11	53.83	71.70	26.62	0.37	45.08
M0389	IBM_182	48.78	7.87	0.16	40.92	70.38	29.97	0.43	40.42
M0390	IBM_183	39.53	1.70	0.04	37.83	72.97	5.02	0.07	67.95
M0391	IBM_184	52.42	2.32	0.05	50.10	79.38	6.62	0.08	72.77
M0396	IBM_185	51.53	6.05	0.12	45.48	79.13	33.27	0.42	45.87
M0401	IBM_187	60.02	7.20	0.12	52.82	71.75	32.05	0.45	39.70
M0404	IBM_188	53.32	1.77	0.03	51.55	75.68	5.95	0.08	69.73
M0405	IBM_189	53.60	1.93	0.04	51.67	70.52	6.07	0.09	64.45
M0407	IBM_190	47.50	7.75	0.17	39.75	77.98	30.65	0.39	47.33
M0412	IBM_191	37.87	7.05	0.19	30.82	74.98	30.13	0.40	44.85
M0414	IBM_192	42.75	6.57	0.16	36.18	68.87	27.23	0.39	41.63
M0422	IBM_194	47.47	1.82	0.04	45.65	77.98	7.70	0.10	70.28
M0424	IBM_195	45.82	4.88	0.11	40.93	67.33	23.18	0.35	44.15
M0427	IBM_196	47.42	8.50	0.18	38.92	77.37	39.40	0.51	37.97
M0428	IBM_197	49.53	8.77	0.18	40.77	74.85	30.78	0.41	44.07
M0429	IBM_198	51.37	6.95	0.14	44.42	74.28	29.80	0.40	44.48
M0430	IBM_199	42.72	8.85	0.20	33.87	74.15	30.12	0.41	44.03
M0431	IBM_200	46.80	1.98	0.04	44.82	77.30	6.02	0.08	71.28
M0433	IBM_201	57.42	8.47	0.15	48.95	79.95	32.02	0.40	47.93
M0434	IBM_202	48.87	6.88	0.14	41.98	68.75	28.70	0.42	40.05
M0436	IBM_203	39.53	5.48	0.14	34.05	68.33	25.87	0.38	42.47
M0438	IBM_204	52.88	9.07	0.17	43.82	69.20	33.87	0.49	35.33
M0443	IBM_206	58.77	1.98	0.03	56.78	72.68	5.62	0.08	67.07
M0444	IBM_207	44.07	5.62	0.13	38.45	68.47	26.90	0.40	41.57

Syn10_ID	Liu et.al-ID	WT_CCMI	MT_CCMI	Ratio_CCMI	Diff_CCMI	WT_CCMII	MT_CCMII	Ratio_CCMII	Diff_CCMII
M0448	IBM_209	59.33	8.03	0.14	51.30	67.35	26.55	0.39	40.80
M0450	IBM_211	47.35	1.60	0.03	45.75	71.05	5.78	0.08	65.27
M0453	IBM_212	55.88	7.80	0.14	48.08	70.57	32.80	0.46	37.77
M0454	IBM_213	50.42	6.72	0.13	43.70	79.88	28.43	0.36	51.45
M0457	IBM_214	53.98	1.77	0.03	52.22	73.25	5.48	0.07	67.77
M0461	IBM_215	43.08	6.00	0.14	37.08	61.73	31.33	0.51	30.40
M0463	IBM_216	63.50	8.72	0.14	54.78	75.70	43.48	0.57	32.22
M0465	IBM_217	56.58	2.38	0.04	54.20	71.60	7.30	0.10	64.30
M0466	IBM_218	49.73	7.50	0.15	42.23	74.17	35.80	0.49	38.37
M0469	IBM_219	55.50	7.00	0.13	48.50	76.85	38.10	0.50	38.75
M0471	IBM_220	48.37	1.82	0.04	46.55	68.92	4.25	0.06	64.67
M0472	IBM_221	58.10	7.40	0.13	50.70	86.20	29.22	0.34	56.98
M0474	IBM_222	52.17	7.60	0.15	44.57	80.38	32.75	0.42	47.63
M0476	IBM_223	50.08	2.15	0.04	47.93	73.85	7.72	0.10	66.13
M0477	IBM_224	44.30	1.88	0.04	42.42	74.03	6.10	0.08	67.93
M0479	IBM_225	46.82	2.08	0.04	44.73	67.73	6.63	0.10	61.10
M0481	IBM_226	57.62	6.23	0.11	51.38	78.85	34.83	0.46	44.02
M0487	IBM_229	58.18	9.67	0.17	48.52	70.98	34.77	0.49	36.22
M0489	IBM_231	51.77	2.52	0.05	49.25	79.43	7.58	0.10	71.85
M0491	IBM_233	50.05	5.70	0.11	44.35	77.30	27.10	0.37	50.20
M0492	IBM_234	59.90	6.88	0.11	53.02	78.62	24.15	0.30	54.47
M0494	IBM_236	54.70	7.95	0.15	46.75	66.37	26.23	0.40	40.13
M0630	IBM_321	46.58	2.05	0.04	44.53	63.67	6.13	0.10	57.53
M0624	IBM_318	52.67	7.05	0.15	45.62	73.20	37.15	0.51	36.05
M0623	IBM_317	49.22	6.38	0.13	42.83	72.95	22.20	0.30	50.75
M0619	IBM_316	55.02	2.72	0.05	52.30	67.22	7.10	0.11	60.12
M0618	IBM_315	49.95	5.50	0.11	44.45	73.27	24.63	0.33	48.63
M0617	IBM_314	51.43	8.30	0.16	43.13	76.12	37.12	0.49	39.00

Syn10_ID	Liu et.al-ID	WT_CCMI	MT_CCMI	Ratio_CCMI	Diff_CCMI	WT_CCMII	MT_CCMII	Ratio_CCMII	Diff_CCMII
M0614	IBM_313	53.55	7.52	0.14	46.03	78.38	30.65	0.39	47.73
M0613	IBM_312	43.05	5.87	0.14	37.18	72.65	28.18	0.39	44.47
M0611	IBM_311	52.82	7.92	0.15	44.90	67.73	23.88	0.35	43.85
M0609	IBM_310	49.28	1.78	0.04	47.50	76.05	5.13	0.07	70.92
M0597	IBM_306	59.10	7.60	0.13	51.50	72.33	39.93	0.56	32.40
M0594	IBM_305	50.00	9.05	0.18	40.95	74.63	35.20	0.47	39.43
M0590	IBM_304	53.37	8.20	0.15	45.17	73.02	25.10	0.34	47.92
M0589	IBM_303	64.10	6.27	0.10	57.83	83.17	35.68	0.43	47.48
M0588	IBM_302	49.58	2.07	0.04	47.52	74.22	5.52	0.07	68.70
M0587	IBM_301	43.30	1.85	0.04	41.45	71.37	4.98	0.07	66.38
M0583	IBM_298	48.10	7.30	0.15	40.80	67.75	30.25	0.45	37.50
M0581	IBM_297	55.30	6.40	0.12	48.90	66.83	23.52	0.35	43.32
M0580	IBM_296	60.83	7.73	0.13	53.10	82.37	29.42	0.36	52.95
M0577	IBM_295	47.55	6.43	0.13	41.12	72.72	29.13	0.41	43.58
M0566	IBM_285	39.68	5.47	0.14	34.22	68.43	30.62	0.45	37.82
M0565	IBM_284	51.77	7.87	0.15	43.90	74.60	27.38	0.37	47.22
M0564	IBM_283	48.85	8.68	0.18	40.17	70.23	28.65	0.41	41.58
M0563	IBM_282	47.48	2.15	0.05	45.33	61.13	6.87	0.11	54.27
M0562	IBM_281	53.05	2.32	0.04	50.73	81.25	6.98	0.09	74.27
M0575	IBM_294	50.62	1.97	0.04	48.65	73.17	7.50	0.10	65.67
M0574	IBM_293	63.78	7.15	0.11	56.63	64.95	33.68	0.52	31.27
M0573	IBM_292	47.10	4.35	0.09	42.75	61.40	31.70	0.52	29.70
M0571	IBM_290	62.95	2.28	0.04	60.67	78.53	7.73	0.10	70.80
M0561	IBM_280	46.85	7.95	0.18	38.90	67.33	25.65	0.39	41.68
M0560	IBM_279	53.15	8.60	0.17	44.55	75.43	26.17	0.35	49.27
M0559	IBM_278	53.45	7.05	0.13	46.40	70.15	29.92	0.43	40.23
M0558	IBM_277	47.20	1.73	0.04	45.47	76.55	5.62	0.07	70.93
M0557	IBM_276	43.90	5.43	0.12	38.47	73.72	23.43	0.32	50.28

Syn10_ID	Liu et.al-ID	WT_CCMI	MT_CCMI	Ratio_CCMI	Diff_CCMI	WT_CCMII	MT_CCMII	Ratio_CCMII	Diff_CCMII
M0556	IBM_275	52.18	2.37	0.05	49.82	75.47	6.35	0.08	69.12
M0553	IBM_274	55.60	6.78	0.12	48.82	67.70	28.51	0.42	39.19
M0551	IBM_272	48.08	1.97	0.04	46.12	69.63	5.35	0.08	64.28
M0550	IBM_271	56.22	7.97	0.14	48.25	63.90	27.78	0.43	36.12
M0549	IBM_270	52.95	6.65	0.13	46.30	69.82	34.95	0.50	34.87
M0548	IBM_269	45.02	1.85	0.04	43.17	66.40	6.27	0.09	60.13
M0546	IBM_267	51.12	7.28	0.15	43.83	71.68	29.15	0.41	42.53
M0545	IBM_266	56.37	5.18	0.10	51.18	71.33	27.17	0.38	44.17
M0543	IBM_264	33.47	5.27	0.16	28.20	69.93	24.73	0.35	45.20
M0544	IBM_265	50.23	1.90	0.04	48.33	71.18	5.58	0.08	65.60
M0540	IBM_261	51.05	7.93	0.16	43.12	68.37	36.37	0.54	32.00
M0538	IBM_260	51.43	5.37	0.11	46.07	74.03	28.32	0.38	45.72
M0537	IBM_259	47.58	7.05	0.15	40.53	77.18	25.87	0.34	51.32
M0535	IBM_257	43.63	8.45	0.20	35.18	75.20	35.52	0.47	39.68
M0534	IBM_256	39.33	7.48	0.19	31.85	73.89	32.98	0.45	40.91
M0533	IBM_255	50.97	6.48	0.13	44.48	76.43	23.78	0.31	52.65
M0532	IBM_254	47.42	5.43	0.12	41.98	68.35	25.87	0.38	42.48
M0527	IBM_253	53.48	6.47	0.12	47.02	70.17	27.63	0.39	42.53
M0525	IBM_252	45.15	6.68	0.15	38.47	64.40	28.92	0.45	35.48
M0519	IBM_251	48.28	7.33	0.15	40.95	68.20	25.50	0.37	42.70
M0517	IBM_250	40.85	5.85	0.14	35.00	70.12	25.77	0.37	44.35
M0513	IBM_249	45.65	6.35	0.14	39.30	73.33	31.82	0.44	41.52
M0512	IBM_248	50.07	6.50	0.13	43.57	87.50	22.70	0.26	64.80
M0510	IBM_247	45.90	7.77	0.17	38.13	75.77	24.77	0.33	51.00
M0509	IBM_246	56.47	1.92	0.03	54.55	76.90	6.35	0.08	70.55
M0506	IBM_244	53.73	2.00	0.04	51.73	68.63	6.23	0.09	62.40
M0502	IBM_241	43.95	5.27	0.12	38.68	67.95	24.40	0.36	43.55
M0500	IBM_239	42.13	7.27	0.18	34.87	76.82	28.00	0.37	48.82

Syn10_ID	Liu et.al-ID	WT_CCMI	MT_CCMI	Ratio_CCMI	Diff_CCMI	WT_CCMII	MT_CCMII	Ratio_CCMII	Diff_CCMII
M0498	IBM_237	44.35	1.82	0.04	42.53	71.73	4.98	0.07	66.75

Table S3. The average values of the CCM traits in wild-type (WT) and mutant (MT) siblings of the F_1 hybrids between *Oy1-N1989/oy1*:B73 (as a pollen-parent) with respective BM-NILs. Data is derived from the field-grown plants with five replications planted in a RCBD. Parental (B73 and Mo17) F_1 crosses were planted as checks in each replication. Multiple plants (2-3) were measured for each genotype (wild-type or mutant) in each replication.

Ear-parent	NIL background	*vey1* status	MT_CCMI	WT_CCMI	Ratio_CCMI	MT_CCMII	WT_CCMII	Ratio_CCMII
B73	**.**	**B73**	**4.75**	**27.49**	**0.17**	**22.15**	**64.55**	**0.34**
Mo17	**.**	**Mo17**	**2.05**	**31.17**	**0.07**	**5.69**	**78.18**	**0.07**
b142	B73	B73	6.07	30.21	0.20	25.26	63.34	0.40
b139	B73	B73	6.26	34.61	0.18	25.25	67.75	0.37
b135	B73	B73	5.73	30.79	0.19	27.88	70.03	0.40
b132	B73	B73	4.95	31.06	0.17	24.91	63.42	0.40
b125	B73	B73	7.17	37.01	0.19	27.15	65.83	0.41
b185	B73	B73	5.89	33.60	0.18	26.88	66.63	0.41
b155	B73	B73	6.17	30.34	0.21	25.64	58.59	0.45
b121	B73	B73	5.51	32.37	0.18	27.26	70.14	0.39
b120	B73	B73	6.75	34.16	0.20	30.36	65.58	0.48
b092	B73	B73	5.03	30.71	0.17	24.97	63.72	0.40
b087	B73	B73	5.03	28.70	0.18	24.13	66.23	0.37
b055	B73	B73	6.79	29.30	0.24	29.99	65.63	0.46
b035	B73	B73	5.55	34.25	0.17	26.87	71.57	0.38
b030	B73	B73	6.15	32.85	0.19	32.26	73.97	0.44
b123	B73	Mo17	2.18	31.38	0.07	5.63	71.50	0.08
b189	B73	Mo17	2.67	29.97	0.09	6.01	68.55	0.09
b182	B73	Mo17	2.24	28.76	0.08	5.39	63.71	0.09
b107	B73	Mo17	1.97	33.01	0.06	5.91	75.01	0.08
b094	B73	Mo17	1.71	32.26	0.05	5.34	73.49	0.07
b049	B73	Mo17	2.32	30.75	0.08	6.41	68.29	0.09
b047	B73	Mo17	1.85	31.44	0.06	6.29	71.44	0.09
b001	B73	Mo17	2.03	33.29	0.06	5.32	71.58	0.07

Ear-parent	NIL background	*vey1* status	MT_CCMI	WT_CCMI	Ratio_CCMI	MT_CCMII	WT_CCMII	Ratio_CCMII
mo24	Mo17	B73	5.73	29.76	0.20	30.65	68.89	0.45
m097	Mo17	B73	5.53	35.29	0.16	29.03	72.02	0.41
mo27	Mo17	Mo17	2.31	28.50	0.08	7.04	71.96	0.10
m022	Mo17	Mo17	2.13	30.65	0.07	6.57	71.69	0.09
m008	Mo17	Mo17	2.37	29.75	0.08	7.20	76.88	0.09
m002	Mo17	Mo17	2.39	31.98	0.08	6.49	66.28	0.10
m093	Mo17	Mo17	1.91	30.85	0.06	7.26	68.09	0.11
m079	Mo17	Mo17	2.31	29.71	0.08	8.50	68.21	0.13
m051	Mo17	Mo17	2.23	30.47	0.07	6.04	69.15	0.09
m048	Mo17	Mo17	2.53	34.06	0.08	7.22	74.83	0.10
m043	Mo17	Mo17	1.85	26.98	0.07	6.76	81.51	0.08
m038	Mo17	Mo17	2.25	29.24	0.08	6.98	75.18	0.09
m035	Mo17	Mo17	2.03	31.19	0.07	7.15	73.66	0.10

Table S4. The BLUP values of the wild-type (WT) and mutant (MT) siblings of the F_1 hybrids of *Oy1-N1989*/*oy1*:B73 with respective maize diversity lines (MDL). Information on the inbred lines from maize association panel (referred to as 302) was adapted from Flint-Garcia *et al.* 2005.

Inbred	State/Country	Panel Type	Pedigree	WT_CCMI	MT_CCMI	Ratio_CCMI	Diff_CCMI	WT_CCMII	MT_CCMII	Ratio_CCMII	Diff_CCMII
F10	Puy-de-Dome, France	Ames	Etoile de Normandie variety	54.91	10.67	0.21	44.34	76.84	32.81	0.37	49.65
F431	.	Ames	.	66.77	9.09	0.12	57.56	78.97	38.01	0.46	44.49
GE440	North Carolina	Ames	Hastings Prolific	60.34	9.42	0.16	51.15	68.42	22.56	0.34	44.04
Hi33	Hawaii	Ames	(M14 x CI187-2)Oh45)BC1	62.22	8.56	0.14	53.79	68.15	28.31	0.43	38.44
HY2	.	Ames	.	57.83	2.74	0.05	52.95	67.11	9.63	0.15	54.00
IA5125B	Iowa	Ames	Unknown	54.52	5.67	0.11	47.32	71.69	14.98	0.21	55.44
LH1	USA	Ames	Check PVP certificate	66.76	7.96	0.11	59.17	78.59	21.81	0.27	58.71
LH119	USA	Ames	Check PVP certificate	58.75	8.70	0.15	49.89	69.25	29.71	0.44	38.67
LH123HT	USA	Ames	Check PVP certificate	59.51	11.22	0.19	49.01	73.16	30.15	0.41	43.64
LH127	USA	Ames	Check PVP certificate	65.34	11.91	0.17	54.93	68.43	24.35	0.37	42.41
LH128	USA	Ames	Check PVP certificate	58.63	10.02	0.17	48.86	72.83	44.43	0.60	30.21
LH132	USA	Ames	Check PVP certificate	56.58	9.53	0.18	46.94	70.95	37.39	0.54	34.02
LH145	USA	Ames	Check PVP certificate	55.76	8.90	0.17	46.48	72.41	21.03	0.29	50.92
LH146Ht	USA	Ames	Check PVP certificate	54.14	7.62	0.15	46.22	67.33	22.08	0.33	44.86
LH149	USA	Ames	Check PVP certificate	60.00	7.94	0.14	51.78	71.48	26.35	0.37	44.79
LH150	USA	Ames	Check PVP certificate	66.99	7.06	0.10	60.05	75.47	17.30	0.23	58.52
LH160	USA	Ames	Check PVP certificate	61.48	8.89	0.15	52.75	78.30	29.55	0.36	51.27
LH193	USA	Ames	Check PVP certificate	61.83	9.03	0.14	53.04	64.83	29.83	0.51	32.48
LH194	USA	Ames	Check PVP certificate	60.00	8.04	0.14	51.71	74.28	22.98	0.31	51.71
LH195	USA	Ames	Check PVP certificate	63.47	10.07	0.15	54.12	71.50	40.72	0.57	31.75
LH196	USA	Ames	Check PVP certificate	53.16	6.81	0.14	45.06	70.76	32.44	0.46	38.26
LH202	USA	Ames	Check PVP certificate	56.62	5.03	0.09	50.06	66.06	25.99	0.41	37.67
LH205	USA	Ames	Check PVP certificate	55.33	.	.	.	69.58	.	.	.
LH208	USA	Ames	Check PVP certificate	61.71	10.84	0.17	51.68	76.11	24.58	0.32	52.78
LH220Ht	USA	Ames	Check PVP certificate	56.60	5.98	0.10	53.00	71.61	23.18	0.34	45.29

Inbred	State/Country	Panel Type	Pedigree	WT_CCMI	MT_CCMI	Ratio_CCMI	Diff_CCMI	WT_CCMII	MT_CCMII	Ratio_CCMII	Diff_CCMII
LH38	USA	Ames	Check PVP certificate	65.04	.	.	.	69.64	.	.	.
LH39	USA	Ames	Check PVP certificate	54.78	6.99	0.14	46.71	62.94	16.94	0.29	41.60
LH51	USA	Ames	Check PVP certificate	64.66	2.98	0.05	60.28	73.93	13.26	0.18	60.08
LH52	USA	Ames	Check PVP certificate	56.92	2.56	0.05	52.07	70.89	9.10	0.13	59.68
LH54	USA	Ames	Check PVP certificate	49.70	3.10	0.07	43.80	75.02	10.90	0.15	63.73
LH57	USA	Ames	Check PVP certificate	58.93	3.17	0.06	53.86	75.36	10.82	0.15	64.27
LH59	USA	Ames	Check PVP certificate	60.65	3.68	0.06	53.68	69.38	13.59	0.21	52.55
LH61	USA	Ames	Check PVP certificate	59.40	2.53	0.05	54.82	77.87	10.60	0.14	67.91
LH65	USA	Ames	Check PVP certificate	64.17	2.56	0.04	60.03	75.25	11.05	0.15	63.91
LH74	USA	Ames	Check PVP certificate	56.16	6.97	0.13	48.24	70.42	32.74	0.47	37.52
LH82	USA	Ames	Check PVP certificate	53.95	8.39	0.17	44.83	69.38	26.02	0.38	42.21
LH85	USA	Ames	Check PVP certificate	61.12	7.77	0.13	53.12	76.72	18.38	0.24	59.26
Mo16W	Missouri	Ames	Pipe Corn	58.03	13.77	0.24	45.64	71.67	46.03	0.64	27.15
Mo20W	Missouri	Ames	N6/Mo22	68.39	8.23	0.12	60.79	70.64	24.42	0.35	45.40
Mo48	Missouri	Ames	(NC33/B52) S6	56.85	12.54	0.24	45.19	74.12	41.86	0.56	34.32
PH9	.	Ames	.	58.96	7.83	0.13	50.72	67.32	19.26	0.30	45.52
PHG29	USA	Ames	Check PVP certificate	59.27	8.80	0.15	50.39	77.11	26.16	0.33	52.71
PHG35	USA	Ames	Check PVP certificate	61.89	7.96	0.13	53.84	75.05	22.92	0.30	52.84
PHG39	USA	Ames	Check PVP certificate	59.66	11.79	0.20	48.78	73.06	39.07	0.53	35.39
PHG47	USA	Ames	Check PVP certificate	61.17	8.55	0.14	52.65	72.70	25.62	0.35	47.14
PHG50	USA	Ames	Check PVP certificate	56.31	8.83	0.16	47.13	72.97	32.05	0.44	41.66
PHG71	USA	Ames	Check PVP certificate	59.68	11.54	0.20	48.97	72.62	25.19	0.35	47.42
PHG72	USA	Ames	Check PVP certificate	63.76	10.24	0.15	54.33	73.25	28.22	0.39	45.52
PHG83	USA	Ames	Check PVP certificate	61.61	2.77	0.05	57.07	72.02	10.75	0.16	59.73
PHG86	USA	Ames	Check PVP certificate	59.73	5.70	0.10	53.01	68.41	15.39	0.23	50.53
PHH93	USA	Ames	Check PVP certificate	61.40	10.16	0.16	51.81	70.23	29.12	0.42	40.54
PHJ31	USA	Ames	Check PVP certificate	64.20	21.74	0.33	46.96	74.87	43.57	0.57	33.79
PHJ33	USA	Ames	Check PVP certificate	59.09	2.49	0.04	54.50	73.34	9.10	0.13	63.05

Inbred	State/Country	Panel Type	Pedigree	WT_CCMI	MT_CCMI	Ratio_CCMI	Diff_CCMI	WT_CCMII	MT_CCMII	Ratio_CCMII	Diff_CCMII
PHJ40	USA	Ames	Check PVP certificate	56.78	20.14	0.42	40.57	71.19	41.25	0.55	35.80
PHJ70	USA	Ames	Check PVP certificate	67.27	9.39	0.13	58.76	74.11	37.60	0.50	38.18
PHJ75	USA	Ames	Check PVP certificate	58.96	9.06	0.16	49.88	73.04	24.75	0.34	48.41
PHK05	USA	Ames	Check PVP certificate	52.00	11.01	0.23	40.91	71.58	28.09	0.39	43.34
PHK29	USA	Ames	Check PVP certificate	56.69	2.89	0.05	51.60	67.55	8.04	0.13	56.06
PHK35	USA	Ames	Check PVP certificate	63.40	10.87	0.17	53.51	72.36	44.11	0.60	29.85
PHK42	USA	Ames	Check PVP certificate	62.88	12.08	0.19	52.11	71.26	28.36	0.41	42.66
PHK76	USA	Ames	Check PVP certificate	68.64	4.02	0.06	63.92	74.93	13.00	0.17	61.69
PHM49	USA	Ames	Check PVP certificate	59.58	6.41	0.11	52.37	77.91	25.16	0.32	54.73
PHM57	USA	Ames	Check PVP certificate	65.84	22.90	0.33	47.97	76.98	47.74	0.60	32.90
PHN11	USA	Ames	Check PVP certificate	59.10	9.53	0.17	49.71	69.96	26.29	0.38	42.76
PHN29	USA	Ames	Check PVP certificate	62.41	7.60	0.12	54.66	75.93	25.19	0.32	51.97
PHN37	USA	Ames	Check PVP certificate	61.86	8.41	0.14	53.50	75.80	27.21	0.35	49.95
PHN73	USA	Ames	Check PVP certificate	56.93	9.69	0.17	49.87	62.67	.	.	.
PHN82	USA	Ames	Check PVP certificate	65.23	11.59	0.17	55.03	74.08	32.56	0.43	42.72
PHP02	USA	Ames	Check PVP certificate	63.62	9.50	0.15	54.68	75.68	30.14	0.39	47.12
PHP55	USA	Ames	Check PVP certificate	61.07	10.85	0.18	50.97	75.52	27.85	0.36	48.99
PHP60	USA	Ames	Check PVP certificate	63.94	9.97	0.15	54.72	74.06	36.72	0.49	38.90
PHR25	USA	Ames	Check PVP certificate	54.72	8.39	0.16	45.68	72.50	28.40	0.39	44.34
PHR32	USA	Ames	Check PVP certificate	62.30	9.21	0.15	53.43	77.68	33.19	0.41	47.10
PHR36	USA	Ames	Check PVP certificate	62.41	8.73	0.14	53.88	71.79	27.43	0.38	44.23
PHR47	USA	Ames	Check PVP certificate	55.99	8.86	0.17	46.76	70.19	33.25	0.48	36.74
PHR62	USA	Ames	Check PVP certificate	63.80	8.39	0.13	55.64	67.50	22.80	0.35	42.55
PHT10	USA	Ames	Check PVP certificate	63.58	9.54	0.15	54.62	72.95	31.09	0.42	42.50
PHT22	USA	Ames	Check PVP certificate	58.87	9.01	0.16	49.81	77.02	35.29	0.44	44.28
PHT55	USA	Ames	Check PVP certificate	66.95	9.71	0.14	58.20	75.85	37.16	0.47	40.97
PHT60	USA	Ames	Check PVP certificate	57.74	7.82	0.14	49.39	70.04	23.09	0.34	45.78
PHT77	USA	Ames	Check PVP certificate	59.59	15.64	0.26	46.07	72.39	42.53	0.58	31.33

Inbred	State/Country	Panel Type	Pedigree	WT_CCMI	MT_CCMI	Ratio_CCMI	Diff_CCMI	WT_CCMII	MT_CCMII	Ratio_CCMII	Diff_CCMII
PHV37	USA	Ames	Check PVP certificate	56.88	2.34	0.05	52.19	68.31	8.61	0.13	56.57
PHV63	USA	Ames	Check PVP certificate	58.98	2.46	0.04	54.41	72.33	8.35	0.12	62.35
PHV78	USA	Ames	Check PVP certificate	59.66	10.15	0.17	49.91	74.08	30.85	0.41	44.29
PHW03	USA	Ames	Check PVP certificate	56.41	10.50	0.19	46.10	71.84	41.70	0.58	31.32
PHW17	USA	Ames	Check PVP certificate	64.98	8.29	0.12	57.01	68.71	31.87	0.47	35.96
PHW20	USA	Ames	Check PVP certificate	62.60	10.81	0.17	52.67	71.14	19.40	0.28	50.65
PHW43	USA	Ames	Check PVP certificate	52.32	6.19	0.13	44.56	69.27	18.80	0.28	48.62
PHW52	USA	Ames	Check PVP certificate	61.06	11.59	0.19	50.46	70.70	35.32	0.50	35.56
PHW65	USA	Ames	Check PVP certificate	58.45	11.37	0.20	47.74	77.79	32.06	0.40	48.28
PHW79	USA	Ames	Check PVP certificate	61.33	9.75	0.16	52.00	73.38	34.47	0.46	40.02
PHZ51	USA	Ames	Check PVP certificate	58.98	9.08	0.16	49.88	75.11	31.88	0.42	44.76
W32	Wisconsin	Ames	Unknown	56.78	9.15	0.18	47.42	69.73	29.23	0.43	39.77
Yu796	North Carolina	Ames	Unknown	61.29	10.62	0.17	51.36	76.65	20.03	0.26	57.66
33-16	Indiana	302	Lux Johnson Country white	61.98	9.77	0.15	52.70	74.69	31.92	0.42	44.14
38-11	Indiana	302	Outcross in line from 176A	56.79	9.11	0.17	47.47	69.26	21.05	0.31	46.57
81-1	USDA	302	Iowa 60*Edisto	56.71	8.35	0.15	47.90	70.84	24.61	0.35	45.50
A188	Minnesota	302	[(4-29*64)4-29(4)]	61.37	6.30	0.10	54.40	79.69	20.40	0.25	61.51
A214N	South Africa	302	(B68*HtN)B68(3)	64.40	10.37	0.15	54.94	71.92	30.15	0.42	41.94
A239	Minnesota	302	A73*A347	57.08	8.70	0.16	48.06	67.52	19.54	0.30	45.54
A441-5	South Africa	302	Robyn*Leamming yellow dent	58.32	8.72	0.15	49.40	66.67	23.86	0.38	40.44
A554	Minnesota	302	[(WD*Wf9)WD(2))]	53.57	7.06	0.14	45.34	72.85	20.96	0.29	51.59
A619	Minnesota	302	[(A171*Oh43)Oh43]	53.91	6.28	0.13	46.24	65.60	17.91	0.29	44.38
A632	Minnesota	302	[(Mt42*B14)B14(3)]	60.64	11.52	0.19	50.03	72.47	29.32	0.40	43.47
A634	Minnesota	302	[(Mt42*B14)B14(2)]	57.20	9.93	0.18	47.35	73.72	26.91	0.36	47.36
A635	Minnesota	302	ND203xB14(3)	53.68	10.07	0.20	43.40	76.54	33.52	0.43	45.23
A641	Minnesota	302	ND203*B14	57.75	8.20	0.15	49.13	75.71	22.08	0.29	54.50
A654	Minnesota	302	A116*Wf9	54.13	6.93	0.14	46.04	66.82	16.01	0.25	47.80
A659	Minnesota	302	Minnesota Synthetic 3	61.39	8.13	0.13	53.18	69.12	34.13	0.50	34.47

Inbred	State/Country	Panel Type	Pedigree	WT_CCMI	MT_CCMI	Ratio_CCMI	Diff_CCMI	WT_CCMII	MT_CCMII	Ratio_CCMII	Diff_CCMII
A661	Minnesota	302	Minnesota Synthetic AS-A	51.08	6.47	0.15	43.00	70.80	21.78	0.31	48.02
A679	Minnesota	302	[(A662*B73) B73(3)]	55.61	8.82	0.17	46.37	70.01	28.38	0.41	40.92
A680	Minnesota	302	[(A662*B73) B73(3)]	59.44	6.07	0.11	52.44	69.20	27.73	0.41	40.40
A682	Minnesota	302	[(AS-D*Mo17) Mo17 (2)]	59.04	2.26	0.04	54.61	68.78	10.21	0.16	55.78
Ab28A	Alabama	302	GT152*38-11	62.70	17.19	0.26	48.42	77.43	51.23	0.64	30.34
B10	Iowa	302	Iowa Stiff Stalk Synthetic	55.86	8.49	0.16	46.86	72.58	32.63	0.45	40.59
B103	Iowa	302	CIMMYT Pool 41 [Northern Temperate Ranges -1 (NTR-1)]	57.27	8.78	0.16	48.21	70.16	25.35	0.37	43.89
B104	Iowa	302	BS13(S)C5	60.10	7.31	0.12	52.32	68.92	37.17	0.55	31.43
B105	Iowa	302	BSSS®C9	60.84	5.94	0.10	54.07	73.65	22.51	0.30	51.27
B109	Iowa	302	[B73 * BS20(S)C1]B73	62.81	9.53	0.15	53.78	70.99	29.01	0.41	41.71
B14A	Iowa	302	Cuzco*B14(8)	60.95	16.62	0.27	46.89	71.32	42.63	0.59	29.76
B164	Minnesota	302	Indiana Reid (Pioneer)	56.08	4.99	0.09	49.50	72.85	15.52	0.22	56.53
B2	Missouri	302	Reid Yellow Dent	61.22	3.39	0.06	56.22	75.90	15.20	0.20	61.02
B37	Iowa	302	Iowa Stiff Stalk Synthetic	68.69	7.75	0.11	61.43	76.37	31.11	0.40	47.19
B46	Iowa	302	W22*B10	61.09	3.99	0.07	55.67	71.68	16.66	0.24	53.89
B57	Iowa	302	Midland	53.59	9.85	0.20	43.45	69.66	30.06	0.44	38.91
B64	Iowa	302	41.2504B*B14(3)	61.87	5.02	0.08	55.82	71.07	15.63	0.23	53.99
B68	Iowa	302	41.2504B*B14(3)	59.76	8.66	0.14	51.03	74.93	26.42	0.35	49.47
B73	Iowa	302	Iowa Stiff Stalk Synthetic C5	57.43	6.84	0.12	50.49	67.19	27.67	0.42	39.36
B73 Htrhm	Iowa	302	Ht1 and rhm1 conversion of B73	63.03	7.77	0.12	55.22	68.45	30.75	0.46	36.63
B76	Iowa	302	[(CL31A*B37)B37]	57.09	7.35	0.13	48.99	72.53	24.07	0.33	48.32
B77	Iowa	302	Pioneer Two-Ear composite(BS11)	59.36	8.40	0.14	50.76	71.02	23.29	0.34	46.95
B79	Iowa	302	Iowa Two-Ear Synthetic No.1(BSTE)	54.85	7.94	0.15	46.13	67.24	21.75	0.34	43.15
B84	Iowa	302	BS13(S2)C0	62.57	10.22	0.16	53.04	74.93	40.73	0.54	36.45
B97	Iowa	302	BSCB1®C9	59.83	9.83	0.17	50.31	75.17	31.34	0.41	45.33
C103	Connecticut	302	Lancaster Surecrop (from Noah Hershey)	66.54	2.45	0.04	62.70	70.16	12.69	0.19	55.40
C49A	Minnesota	302	Minn 13	59.91	10.26	0.17	50.10	68.52	34.57	0.51	33.25
CH701-30	Canada - Harrow	302	unknown	63.79	3.74	0.06	58.81	75.33	12.19	0.16	62.97

Inbred	State/Country	Panel Type	Pedigree	WT_CCMI	MT_CCMI	Ratio_CCMI	Diff_CCMI	WT_CCMII	MT_CCMII	Ratio_CCMII	Diff_CCMII
CH9	Canada - Harrow	302	Funk's G176	63.08	7.22	0.11	55.65	78.91	19.47	0.24	61.27
CI187-2	USDA	302	Krug	63.56	13.71	0.21	51.74	75.76	44.70	0.58	33.99
CI21E	USDA	302	Hy*C.I.21	60.84	16.08	0.26	47.14	69.99	36.02	0.53	33.95
CI28A	USDA	302	Recovered Blight Resistance B2	58.17	4.11	0.07	52.39	75.88	16.30	0.22	59.99
CI31A	USDA	302	Midland OP	60.45	7.91	0.13	52.29	64.94	24.96	0.41	37.06
CI3A	USDA	302	[(C.I.3*related inbred) C.I.3 (2)]	49.55	7.67	0.21	40.52	70.63	25.01	0.36	44.85
CI44	USDA	302	L97*Oh07(2)	56.54	5.27	0.10	49.81	70.45	21.40	0.31	47.88
CI64	USDA	302	K64*Mo21A	54.98	5.48	0.11	47.95	69.49	19.94	0.29	47.88
CI66	USDA	302	L97*K55 (2)	59.06	7.29	0.13	51.20	73.93	19.74	0.27	54.18
CI7	USDA	302	[(L317*33-16)33-16(2)]	58.49	6.56	0.11	51.07	70.70	18.74	0.27	50.64
CI90C	USDA	302	CI90A = L97*M14	62.79	7.88	0.12	54.88	76.14	24.17	0.31	53.19
CI91B	USDA	302	L97*A71	58.21	13.98	0.25	45.69	77.83	40.98	0.51	40.22
CM105	Canada-Morden	302	CMV3xB14(2)	63.47	2.56	0.04	59.25	72.23	5.87	0.09	64.46
CM174	Canada-Morden	302	CMV3xB14(2)	57.27	6.95	0.13	49.46	73.59	18.45	0.25	54.88
CM37	Canada-Morden	302	KE3	59.22	9.31	0.16	49.99	80.90	22.51	0.27	61.25
CM7	Canada-Morden	302	W85*CMV3	66.55	8.75	0.13	58.41	79.58	21.20	0.26	60.63
CML10	Mexico	302	Pop.21 = Tuxpeño	62.06	11.89	0.19	51.34	64.26	38.38	0.64	23.91
CML103	Mexico	302	Pop. 44	57.10	6.43	0.12	49.63	74.36	18.01	0.24	56.35
CML108	Mexico	302	Pop. 44	55.48	3.00	0.06	50.20	61.44	10.96	0.20	44.98
CML154Q	Mexico	302	Pop. 62	65.55	20.31	0.29	49.41	75.77	47.79	0.61	31.19
CML157Q	Mexico	302	Pop. 62	61.28	4.63	0.08	55.44	72.21	13.10	0.18	57.86
CML158Q	Mexico	302	Pop. 62	66.27	4.47	0.07	61.03	75.18	18.79	0.25	56.76
CML218	Mexico	302	EV = Streak resist. source	59.32	16.62	0.28	45.11	75.69	44.61	0.58	33.98
CML228	Mexico	302	Suwan-1/SR	62.14	6.65	0.11	55.01	70.61	28.45	0.41	41.68
CML247	Mexico	302	Pool 24 (Tuxpeño)	66.25	3.37	0.05	61.75	76.57	14.70	0.19	62.39
CML254	Mexico	302	Pop. 21 = Tuxpeño Sequia	59.30	4.41	0.08	53.43	73.09	14.61	0.20	57.69
CML277	Mexico	302	Pop. 43 = La Posta (Tux.)	63.36	6.02	0.09	56.78	69.61	16.30	0.24	51.38
CML311	Mexico	302	Pop. 500 = Inter. Mat. Wh. Dent Mix	61.10	8.25	0.13	52.77	79.29	32.21	0.39	50.22

Inbred	State/Country	Panel Type	Pedigree	WT_CCMI	MT_CCMI	Ratio_CCMI	Diff_CCMI	WT_CCMII	MT_CCMII	Ratio_CCMII	Diff_CCMII
CML314	Mexico	302	Pop. 600 = Late Mat. Wh. Dent Mix	60.27	16.98	0.28	45.90	73.43	34.86	0.47	39.73
CML321	Mexico	302	Pop. 502 = Mex. DK + US	59.25	4.36	0.08	53.40	70.57	11.21	0.17	57.32
CML322	Mexico	302	Recyc. US + Mex	61.10	4.83	0.08	55.11	72.34	21.38	0.30	50.51
CML323	Mexico	302	Pop. 33 Amar. Subtrop. Mix	57.09	7.48	0.15	48.91	71.55	24.61	0.35	46.48
CML331	Mexico	302	Suwan/Pop.47 * Mp78:518	58.16	8.07	0.14	49.68	69.91	21.71	0.32	46.86
CML332	Mexico	302	Suwan/Pop.47 * Mp78:518	62.01	8.76	0.14	53.42	66.04	19.03	0.31	43.98
CML333	Mexico	302	Pop. 590	57.37	2.84	0.05	52.39	71.12	12.82	0.19	56.61
CML341	Mexico	302	Pop. 43 = La Posta (Tux.)	60.23	3.19	0.06	55.27	75.88	9.37	0.13	66.30
CML38	Mexico	302	Pop. 32	61.54	17.38	0.28	47.01	70.83	45.41	0.66	26.56
CML45	Mexico	302	Pop. 43 = La Posta (Tux.)	56.35	2.91	0.06	51.22	79.84	9.89	0.12	71.28
CML52	Mexico	302	Pop. 79 = STA ROSA	61.78	7.28	0.12	54.18	69.73	19.12	0.28	48.97
CML69	Mexico	302	Pop. 36 = Cogollero (Caribbean)	66.51	9.85	0.14	57.61	70.75	27.43	0.39	42.80
CML91	Mexico	302	Pop. 42 Northern Temp./German Mix	61.61	13.54	0.22	49.73	72.14	36.41	0.51	36.55
CML92	Mexico	302	Pop. 42 Northern Temp./German Mix	60.28	10.45	0.17	50.37	71.72	31.62	0.45	40.32
CMV3	Minnesota	302	A21*W185	55.23	6.42	0.13	47.60	68.41	20.90	0.32	45.52
Co106	Canada-Ottawa	302	University of Wisconsin CR11	51.81	7.90	0.17	42.83	74.51	22.44	0.30	52.53
Co125	Canada-Ontario	302	unknown	57.04	5.44	0.10	50.24	74.53	14.53	0.20	59.75
Co255	Canada-Ottawa	302	INRA 258	60.58	12.23	0.20	49.49	80.68	37.28	0.44	47.51
D940Y	South Africa	302	BO60W(A166NxB566Y-B560Y)B557Y	61.40	12.91	0.21	49.92	68.22	28.54	0.43	38.31
DE1	Delaware B	302	P3140*P3751	56.48	6.84	0.13	48.67	70.30	22.49	0.33	46.69
DE2	Delaware B	302	P3140*P3751	56.78	7.30	0.13	48.69	68.88	23.87	0.36	43.47
DE811	Delaware	302	[B68*[B37Ht*(C103*Mp3204 double cross) Selection]]	66.41	2.42	0.04	62.58	72.05	9.14	0.13	61.24
E2558W	South Africa	302	N6*M162W^3	53.53	11.82	0.24	42.04	71.70	34.47	0.48	37.71
EP1	Spain	302	Spanish population ‘Lizargarate’	53.66	10.60	0.21	43.02	82.44	49.75	0.56	38.58
F2	Puy-de-Dome, France	302	OP Lacaune	59.08	18.41	0.31	43.63	69.57	50.25	0.74	20.42
F2834T	South Africa	302	Teko Yellow	60.56	5.35	0.09	54.17	72.68	21.35	0.29	50.99
F44	Florida	302	Smith (Old Florida variety)	59.76	9.07	0.15	50.75	69.99	32.62	0.47	37.03
F7	France-Peronne	302	OP Lacaune	56.66	8.48	0.16	47.75	77.82	26.52	0.33	53.36

Inbred	State/Country	Panel Type	Pedigree	WT_CCMI	MT_CCMI	Ratio_CCMI	Diff_CCMI	WT_CCMII	MT_CCMII	Ratio_CCMII	Diff_CCMII
GA209	Georgia	302	T61*NC37	61.35	5.80	0.09	54.73	72.56	13.78	0.19	57.72
GT112	Georgia	302	Multiple cross (includes Whatley, Cuban, Garrick, Creole, and 12% other)	59.51	11.22	0.19	49.01	67.22	32.41	0.50	33.42
H100	Indiana	302	N28*H91	61.42	9.92	0.16	51.99	78.21	28.77	0.35	51.85
H105W	Indiana	302	33-16*A632(3)	62.39	8.77	0.14	53.83	73.13	21.87	0.30	51.14
H84	Indiana	302	[B37*GE440)Ht Ht	63.78	14.29	0.22	51.59	75.77	41.42	0.53	36.99
H91	Indiana	302	[B37*GE440)B14(4)]Ht Ht	53.67	9.80	0.20	43.57	74.45	24.65	0.33	50.43
H95	Indiana	302	Oh43*C.L90A	62.32	8.09	0.13	54.22	67.40	22.83	0.35	42.38
H99	Indiana	302	Illinois Synthetic 60C	60.75	8.25	0.13	52.39	71.45	32.16	0.46	39.46
Hi27	Hawaii	302	[CM104(India)*MV source]BC6	63.64	9.73	0.15	54.55	69.52	25.36	0.38	42.99
Hp301	Indiana	302	Supergold	52.11	6.64	0.14	44.02	70.13	18.87	0.27	49.75
I205	Iowa	302	Iodent	60.77	10.94	0.18	50.58	75.36	50.89	0.66	27.81
IA2132	Iowa	302	[(TSR * 45) * 4329]	53.74	8.58	0.18	44.48	66.72	36.81	0.57	28.73
IA5125	Iowa	302	[(IP39*Tendermost)*IP39]	53.59	5.19	0.11	46.63	72.79	16.42	0.23	55.63
IDS28	Iowa	302	Yellow Pearl	60.93	10.08	0.16	51.34	68.59	30.26	0.45	37.27
IDS69	Iowa	302	South American Popcorn	58.35	7.13	0.13	50.52	72.43	22.91	0.32	49.24
IL677A	Illinois	302	[(Bolivia 1035*IL44b)*IL422a]	54.95	5.33	0.10	48.03	74.06	23.98	0.32	50.51
Ill.Hy	Illinois	302	Illinois High Yield	53.59	2.84	0.06	48.24	66.28	9.17	0.15	53.27
K148	Kansas	302	Yellow selection No. 1 (Pride of Saline, yellow strain)	57.56	11.22	0.20	46.87	73.47	37.51	0.50	37.37
K4	Kansas	302	Kansas Sunflower	54.30	8.04	0.16	45.47	71.01	25.19	0.36	45.21
K55	Kansas	302	Pride of Saline	54.84	6.59	0.13	47.04	72.91	22.32	0.30	50.43
K64	Kansas	302	Pride of Saline	55.14	5.40	0.11	48.18	70.63	21.34	0.31	48.17
Ki11	Thailand	302	Suwan 1(S)C4-S8-18-7	68.56	7.91	0.11	61.18	76.33	20.46	0.26	56.83
Ki14	Thailand	302	Suwan 1(S)C4-S8-19-5	58.54	6.76	0.12	50.99	70.13	23.45	0.34	45.58
Ki21	Thailand	302	Pacific 9-S8-45	57.53	9.20	0.16	48.21	70.90	28.99	0.42	41.60
Ki3	Thailand	302	Suwan 1(S)C4-S8-5-3	59.69	4.25	0.07	53.97	70.94	20.18	0.29	49.67
Ki43	Thailand	302	Suwan 3(S)C3-S7-138	64.98	9.56	0.14	56.13	75.48	26.71	0.35	49.96
KUl2007	Thailand	302	DK version of Ki3; Suwan 1(S)C4-S8-5-3	58.67	10.46	0.18	48.60	74.66	39.38	0.52	37.31
KUl2021	Thailand	302	DK version of Ki9; Suwan 1(S)C4-S8-16-7	59.28	14.00	0.24	46.85	72.12	44.86	0.62	28.82

Inbred	State/Country	Panel Type	Pedigree	WT_CCMI	MT_CCMI	Ratio_CCMI	Diff_CCMI	WT_CCMII	MT_CCMII	Ratio_CCMII	Diff_CCMII
KUI44	Thailand	302	KS 6(S)C2-S7-366	61.64	14.62	0.23	49.02	73.98	44.33	0.59	31.87
Ky21	Kentucky	302	Boone County White	60.72	13.49	0.22	48.78	71.43	38.98	0.55	33.24
Ky226	Kentucky	302	NCLauDA*Coahuila 8	64.84	11.52	0.17	54.64	71.08	39.18	0.55	32.57
Ky228	Kentucky	302	Pride of Saline	65.59	12.30	0.18	54.93	76.97	34.62	0.44	44.83
L317	Iowa	302	Lancaster surecrop (from Noah Hershey)	64.05	20.82	0.31	47.42	75.80	44.90	0.58	33.86
L578	Louisiana	302	Unknown	56.89	8.05	0.15	48.30	69.63	27.87	0.41	40.86
M162W	South Africa	302	K64R**2 x B1138T	56.04	6.47	0.12	48.44	68.50	18.32	0.28	48.00
M37W	South Africa	302	21A**2 x Jellicorse	59.58	8.32	0.14	51.06	71.41	17.06	0.24	53.16
Mo.G	Missouri	302	Mastadon variety from Pennsylvania	63.13	15.29	0.23	50.19	69.25	39.54	0.59	29.72
Mo17	Missouri	302	C.I.187-2*C103	57.94	2.30	0.04	55.39	76.23	9.82	0.13	66.40
Mo18W	Missouri	302	Wf9*Mo22(2)	64.81	9.07	0.13	56.28	74.11	24.47	0.33	50.12
Mo1W	Missouri	302	[Mo22*Wf9(2)]	61.75	8.03	0.13	53.64	76.45	22.68	0.29	54.96
Mo24W	Missouri	302	(K10*K49/Ziler Hi-cob) (pipe corn)	51.29	6.52	0.14	43.20	66.78	17.10	0.27	46.74
Mo44	Missouri	302	Mo22*Pioneer Mexican Synthetic 17	63.21	3.25	0.05	58.51	71.11	11.41	0.17	57.88
Mo45	Missouri	302	Race Negro de Tierra Caliente (Guatemala)	65.70	12.95	0.19	54.61	77.98	44.41	0.55	37.30
Mo46	Missouri	302	Race Cravo Paulista (Brazil)	63.52	3.03	0.05	58.99	76.08	8.55	0.12	67.32
Mo47	Missouri	302	Race Candela (Ecuador)	64.09	12.78	0.19	52.95	76.83	32.07	0.40	46.96
Mp339	Mississippi	302	T61*Hill Yellow Dent	59.85	12.69	0.21	48.38	80.20	30.14	0.36	53.34
MS1334	Michigan	302	[(Golden glow * Maize Amargo)*Golden Glow]	60.06	6.37	0.11	52.92	77.16	14.04	0.18	63.81
MS153	Michigan	302	Iowa stiff stalk synthetic	56.63	12.36	0.23	45.07	72.57	37.49	0.52	36.16
MS71	Michigan	302	A619*R168	60.19	6.97	0.12	52.65	71.53	13.47	0.19	56.58
Mt42	Minnesota	302	Minnesota No.13 (Owen's)	56.32	10.40	0.19	46.07	77.29	29.75	0.38	49.69
N192	Nebraska	302	CM105*B73	56.42	7.84	0.14	47.93	71.46	33.15	0.47	38.57
N28Ht	Nebraska	302	N28= BSSS	60.50	8.91	0.15	51.66	77.25	31.74	0.40	47.84
N6	Nebraska	302	Hays Golden	61.95	6.97	0.11	54.58	68.05	23.57	0.36	42.61
N7A	Nebraska	302	Oh07*Stiff stalk Synthetic	58.32	8.29	0.15	49.70	70.41	27.93	0.40	41.88
NC222	North Carolina	302	Jarvis Golden Prolific	60.77	13.75	0.22	48.66	71.34	34.26	0.48	37.41
NC230	North Carolina	302	K55*Yellow line or inbred	54.70	7.27	0.14	46.43	74.31	21.31	0.29	53.27

Inbred	State/Country	Panel Type	Pedigree	WT_CCMI	MT_CCMI	Ratio_CCMI	Diff_CCMI	WT_CCMII	MT_CCMII	Ratio_CCMII	Diff_CCMII
NC232	North Carolina	302	[(T204*Low Ear outcross) T204 (2)]	59.98	6.19	0.11	52.96	68.03	20.89	0.32	45.02
NC250	North Carolina	302	[(Nigeria Composite ARb*B37)B37)	68.20	7.90	0.11	60.80	72.88	25.18	0.35	47.79
NC258	North Carolina	302	TZ(2)*[(NC248*246)*C103]	61.20	16.51	0.27	47.24	73.03	47.65	0.65	27.55
NC260	North Carolina	302	[(Mo44*Mo17)Mo44(3)]	57.49	4.78	0.09	51.18	74.29	12.88	0.18	60.91
NC262	North Carolina	302	TZ (TZ=McNair 14*18)	60.53	11.92	0.20	49.64	74.36	39.19	0.52	37.07
NC264	North Carolina	302	[(SC76*Gaspe)Gaspe]SC76(3)	61.33	10.71	0.17	51.34	70.65	29.13	0.42	41.12
NC268	North Carolina	302	(B73*NC250) B73	53.70	5.96	0.12	46.23	70.88	18.16	0.27	51.42
NC290A	North Carolina	302	McNair inbred lines 14*18 (largely of C103 origin); sister line of NC290	65.40	7.56	0.11	57.95	68.90	27.40	0.41	40.29
NC292	North Carolina	302	[(B73*NC250) B73 (3)]	63.51	8.02	0.12	55.57	68.87	27.12	0.41	40.51
NC294	North Carolina	302	[(B73*NC250) B73]	60.97	6.72	0.11	53.67	72.05	23.46	0.33	48.20
NC298	North Carolina	302	PioneerX105A * H-5 * Agroceres155	69.17	4.77	0.07	63.99	75.13	19.84	0.26	55.75
NC304	North Carolina	302	(H5*PioneerX105A)*H101	67.07	4.32	0.06	62.00	73.12	16.72	0.23	55.81
NC306	North Carolina	302	(B73*NC250)*B73	63.65	6.53	0.10	56.74	73.78	21.67	0.30	52.21
NC308	North Carolina	302	(B73*NC250)*B73	64.38	8.88	0.13	55.94	68.33	27.60	0.42	39.32
NC310	North Carolina	302	improved B73-type derived from NC250*B73^3	61.34	7.39	0.12	53.63	69.16	24.38	0.36	43.40
NC312	North Carolina	302	(B73*NC250)*B73	67.22	9.15	0.13	58.87	72.25	20.87	0.29	50.84
NC314	North Carolina	302	B73*NC250	61.96	4.91	0.08	56.00	71.31	19.30	0.27	50.97
NC316	North Carolina	302	(B73Ht1rhm1*NC250)B73Ht1rhm1^3	62.63	7.14	0.11	55.21	69.65	25.95	0.38	42.64
NC318	North Carolina	302	[(SC76*B52)SC76(3)]	63.30	11.22	0.17	53.16	77.57	33.46	0.42	46.70
NC320	North Carolina	302	[(SC76*B52)SC76(3)]	64.47	10.25	0.15	55.11	74.84	28.38	0.37	47.57
NC322	North Carolina	302	[(SC76*B52)SC76(3)]; sister line to NC318	65.82	10.38	0.15	56.50	73.39	39.53	0.53	35.43
NC324	North Carolina	302	B73*NC250	50.52	3.43	0.08	44.48	63.88	13.55	0.23	45.98
NC326	North Carolina	302	[(B73*NC250)*B73(3)]	59.72	7.92	0.13	51.48	73.83	31.30	0.42	43.52
NC328	North Carolina	302	[(B73*NC250)*B73(3)]	62.25	10.04	0.16	52.81	73.60	33.84	0.45	40.90
NC33	North Carolina	302	Weekley's Improved	62.66	7.90	0.12	54.73	73.19	23.84	0.33	49.43
NC330	North Carolina	302	[(B73*NC250)*B73(4)]	57.41	8.51	0.15	48.55	65.65	28.62	0.46	34.70
NC332	North Carolina	302	(SC76*B52); sister line of NC334	61.60	11.57	0.19	51.06	71.41	32.63	0.46	38.99
NC334	North Carolina	302	(SC76*B52); sister line of NC332	62.67	10.45	0.16	52.99	77.66	31.32	0.39	48.77

Inbred	State/Country	Panel Type	Pedigree	WT_CCMI	MT_CCMI	Ratio_CCMI	Diff_CCMI	WT_CCMII	MT_CCMII	Ratio_CCMII	Diff_CCMII
NC338	North Carolina	302	[PioneerX105A*H5] * [Pioneer304B*Agroceres504]	58.84	4.86	0.09	52.61	73.27	22.05	0.30	51.17
NC342	North Carolina	302	McNair inbreds 14*18(of Coker 811A x C103 origin)	60.80	19.84	0.33	44.53	74.63	39.86	0.53	36.83
NC344	North Carolina	302	TZ(2)*[(NC248*246)*C103]; Sister line of NC258	58.79	11.66	0.20	47.91	69.82	38.01	0.56	31.91
NC348	North Carolina	302	PioneerX105A * H-5 * Agroceres155	70.55	4.17	0.06	65.92	75.26	18.40	0.24	57.23
NC350	North Carolina	302	(H5*PioneerX105A)*H101	64.79	12.52	0.18	53.91	75.01	35.80	0.47	41.05
NC356	North Carolina	302	TROPHY SYN	56.74	6.38	0.12	49.27	70.27	22.63	0.33	46.51
NC358	North Carolina	302	TROPHY SYN	56.07	12.42	0.23	44.42	71.03	36.50	0.53	34.95
NC360	North Carolina	302	Agroceres155*PioneerX105A/NC262	60.59	10.04	0.16	50.99	70.06	26.07	0.38	43.10
NC362	North Carolina	302	Agroceres155*PioneerX105A/NC262	57.20	11.25	0.20	46.46	72.53	33.78	0.47	39.48
NC364	North Carolina	302	Agroceres155*PioneerX105A/NC262	56.88	6.85	0.13	49.10	69.40	22.23	0.34	45.68
NC366	North Carolina	302	FLA Syn	64.51	14.47	0.21	52.26	75.73	46.23	0.60	32.55
NC368	North Carolina	302	[B73*NC250]/[(B73*NC250)*B73]	62.83	7.25	0.11	55.36	66.27	24.75	0.40	39.08
NC370	North Carolina	302	[(SC76*B52)SC76(3)]	61.06	7.88	0.13	52.99	72.96	30.66	0.42	42.90
NC372	North Carolina	302	[(B73*Pa91)*B73]	57.36	8.05	0.14	48.81	68.52	30.82	0.47	36.65
ND246	North Dakota	302	W755*W771	65.04	7.89	0.12	57.34	80.30	19.88	0.24	62.82
Oh40B	Ohio	302	Eight line composite of Lancaster Surecrop lines	60.81	6.77	0.11	53.47	72.40	17.38	0.24	54.22
Oh43	Ohio	302	Oh40B*W8	59.08	8.67	0.15	50.27	63.18	24.46	0.42	35.10
Oh43E	Ohio	302	ERF/Oh43; ERF=LeamingxReid + other Pioneer inbreds	61.59	7.04	0.11	54.14	70.23	27.88	0.40	41.68
Oh603	Ohio	302	« Syn of Va58, OhS3267, H95, Va26, Coas. Trop. FL. »	54.92	9.13	0.18	45.40	66.62	23.71	0.37	40.51
Oh7b	Ohio	302	[(Oh07*38-11)Oh07]	56.58	6.63	0.12	48.92	71.07	24.73	0.35	45.70
Os420	Iowa	302	Osterland yellow dent	54.31	7.19	0.14	46.06	71.76	21.03	0.30	50.03
P39	Indiana	302	Purdue Bantam	49.16	6.65	0.16	40.77	67.47	17.38	0.27	47.44
Pa762	Pennsylvania	302	Oh43*Pa70L	59.10	10.38	0.18	49.12	62.68	23.58	0.42	35.21
Pa875	Pennsylvania	302	Wf9 Synthetic (original)	63.00	9.40	0.15	54.07	66.24	27.52	0.44	36.52
Pa880	Pennsylvania	302	Wf9 Synthetic C3	59.52	7.94	0.14	51.25	66.68	20.01	0.31	43.97
Pa91	Pennsylvania	302	(Wf9*Oh43)S4*[(38-11*L317)38-11]S4	62.96	10.57	0.16	53.23	72.59	30.19	0.42	42.84
R168	Illinois	302	Illinois Synthetic 60C	63.65	12.39	0.19	52.74	72.66	30.44	0.42	42.69
R177	Illinois	302	Germplasm 230B(Snelling Corn Borer Synthetic)	65.82	9.00	0.13	57.44	80.44	38.04	0.45	46.48

Inbred	State/Country	Panel Type	Pedigree	WT_CCMI	MT_CCMI	Ratio_CCMI	Diff_CCMI	WT_CCMII	MT_CCMII	Ratio_CCMII	Diff_CCMII
R229	Illinois	302	[(479*B73)B73(2)]S6; 479 is a Brazilian inbred of Tuxpeño type	64.34	6.98	0.11	57.19	69.36	29.21	0.43	39.28
R4	Illinois	302	Funk Yellow dent	54.72	7.36	0.16	46.38	69.69	18.43	0.27	49.54
SC357	South Carolina	302	[(Whately yellow * Tennessee Redcob) Young]	61.48	15.03	0.24	48.56	67.97	38.66	0.59	28.77
SC55	South Carolina	302	[(L501*L503)*(L548*L569)]	61.76	11.67	0.19	51.16	73.04	36.15	0.49	38.03
SD40	South Dakota	302	Pioneer hybrid 3709	64.00	9.58	0.15	55.04	71.69	21.67	0.31	49.34
SD44	South Dakota	302	SDp309*SD30	62.06	7.36	0.12	54.43	72.75	21.35	0.29	51.09
Sg1533	Indiana	302	Super gold	52.23	7.86	0.17	43.32	64.42	24.92	0.41	36.39
SG18	Indiana	302	Super gold	51.28	7.47	0.16	42.54	68.10	20.82	0.32	45.17
T232	Tennessee	302	Jellicorse*Teko yellow	63.07	11.42	0.18	52.77	76.34	44.39	0.57	35.07
T234	Tennessee	302	[T111*RB.L*III.A)]T111(4)	59.80	13.36	0.22	47.85	72.66	34.61	0.47	38.90
T8	Tennessee	302	Jarvis Golden Prolific	61.60	24.32	0.38	42.35	69.86	46.28	0.67	24.43
Tx303	Texas	302	Yellow Surcropper	65.09	6.58	0.10	58.29	75.85	19.23	0.25	57.28
Tx601	Texas	302	Yellow Tuxpan	61.01	17.53	0.28	46.34	71.22	45.18	0.64	27.31
Tzi10	Nigeria	302	Tlaltizapan 7844 x TZSR	54.31	10.26	0.21	43.95	68.29	36.56	0.55	31.12
Tzi11	Nigeria	302	Mo17 x RppSR	64.40	6.22	0.09	57.78	72.17	28.76	0.40	43.54
Tzi16	Nigeria	302	PI 540747 = N28/RPPTZSR-Y	59.69	7.18	0.12	51.96	70.55	27.47	0.39	42.50
Tzi18	Nigeria	302	Sete Lagoas 7728 x TZSR	60.51	7.52	0.13	52.62	69.97	20.53	0.30	48.01
Tzi25	Nigeria	302	[(B73*RPPSR-TZ)*B73(2)]	64.17	15.66	0.24	51.07	71.41	45.72	0.65	27.06
Tzi8	Nigeria	302	TZB x TZSR	65.70	2.39	0.04	63.11	74.74	5.76	0.08	68.88
Tzi9	Nigeria	302	SIDS7734/TZSR	65.49	14.04	0.20	53.64	73.21	33.80	0.46	40.39
U267Y	South Africa	302	WF9r*Mex.155^3	58.09	5.57	0.10	51.30	76.00	17.50	0.23	59.07
Va102	Virginia	302	Va59*Va60	57.44	7.03	0.13	49.60	72.08	26.04	0.37	45.90
Va14	Virginia	302	[(VaCBS selection*Va17)Va17]	59.78	15.51	0.26	46.37	71.29	41.64	0.59	30.61
Va17	Virginia	302	Wf9*T8	67.27	16.42	0.23	53.97	82.24	49.53	0.56	38.51
Va22	Virginia	302	Va17*C103 backcross	58.19	21.26	0.37	40.70	72.74	46.71	0.64	28.00
Va26	Virginia	302	Oh43*K155	55.62	7.27	0.14	47.44	75.55	20.61	0.27	55.61
Va35	Virginia	302	[(C103*T8)T8]	61.41	18.62	0.29	46.03	72.50	41.19	0.57	32.69
Va59	Virginia	302	[(C103*T8(2))*(K4*C103(2))]	64.26	9.98	0.15	55.06	73.68	33.11	0.45	41.67

Inbred	State/Country	Panel Type	Pedigree	WT_CCMI	MT_CCMI	Ratio_CCMI	Diff_CCMI	WT_CCMII	MT_CCMII	Ratio_CCMII	Diff_CCMII
Va85	Virginia	302	Virginia Long Ear Synthetic	54.30	7.97	0.16	45.51	67.81	23.53	0.36	42.31
Va99	Virginia	302	Oh07B*Pa91	63.49	8.10	0.13	55.49	76.12	31.44	0.40	46.55
VaW6	Virginia	302	unknown	63.00	2.74	0.05	58.61	75.66	9.06	0.12	66.28
W117HT	Wisconsin	302	W117=643*Minnesota No.13	57.68	8.94	0.16	48.55	77.54	32.83	0.41	47.23
W153R	Wisconsin	302	[(la153*W8)la153]	65.49	16.23	0.23	52.14	73.54	53.63	0.72	22.80
W182B	Wisconsin	302	WD*W22	55.18	9.12	0.18	45.69	70.58	27.21	0.39	42.77
W22	Wisconsin	302	III.B10*W25	59.82	7.78	0.13	52.00	75.36	31.99	0.42	43.54
W401	Wisconsin	302	[(33*Wisconsin No.25)*67C]	63.81	16.10	0.24	50.39	75.81	50.00	0.64	29.24
W64A	Wisconsin	302	Wf9*CI.187-2	59.77	8.66	0.15	51.04	73.94	24.68	0.33	49.70
Wf9	Indiana	302	Reid yellow dent (Indiana station strain)	61.20	7.66	0.13	53.28	75.95	22.09	0.29	54.83

Table S5. The summary of the HapMap3 variants before and after filtering to remove SNPs with minor allele frequency < 0.05 (5%) and missing > 0.1 (10%).

Chromosome	Sites_before_filtering	Sites_after_filtering
1	12550106	2900472
2	9620462	2247603
3	9415581	2208140
4	9862608	2146099
5	8226794	1855240
6	6502278	1430027
7	6902443	1632102
8	6619311	1510768
9	6112165	1528972
10	5875644	1327869
Total	**81687392**	**18787292**

Table S6. The chlorophyll accumulation in the third fully-expanded leaf at the V3 stage of greenhouse-grown maize seedlings.

Genotype	CCM (Index)	Chlorophyll *a* (mg/g FW)	Chlorophyll *b* (mg/g FW)	Total Chlorophyll (mg/g FW)	Chl *a*/*b* ratio	Total Carotenoids (mg/g FW)
Mo17/B73	27.04±2.11^{a}	1.48±0.10^{a}	0.42±0.026^{a}	1.90±0.12^{a}	3.50±0.05^{d}	0.20±0.011^{a}
Oy1-N1989/oy1:Mo17/B73	5.74±0.11^{e}	0.38±0.02^{d}	0.07±0.005^{d}	0.45±0.02^{d}	5.48±0.16^{b}	0.04±0.002^{e}
B73/Mo17	22.86±0.29^{b}	1.15±0.04^{b}	0.32±0.015^{b}	1.47±0.05^{b}	3.57±0.10^{d}	0.16±0.004^{b}
Oy1-N1989/oy1:B73/Mo17	4.35±0.22^{e}	0.36±0.03^{d}	0.06±0.008^{d}	0.42±0.04^{d}	6.03±0.25^{a}	0.05±0.002^{de}
B73	25.19±1.12^{ab}	1.13±0.03^{b}	0.32±0.008^{b}	1.47±0.04^{b}	3.54±0.03^{d}	0.16±0.003^{bc}
Mo17	16.18±0.97^{c}	0.98±0.03^{b}	0.29±0.008^{b}	1.27±0.04^{b}	3.44±0.03^{d}	0.14±0.001^{c}
Oy1-N1989/oy1:B73	10.18±0.42^{d}	0.57±0.03^{c}	0.13±0.008^{c}	0.70±0.03^{c}	4.40±0.07^{c}	0.06±0.003^{d}
Oy1-N1989/Oy1-N1989$^{\&}$	1.00±0.00^{f}	n.d	n.d	-	-	0.01±0.001^{f}

Data are presented as means ± standard deviation. Each values is a mean of three biological replicates except for Mo17 with two replications. The connecting letter report between data within each trait indicates statistical significance determined using ANOVA with post-hoc analysis to compare means between genotypes using Tukey's HSD at $p<0.05$. CCM meter reads a value of 1.00 for blank.

$^{\&}$Homozygote seedlings were obtained in B73 background and the measurements were performed on first leaf of 10 days old seedlings, n=5.

Table S7. Means and standard deviation of pigment absorbance (index) from mutant (*Oy1-N1989/oy1*) and wild-type plants grown at the Purdue Agronomy Farm.

Genotype	CCMI	CCMII
B73	57.3±8.0[a]	67.0±5.2[a]
Mo17/B73	57.8±7.3[a]	76.4±5.6[b]
Oy1-1989/oy1:B73	6.8±1.3[b]	27.7±3.2[c]
Oy1-1989/oy1:Mo17/B73	2.3±0.5[c]	9.8±1.7[d]

The connecting letter report indicates statistical significance determined using ANOVA followed by mean comparisons between the genotypes using Tukey's HSD at $p<0.01$. Check materials and methods for trait descriptions.

Table S8. The trait correlations among the CCM traits in IBM x *Oy1-N1989/oy1*:B73 F_1 hybrid populations.

	WT_CCMI	MT_CCMI	Ratio_CCMI	Diff_CCMI	WT_CCMII	MT_CCMII	Ratio_CCMII	Diff_CCMII
WT_CCMI		0.069	-0.222	0.901	0.368	0.062	-0.045	0.235
MT_CCMI	0.312		0.948	-0.371	0.059	0.875	0.859	-0.616
Ratio_CCMI	0.001	<.0001		-0.619	-0.062	0.829	0.855	-0.673
Diff_CCMI	<.0001	<.0001	<.0001		0.317	-0.323	-0.416	0.487
WT_CCMII	<.0001	0.39	0.363	<.0001		0.136	-0.156	0.664
MT_CCMII	0.361	<.0001	<.0001	<.0001	0.046		0.947	-0.651
Ratio_CCMII	0.513	<.0001	<.0001	<.0001	0.021	<.0001		-0.835
Diff_CCMII	0.001	<.0001	<.0001	<.0001	<.0001	<.0001	<.0001	

The upper half contains Pearson's correlation coefficient and the lower half contains correlation p-values for each pairwise trait comparison. Self-comparisons (diagonal) are left blank.

Table S9. The trait Correlations among the CCM traits in Syn10 x *Oy1-N1989/oy1*:B73 F_1 hybrid populations.

	WT_CCMI	MT_CCMI	Ratio_CCMI	Diff_CCMI	WT_CCMII	MT_CCMII	Ratio_CCMII	Diff_CCMII
WT_CCMI		0.107	-0.118	0.899	0.367	0.156	0.077	0.032
MT_CCMI	0.0926		0.965	-0.340	-0.035	0.889	0.910	-0.852
Ratio_CCMI	0.0628	<.0001		-0.537	-0.084	0.858	0.887	-0.846
Diff_CCMI	<.0001	<.0001	<.0001		0.365	-0.244	-0.329	0.406
WT_CCMII	<.0001	0.583	0.185	<.0001		0.125	-0.124	0.370
MT_CCMII	0.014	<.0001	<.0001	<.0001	0.049		0.960	-0.876
Ratio_CCMII	0.228	<.0001	<.0001	<.0001	0.05	<.0001		-0.960
Diff_CCMII	0.613	<.0001	<.0001	<.0001	<.0001	<.0001	<.0001	

The upper half contains Pearson's correlation coefficient and the lower half contains correlation p-values for each pairwise trait comparison. Self-comparisons (diagonal) are left blank.

Table S10. The summary of the QTL detected for CCM traits in IBM x *Oy1-N1989/oy1*:B73 F_1 hybrid populations.

							LOD-2 Interval[e]			Mean±SE[g]		
Trait Identifier	QTL[a]	Chr[b]	LOD[c]	Position[d]	Left Marker	Right Marker	Left	Right	PVE[f]	B73	Mo17	Greater Allele
MT_CCMI	1	10	46.9	139	AI795367	AY109994	137	141	53.68	8.81±0.188	4.16±0.226	B73
WT_CCMI	1	1	3.6	523	bnl5.59a	php20654	519	534	7.12	47.27±0.548	43.51±0.734	B73
MT_CCMII	1	10	45.0	139	AI795367	AY109994	128	141	51.48	18.27±0.448	7.38±0.585	B73
WT_CCMII	0											
Ratio_CCMI	1	10	39.7	139	AI795367	AY109994	137	145	50.19	0.19±0.004	0.09±0.005	B73
Ratio_CCMII	1	10	44.4	139	AI795367	AY109994	137	142	55.38	0.36±0.009	0.14±0.01	B73
Diff_CCMI	1	10	6.6	145	phi059	isu85b	126	153	13.18	36.89±0.576	42.24±0.724	B73
Diff_CCMII	1	10	22.4	138	AI795367	AY109994	129	142	36.80	32.95±0.687	44.77±0.912	B73

[a]Number of QTL detected for a given trait
[b]Chromosome location of a QTL
[c]LOD score at the peak of a given QTL
[d]Peak position and [e]LOD-2 interval of the QTL in terms of genetic position in centiMorgan(cM)
[f]PVE is percent of variance explained by the QTL at this position as estimated by regression and reported as an R^2 value*100
[g]Mean and standard error of the trait with B73 and Mo17 genotype at the peak marker of the detected QTL

Table S11. The summary of the QTL detected from CCM traits in Syn10 x *Oy1-N1989/oy1*:B73 F_1 hybrid populations.

							LOD-2 Interval[e]			Mean±SE[g]		
Trait	QTL[a]	Chr[b]	LOD[c]	Position[d]	Left Marker	Right Marker	Left	Right	PVE[f]	B73	Mo17	Greater allele
MT_CCMI	1	10	59.9	189	chr10.90.5	chr10.93	189	193	65.2	7.00±0.117	2.65±0.174	B73
WT_CCMI	0											
Ratio_CCMI	1	10	54.0	189	chr10.90.5	chr10.93	189	192	62.1	0.14±0.002	0.05±0.003	B73
Diff_CCMI	0											
MT_CCMII	1	10	83.6	192	chr10.94.5	chr10.95.5	190	193	66.5	29.07±0.478	8.39±0.731	B73
WT_CCMII	0											
Ratio_CCMII	1	10	78.1	192	chr10.94.5	chr10.95.5	190	193	66.9	0.40±0.006	0.11±0.010	B73
Diff_CCMII	1	10	52.1	189	chr10.90.5	chr10.93	189	191	60.3	42.46±0.623	63.39±0.926	B73

[a]Number of QTL detected for a given trait
[b]Chromosome location of a QTL
[c]LOD score at the peak of a given QTL
[d]Peak position and [e]LOD-2 interval of the QTL in terms of genetic position in centiMorgan(cM)
[f]PVE is percent of variance explained by the QTL at this position as estimated by regression and reported as an R^2 value*100
[g]Mean and standard error of the trait with B73 and Mo17 genotype at the peak marker of the detected QTL

Table S12. Recombinants within the *vey1* region derived from Syn10 x *Oy1-N1989/oy1*:B73 F_1 populations.

Line ID	MT_CCMI	Ratio_CCMI	MT_CCMII	Ratio_CCMII	chr10.90.5	chr10.93	chr10.94.5	chr10.95.5	Category[1]
IBM_31	7.0	0.13	33.2	0.46	B	A	A	A	Suppressed
IBM_41	2.3	0.05	7.0	0.10	B	B	A	A	Enhanced
IBM_149	1.7	0.03	5.7	0.09	B	B	B	A	Enhanced
IBM_144	1.7	0.03	5.6	0.07	B	B	B	A	Enhanced
IBM_199	8.9	0.20	30.1	0.41	A	A	A	B	Suppressed
IBM_201	8.5	0.15	32.0	0.40	A	A	A	B	Suppressed
IBM_214	1.8	0.03	5.5	0.07	B	B	B	A	Enhanced
IBM_217	2.4	0.04	7.3	0.10	B	B	B	A	Enhanced
IBM_229	9.7	0.17	34.8	0.49	B	A	A	A	Suppressed

The genotype code ‘A’ and ‘B’ for each marker denote B73 and Mo17 genotype, respectively.

[1]Severity of the mutation. Check the respective CCM trait value for quantitative assessment of severity.

Table S13. The trait correlations of various CCM traits using mean values of MDL x *Oy1-N1989/oy1*:B73 F_1 hybrid populations.

	WT_CCMI	MT_CCMI	Ratio_CCMI	Diff_CCMI	WT_CCMII	MT_CCMII	Ratio_CCMII	Diff_CCMII
WT_CCMI		0.182	-0.047	0.825	0.329	0.178	0.124	0.007
MT_CCMI	0.001		0.964	-0.405	0.135	0.861	0.846	-0.750
Ratio_CCMI	0.410	<.0001		-0.596	0.080	0.823	0.818	-0.746
Diff_CCMI	<.0001	<.0001	<.0001		0.231	-0.329	-0.372	0.438
WT_CCMII	<.0001	0.012	0.142	<.0001		0.171	-0.028	0.351
MT_CCMII	0.002	<.0001	<.0001	<.0001	0.002		0.976	-0.862
Ratio_CCMII	0.030	<.0001	<.0001	<.0001	0.601	<.0001		-0.942
Diff_CCMII	0.904	<.0001	<.0001	<.0001	<.0001	<.0001	<.0001	

The upper half contains Pearson's correlation coefficient and the lower half contains correlation p-values for each pairwise trait comparison. Self-comparisons (diagonal) are left blank.

Table S14. The broad sense heritability and variance estimates of CCM traits measured in MDL x *Oy1-N1989/oy1*:B73 F_1 hybrid populations.

Trait	Heritability	LSD	Variance
WT_CCMI	0.59	14.56	80.64
MT_CCMI	0.95	3.22	18.77
Ratio_CCMI	0.92	0.06	0.01
Diff_CCMI	0.65	14.53	88.81
WT_CCMII	0.63	11.74	57.20
MT_CCMII	0.96	7.36	126.66
Ratio_CCMII	0.94	0.12	0.02
Diff_CCMII	0.87	13.37	169.53

Table S15. The summary of the top four statistically significant SNP markers associated with CCM traits by GWAS and top SNP following the addition of S10_9161643 as a covariate for each trait.

Trait	SNP[1]	P-value	MAF[2]	PVE[3]	FDR[4]
MT_CCMI	S10_9161643	2.12E-10	0.49	11.38	0.000281683
	S10_8785697	1.70E-09	0.46	10.16	0.001131981
	S10_8994665	1.29E-08	0.36	9.00	0.002713112
	S10_8937688	1.41E-08	0.38	8.95	0.002713112
	S10_9179932	2.04E-08	0.08	8.73	0.002713112
MT_CCMI with S10_9161643 covariate	S10_9179932	6.58E-08	0.08	6.82	0.063
Ratio_CCMI	S10_9161643	5.43E-09	0.49	9.93	0.003601250
	S10_9326761	6.87E-09	0.10	9.79	0.003601250
	S10_9327646	9.04E-09	0.11	9.62	0.003601250
	S10_9179932	1.08E-08	0.08	9.51	0.003601250
Ratio_CCMI covariate with S10_9161643 covariate	S10_9179932	5.16E-08	0.08	7.57	0.043
MT_CCMII	S10_9161643	1.61E-15	0.49	18.41	0.000000002
	S10_8937688	6.76E-12	0.38	13.27	0.000004489
	S10_9047937	1.33E-11	0.38	12.86	0.000004524
	S10_9104770	1.36E-11	0.36	12.85	0.000004524
	S10_9179932	2.16E-08	0.08	8.59	0.000073403
MT_CCMII covariate with S10_9161643 covariate	S10_9179932	3.60E-09	0.08	7.29	0.005
Ratio_CCMII	S10_9161643	1.98E-14	0.49	16.82	0.000000026
	S10_8937688	1.42E-12	0.38	14.20	0.000000653
	S10_9001249	1.63E-12	0.34	14.12	0.000000653
	S10_8996692	3.78E-12	0.33	13.61	0.000000653
	S10_9179932	1.24E-08	0.08	8.90	0.000034587

Trait	SNP[1]	P-value	MAF[2]	PVE[3]	FDR[4]
Ratio_CCMII covariate with S10_9161643 covariate	S10_9179932	2.39E-09	0.08	7.64	0.003

Except for Ratio_CCMI trait, the S10_9179932 marker was not among the top four SNP associations in no covariate model and is thus provided for comparison with the covariate model. [1]SNP markers associated with the respective traits. S10 denotes SNP markers on chromosome 10 followed by the physical position of the markers from the B73 v4 assembly; [2]Minor allele frequency (MAF) of the SNP marker; [3]Phenotypic variance explained (PVE) by the SNP marker; [4]Chromosome-wide FDR adjusted P-value.

Table S16. Haplotypes at two SNPs at *vey1* locus associated with *Oy1-N1989* suppression and its effect on CCM traits in MDL x *Oy1-N1989*/*oy1*:B73 F_1 populations.

Haplotype[&]	Sample (n)	WT_CCMI	MT_CCMI	Ratio_CCMI	WT_CCMII	MT_CCMII	Ratio_CCMII
AG	153	60.86±3.69[a]	10.00±4.13[a]	0.16±0.06[a]	72.57±3.45	30.99±9.19[a]	0.43±0.12[a]
CG	121	59.00±4.21[b]	7.65±2.42[b]	0.13±0.04[b]	72.04±3.97	22.65±6.69[b]	0.32±0.09[b]
AA	8	58.56±2.43[ab]	3.93±1.17[c]	0.07±0.02[c]	73.78±3.74	15.28±4.90[c]	0.21±0.07[c]
CA	23	60.53±4.45[ab]	2.78±0.99[c]	0.05±0.02[c]	72.99±3.08	10.63±2.82[c]	0.15±0.03[c]

[&]The first nucleotide of the haplotype denotes variant (A/C) at SNP S10_9161643 and the second nucleotide of the haplotype denotes variant (G/A) at SNP S10_9179932. The physical positions of these SNPs are from the B73 v4 assembly.

Table S17. The chlorophyll quantification of plants segregating for the allelic interaction between *Oy1-N1989* and *oy1-yg* alleles at *oy1*.

Cross	Days after planting	*Oy1-N1989/oy1-yg*	*Oy1-N1989/+*	*oy1-yg/+*	*oy1-yg/oy1-yg*
(Mo17 x *oy1-yg/oy1-yg*) x *Oy1-N1989*/+:B73	21	1.7±0.4[a]	3.0±0.6[a]	.	.
(B73 x *oy1-yg/oy1-yg*) x *Oy1-N1989*/+:B73	21	2.9±0.5[b]	5.1±0.8[b]	.	.
(Mo17 x *oy1-yg/oy1-yg*) x *Oy1-N1989*/+:B73	40	3.7±0.6[c]	7.0±0.3[c]	.	.
(B73 x *oy1-yg/oy1-yg*) x *Oy1-N1989*/+:B73	40	7.5±0.9[d]	17.1±3.3[d]	.	.
(Mo17 x *oy1-yg/oy1-yg*) x *oy1-yg/oy1-yg*	21	.	.	27.6±5.7[a]	7.6±2.8[a]
(B73 x *oy1-yg/oy1-yg*) x *oy1-yg/oy1-yg*	21	.	.	27.8±6.8[a]	8.1±2.8[a]
(Mo17 x *oy1-yg/oy1-yg*) x *oy1-yg/oy1-yg*	40	.	.	32.2±4.9[b]	16.7±5[b]
(B73 x *oy1-yg/oy1-yg*) x *oy1-yg/oy1-yg*	40	.	.	38.7±6.1[b]	21±6.2[b]

Data are presented as means and standard deviations. The sample size in each category varies from 5-20 plants. Comparisons to declare statistical significance were done only between the crosses with B73 and Mo17 as a parent within each genotype class of the progenies quantified on the same day (i.e. within 21 or 40 days after planting). The connecting letter report between the two samples indicates the statistical significance at $p < 0.05$ using student's t-test.

Table S18. The summary of the average CCM value of the F_1 hybrids of inbred lines crossed with *Oy1-N1989/oy1*:B73, and allelic state at the 6 bp (two amino acids) indel in the coding sequence of OY1 transcript in the respective parental inbred line.

Inbred	Insertion[a]	MT_CCMI	WT_CCMI	Ratio_CCMI	MT_CCMII	WT_CCMII	Ratio_CCMII	Category[b]
NC350	AT	12.7	68.1	0.19	36.2	76.6	0.48	sup
NC358	AT	12.6	53.3	0.24	36.9	70.3	0.54	sup
CML69	AT	9.9	71.0	0.14	27.5	69.9	0.39	sup
B97	AS	9.9	59.7	0.17	31.5	76.9	0.41	sup
Mo18W	AS	9.1	68.1	0.13	24.4	75.2	0.33	sup
Oh43	AS	8.7	58.4	0.15	24.3	57.9	0.42	sup
W22	AT	8.5	64.4	0.13	37.8	74.6	0.51	sup
IL14H	AT	7.7	50.3	0.15	22.5	68.8	0.33	sup
B73	-	7.0	57.2	0.12	26.3	69.4	0.38	sup
MS71	AS	6.9	60.3	0.11	12.9	71.1	0.18	sup
P39	AT	6.5	41.6	0.16	16.9	64.7	0.26	sup
Oh7b	AS	6.5	54.2	0.12	24.6	70.4	0.35	sup
CML103	-	6.3	55.1	0.12	17.6	75.6	0.23	sup
CML322	-	4.6	61.9	0.07	21.1	72.4	0.29	enh
Ki3	AT	4.0	59.5	0.07	19.9	70.2	0.28	enh
CML247	AT	3.1	70.6	0.04	14.1	79.1	0.18	enh
Tzi8	AT	2.4	71.0	0.03	5.4	78.8	0.07	enh
Mo17	AS	2.0	53.7	0.04	9.6	76.5	0.13	enh
Linear Fit (R^2)[c]		**0.009**	**0.00003**	**0.005**	**0.002**	**0.008**	**0.0009**	
P-value[d]		**0.49**	**0.66**	**0.56**	**0.56**	**0.87**	**0.64**	

Data were derived from three replications planted in a RCBD.

[a]Coding sequence polymorphism in the third exon of OY1 protein with three alternate alleles. Abbreviated symbols are A:Alanine, T:Threonine, S:Serine, -:Deletion of both amino acids.

[b]Category of the genotypes in terms of the severity of *Oy1-N1989/oy1*:B73/inbred F_1 mutant individuals assigned based on CCMI and Ratio_CCMI trait value. Abbreviated symbols are sup:suppressed mutants, enh:enhanced/severe mutants.

[c]R^2 of the linear regression model using Indel polymorphism as an explanatory variable onto a given trait as a response variable.

[d]P-value of the analysis of variance for effect of Indel polymorphism on the respective trait value.

Table S19. The linear regression of the top *vey1* linked marker (isu085b) and CCM traits from wild-type and mutant siblings of IBM x *Oy1-N1989/oy1*:B73 F_1 populations on to OY1 expression (RPKM values) of the respective IBM line (n=74).

Trait/Marker	R^2 (%)	P-value
isu085b	19.2	<0.0001
MT_CCMI	25.2	<0.0001
WT_CCMI	4.8	0.06
MT_CCMII	27.3	<0.0001
WT_CCMII	0.9	0.40
Ratio_CCMI	31.3	<0.0001
Ratio_CCMII	22.5	<0.0001

Table S20. The allele expression bias at *oy1* in leaf tissue from the top fully-expanded leaf at the V3 stage.

Genotype	SNP_252[1]	SNP252_Ref[2]	SNP_252_Alt[3]	SNP_317	SNP317_Ref	SNP317_Alt	Ratio_SNP252[Ψ]	Ratio_SNP317[+]	Average[%]
oy1/*oy1*:B/M[&]	.	.	.	.	.	.	.	.	1.19±0.07
oy1/*oy1*:B/M	C/C	.	.	C/T	2635±51.60	2430±67.28	.	1.08±0.01[a]	1.08±0.01[a]
Oy1-N1989/*oy1*:M/B	C/T	2044±149.77	2291±152.87	C/T	2782±120.79	2522±67.29	1.12±0.01[a]	1.10±0.02[a]	1.11±0.01[a]
Oy1-N1989/*oy1*:B/M	C/T	2138±142.51	2456±122.46	C/T	2677.33±99.71	2425±95.50	1.15±0.03[a]	1.10±0.01[a]	1.13±0.02[a]
Oy1-N1989/*oy1*:B	C/T	2261±109.33	2290±76.62	C/C	.	.	1.01±0.02[b]	.	1.01±0.02[b]

The connecting letter report in all columns indicate statistical significance calculated using ANOVA with post-hoc analysis using Tukey's HSD with $p<0.01$.

[1]SNP position 252 with two alternate alleles. C corresponds to the wild-type/reference allele and T corresponds to the mutant/alternate allele. Same applies to SNP_317 column, except this SNP is polymorphic only between B73 and Mo17; *Oy1-N1989* allele is monomorphic with B73 at SNP_317.

[2]Mean ± standard deviation of allele count for the reference allele using three biological replications. Same applies to SNP317_Ref column. Same applies to SNP317_Ref column.

[3]Mean ± standard deviation of allele count for the alternate allele using three biological replications. Same applies to SNP317_Alt column. Same applies to SNP317_Alt column.

[&]Data obtained from Waters *et al*. 2017. Allele bias at *oy1* locus for plants grown under control condition.

[Ψ]Mean ± standard deviation of the ratios of the read count from reference allele to the alternate allele at SNP252.

[+]Mean ± standard deviation of the ratios of the read count from reference allele to the alternate allele at SNP317.

[%]Mean ± standard deviation of the average of the ratios at SNP position 252 and 317.

Table S21. The chlorophyll approximation (using CCM) from the middle of the third leaf at the V3 stage on greenhouse-grown maize seedlings from a cross of B73, Mo17, and PH207 inbred lines (ear-parents) with *Oy1-N1989/oy1*:B73 plants (pollen-parent).

Pedigree	Genotype	Sample size	CCM (Index)
B73	wild-type	8	21.16±2.65[a]
B73	mutant	5	7.95±0.45[b]
PH207/B73	wild-type	5	28.20±1.57[c]
PH207/B73	mutant	6	5.53±0.23[d]
Mo17/B73	wild-type	5	15.62±1.83[e]
Mo17/B73	mutant	5	3.90±0.12[d]

Data are presented as mean ± standard deviation. The connecting letter report indicates statistical significance calculated using ANOVA with post-hoc analysis using Tukey's HSD with $p<0.05$.

Table S22. The distribution of normalized OY1 expression in the emerging shoot tissue of maize diversity lines (Kremling *et al*. 2018) at two SNPs associated with suppression of *Oy1-N1989* phenotype in MDL x *Oy1-N1989*/*oy1*:B73 F_1 populations.

Variant	Allele/Haplotype	Sample Size	OY1 (count)	R^2 (%)[a]
S10_9161643	A	138	3.94 ± 0.24*	7.14
	C	119	3.79 ± 0.30	
S10_9179932	A	15	3.62 ± 0.20*	4.80
	G	242	3.89 ± 0.28	
Haplotypes	AG	132	3.95 ± 0.24[a]	11.24
	CG	110	3.81 ± 0.30[b]	
	AA	6	3.68 ± 0.17[bc]	
	CA	9	3.58 ± 0.23[c]	

Data are presented as mean ± standard error. An asterisk and the connecting letter report denotes the significant statistical difference between the means in each variant category determined using ANOVA, followed by mean comparisons using student's t-test at $p<0.05$.

[a]Variation explained by a given variant (first column) in OY1 expression. All the linear regression models were significant at $p<0.001$.

Table S23. The pairwise trait correlations between OY1 transcript abundance in the emerging shoots of maize inbred lines and the CCM traits of corresponding F_1 hybrids with *Oy1-N1989*/*oy1*:B73 for the 198 inbred lines common between the current study and Kremling *et al*. 2018.

	OY1 (count)	WT_CCMI	MT_CCMI	Ratio_CCMI	WT_CCMII	MT_CCMII	Ratio_CCMII
OY1 (count)		0.110	0.219	0.196	-0.075	0.169	0.191
WT_CCMI	0.133		0.231	0.004	0.295	0.212	0.162
MT_CCMI	0.003	0.001		0.967	0.154	0.865	0.853
Ratio_CCMI	0.007	0.958	<.0001		0.093	0.837	0.837
WT_CCMII	0.303	<.0001	0.030	0.194		0.209	-0.007
MT_CCMII	0.020	0.003	<.0001	<.0001	0.003		0.973
Ratio_CCMII	0.009	0.023	<.0001	<.0001	0.921	<.0001	

The upper half contains Pearson's correlation coefficient and the lower half contains correlation p-values for each pairwise trait comparison. Self-comparisons (diagonal) are left blank.

Figures

A *Very Oil Yellow1* modifier of the *Oil Yellow1-N1989* allele uncovers a cryptic phenotypic impact of cis-regulatory variation in maize

Rajdeep S. Khangura, Sandeep Marla, Bala P. Venkata, Nicholas J. Heller, Gurmukh S. Johal, and Brian P. Dilkes

Figure 1. The chlorophyll pigment accumulation differs in severity for *Oy1-N1989/oy1* heterozygotes in the B73 and B73 x Mo17 hybrid backgrounds. The representative wild-type (*oy1*/*oy1*) and mutant (*Oy1-N1989/oy1*) sibling from (a) B73 x *Oy1-N1989/oy1*:B73 and (b) Mo17 x *Oy1-N1989/oy1*:B73 F_1 crosses in the field-grown plants. The measuring stick in panel a and b is 243 cm. (c) Non-destructive chlorophyll approximation in mutant and wild-type siblings at an ~3 weeks (CCMI) and ~6 weeks (CCMII) after planting; data for each class of genotype is derived from 39 replications planted in RCBD. The asterisk indicates statistical significance between the means in each genotype category at $p < 0.01$ determined using student's t-test.

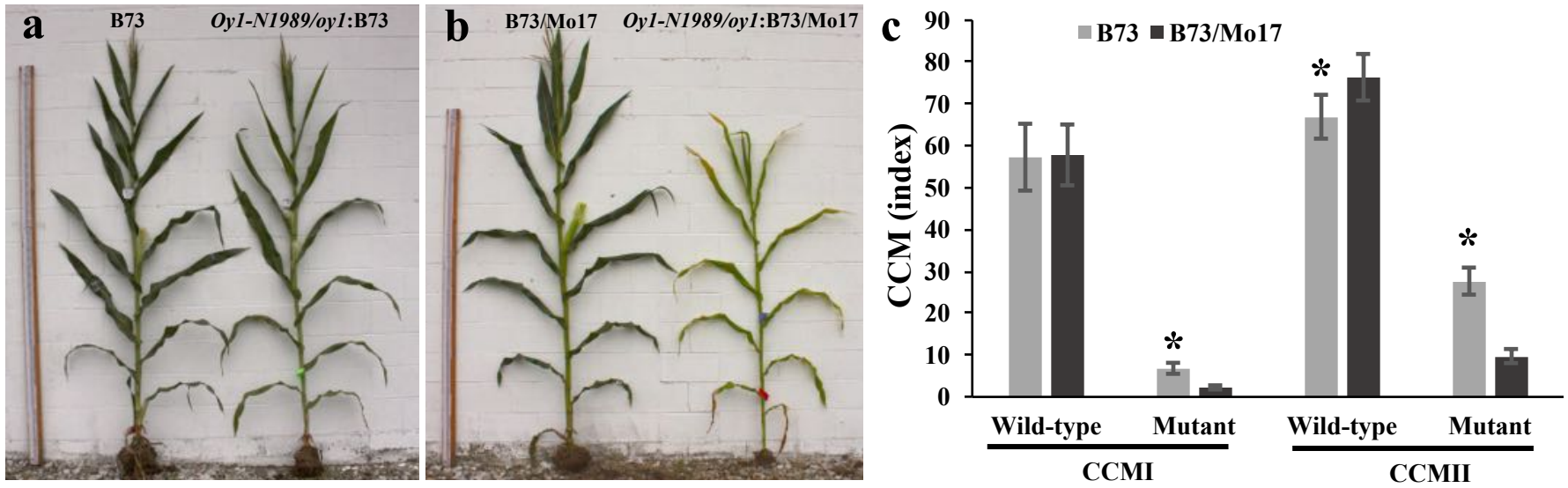

Figure 2. The crossing scheme used to map *Oy1-N1989* enhancer/suppressor loci in IBM and Syn10 populations. Red, blue and white colors indicate B73, Mo17, and missing genotypes. The heterozygous tester (*Oy1-N1989/oy1*:B73) shows chromosome 10 with a black dot indicating *Oy1-N1989* mutant allele. The F_1 progenies depicted here shows a hypothetical state of chromosome 10 for each F_1 progeny showing segregation of wild-type and mutant (with the black spot) siblings.

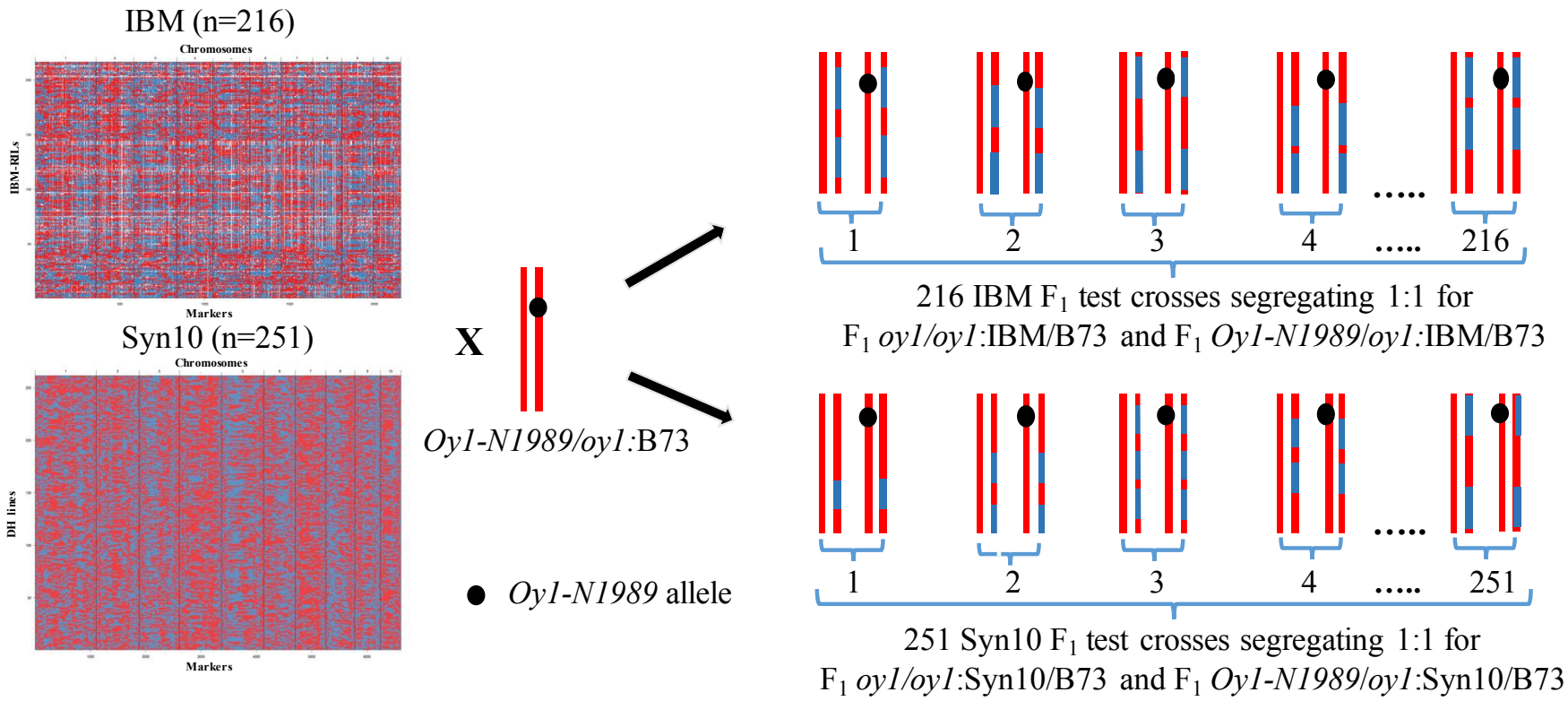

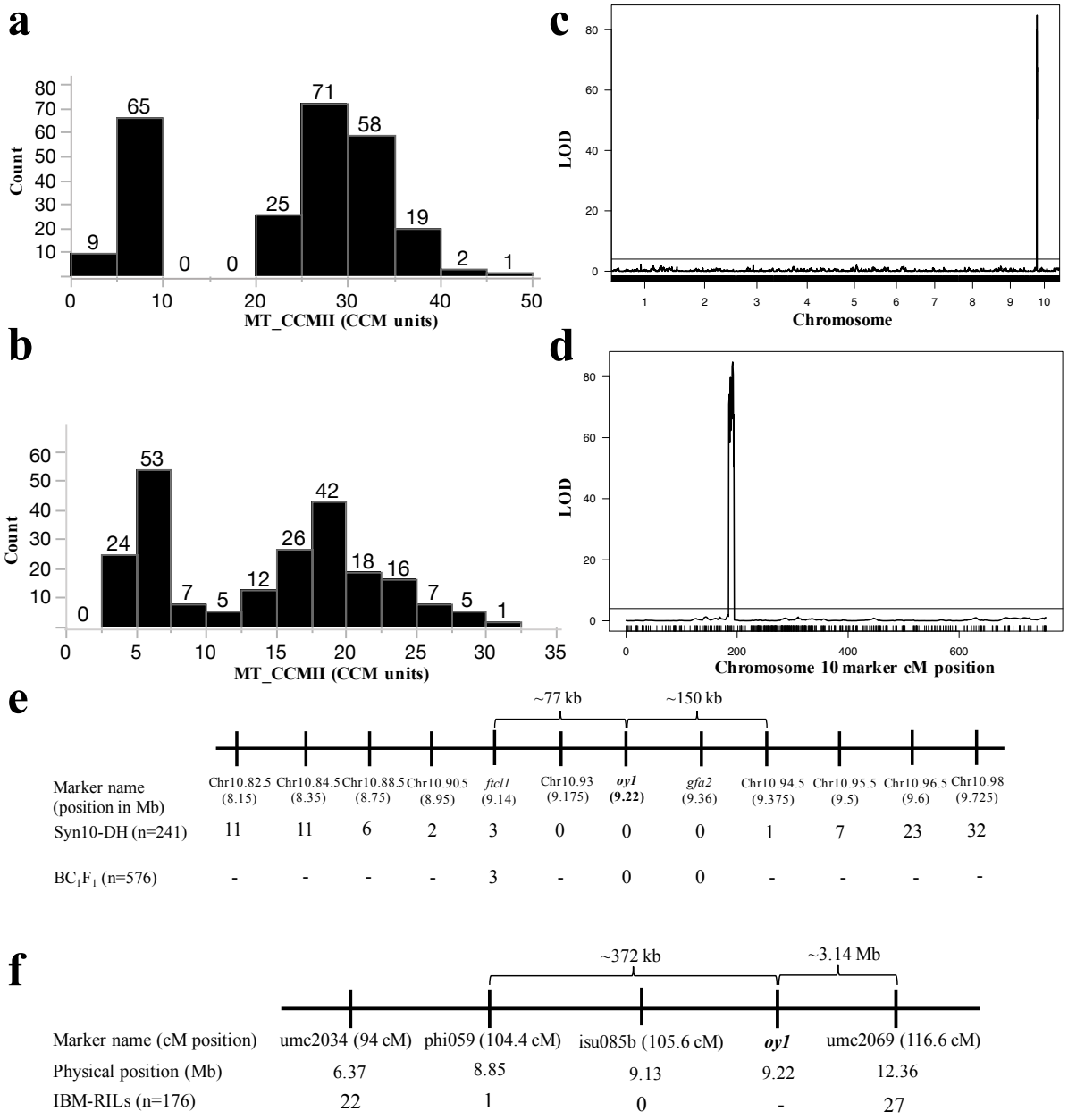

Figure 3. The phenotypic distribution, QTL analysis, and fine mapping results of MT_CCMII trait. The distribution of MT_CCMII in (a) Syn10 x *Oy1-N1989/oy1*:B73 F_1 population and (b) IBM x *Oy1-N1989/oy1*:B73 F_1 population. (c) Genome-wide QTL plot of MT_CCMII in Syn10 x *Oy1-N1989/oy1*:B73 F_1 population. The x-axis indicates the chromosome number and Y-axis indicates the logarithm to the base 10 of odds (LOD) of tested markers. Black horizontal bar indicates the permutation testing-based threshold to declare statistical significance of the QTL. (d) Close-up view of the vey1 locus on chromosome 10. The x-axis indicates the centiMorgan (cM) position of the molecular markers. Recombinants detected in F_1 crosses of *Oy1-N1989/oy1*:B73 as pollen-parent with (e) Syn10 lines and B73 x Mo17 F_1 (BC_1F_1), and (f) IBM. A number at a given marker and population intersection in (e) and (f) indicates the total number of recombinants between the respective marker genotype and phenotype; hyphen denotes no genotyping. dCAPS marker at *oy1* is highlighted in bold.

Figure 4. The Manhattan plots of SNPs associations with MT_CCMII trait in MDL x *Oy1-N1989/oy1*:B73 F_1 populations. The genome-wide association of (a) MT_CCMII, (b) MT_CCMII using S10_9161643 as a covariate. The close-up view of the region on chromosome 10 for (c) MT_CCMII result shown in panel a, (d) MT_CCMII results shown in panel b. Arrows in panels a-d identify the data point corresponding to SNPs S10_9161643 and S10_9179932. The horizontal red and hashed red lines in panels a-d indicates the genome-wide Bonferroni cut-off at p<0.05 and hashed golden line in panels c-d is the chromosome-wide FDR-adjusted threshold at p<0.05. The linkage disequilibrium of all SNPs in a ~450 kb region around *oy1* with SNPs (e) S10_9161643, and (f) S10_9179932. Vertical lines in panels c-f from left to right represent the genomic position of *ftcl1*, *ereb28*, *oy1* (green), and *gfa2* loci.

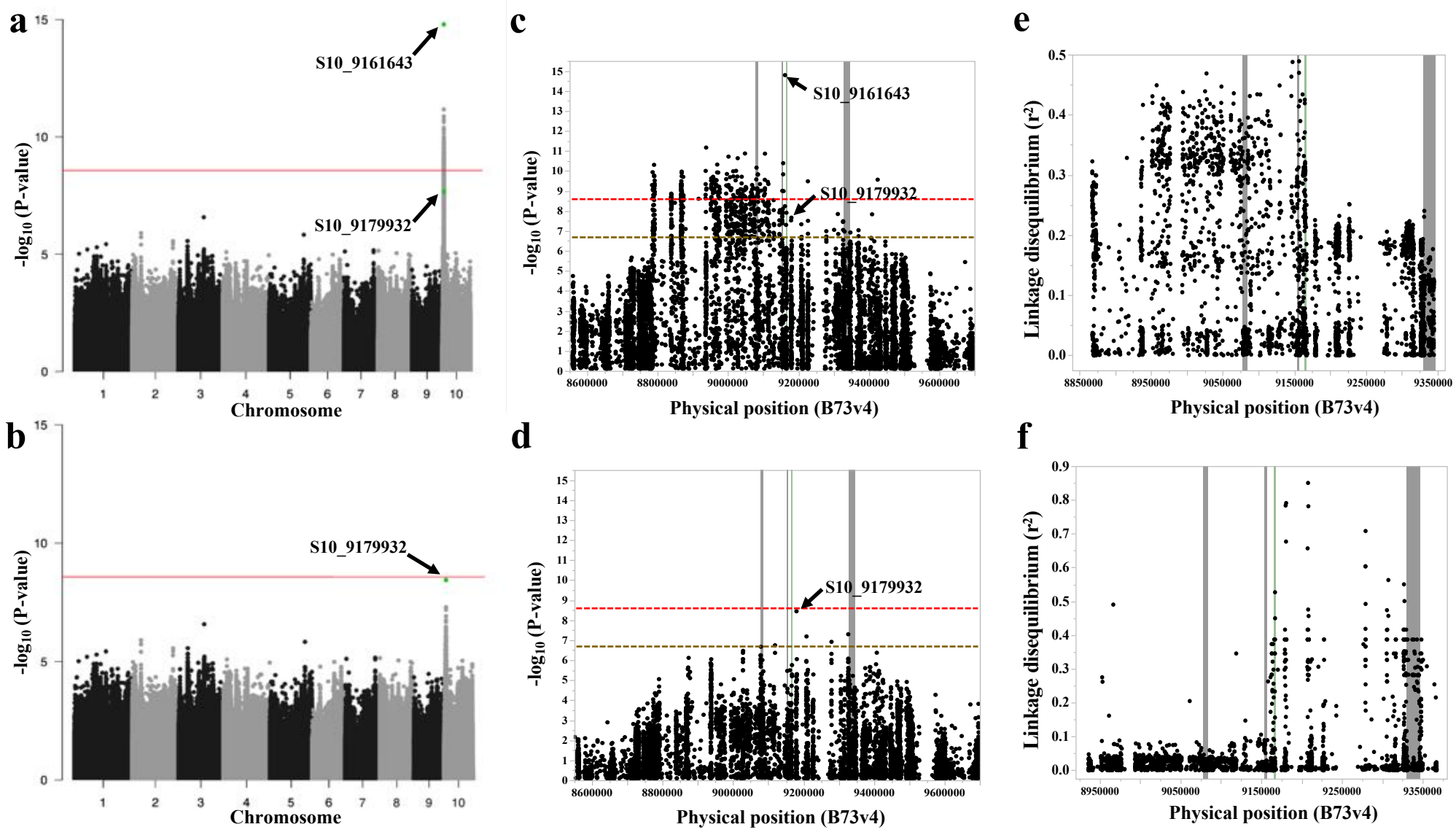

Figure 5. The single locus test of *oy1* showing the interaction between wild-type alleles of *oy1* from B73 and Mo17 with semi-dominant and recessive mutant alleles *Oy1-N1989* and *oy1-yg*, respectively. (a) Mutant (two severity groups) and wild-type individuals segregating in a cross (B73 x *oy1-yg/oy1-yg*) x *Oy1-N1989/oy1*:B73. White-fill arrows indicate *Oy1-N1989/oy1* plants (pale-green and suppressed), whereas yellow-fill arrows indicate *Oy1-N1989/oy1-yg* (yellow-green and severe) plants. The CCM measurements of testcrosses at 21 and 40 days after planting in the (b) mutant siblings (*Oy1-N1989/oy1-yg* and *Oy1-N1989*/+) of (Mo17 x *oy1-yg/oy1-yg*) x *Oy1-N1989*/+:B73, and (B73 x *oy1-yg/oy1-yg*) x *Oy1-N1989*/+:B73 crosses, (c) mutant (*oy1-yg/oy1-yg*) and wild-type (*oy1-yg*/+) siblings of (Mo17 x *oy1-yg/oy1-yg*) x *oy1-yg/ oy1-yg* and (B73 x *oy1-yg/oy1-yg*) x *oy1-yg/ oy1-yg* crosses. Asterisks in panel b-c indicate the significant difference of mean between the genotypes in a given cross at $p<0.01$ determined using student's t-test. Check supplemental information for details.

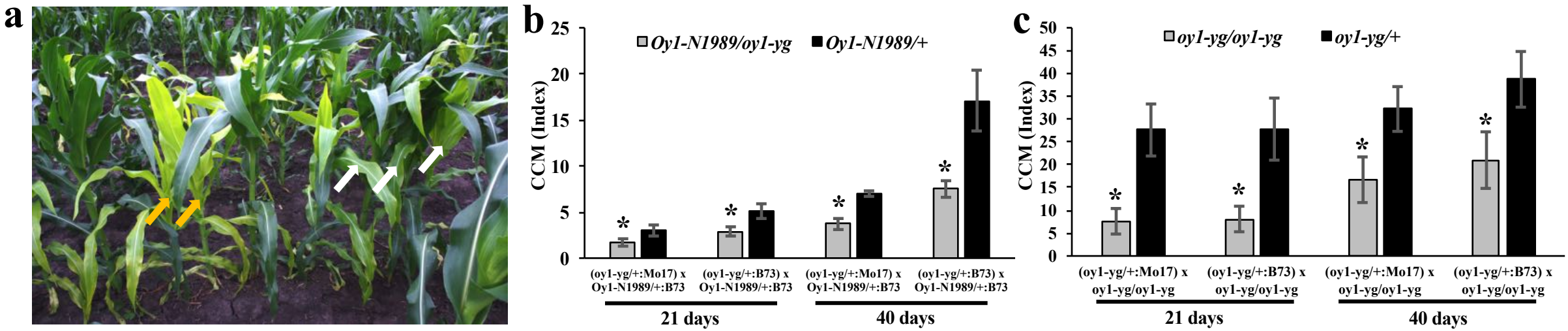

Figure 6. The distributions of CCM trait measurements in the F_1 progenies of a sub-set of maize inbred lines crossed with *Oy1-N1989/oy1*:B73 at three allelic variants in the *oy1* coding sequence identified in respective inbred lines. The phenotypic distribution of (a) MT_CCMI, (b) WT_CCMI, (c) MT_CCMII, and (d) WT_CCMII. Symbols "-", "AS", and "AT" on the X-axis denote deletion of 6 base pairs (bp), insertion of amino acid residues Alanine-Serine (AS), and Alanine-Threonine (AT), respectively. Three inbred lines including B73 carried "-" allele, six inbred lines carried "AS" insertion, nine inbred lines carried "AT" insertion. No statistically significant difference was found among the three distributions in all panels using ANOVA. Check the supplemental information for more details.

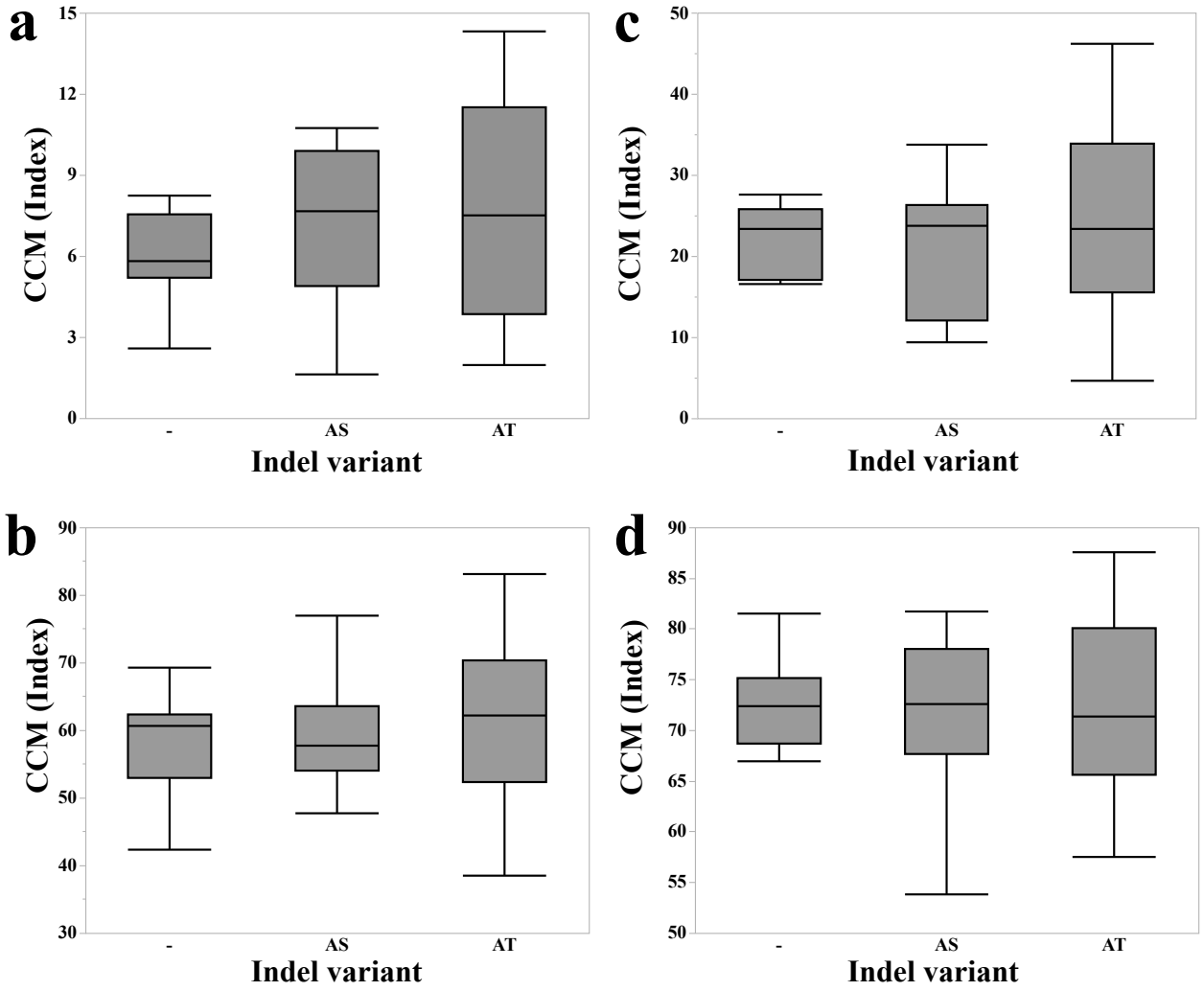

Figure 7. Expression of OY1 in the shoot apices of 14 days old IBM seedlings co-segregates with *vey1*. (a) Genotypic distribution of OY1 RPKM (X-axis) at the marker isu085b (linked to *vey1*). An asterisk indicates the significant difference in the mean between two groups using Student's t-test at p<0.01. The linear regression of OY1 expression in IBM on CCMII in the (b) wild-type and (c) mutant siblings derived from IBM x *Oy1-N1989/oy1*:B73 crosses.

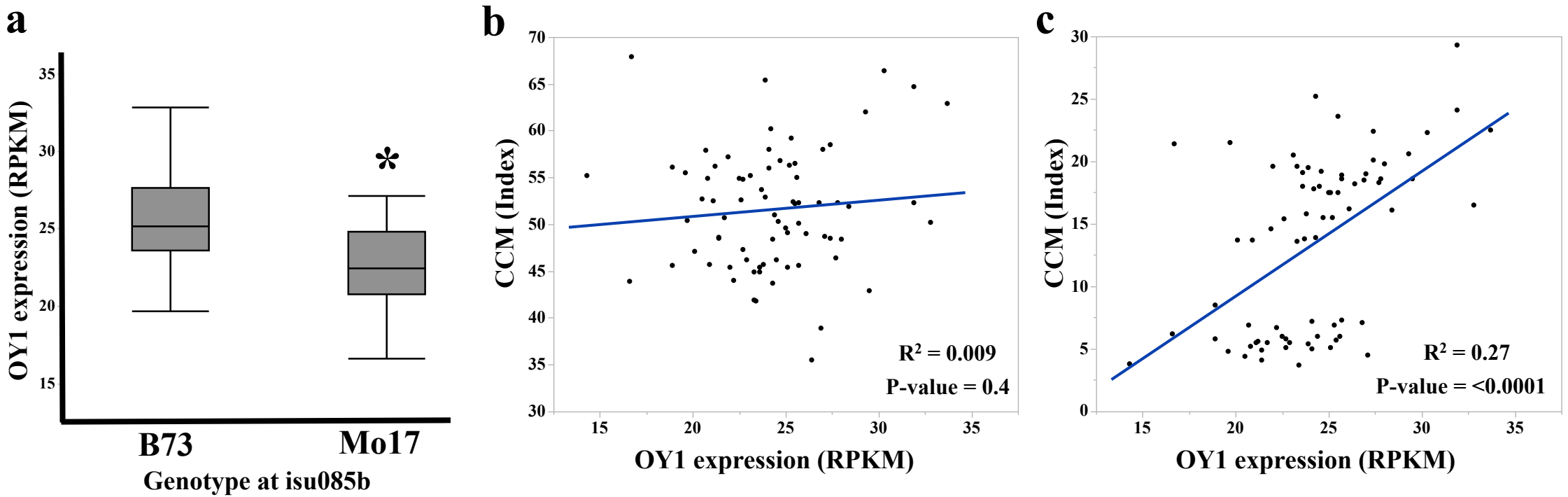

Supplemental Figures

Figure S1. The linear regression of the chlorophyll pigment measurements using non-destructive CCM-200 plus meter (expressed as CCM index) and absolute chlorophyll pigment quantification using the spectrophotometric method from the same leaf. The linear fit of CCM readings with (a) Chlorophyll *a* (Chl*a*), (b) Chlorophyll *b* (Chl*b*), (c) Total chlorophyll, (d) Chlorophyll *a*/*b* ratio (chl*a*/*b* ratio). The absolute amount of chl*a*, chl*b*, and total chlorophyll was quantified using the spectrophotometer; expressed as mg/g fresh weight (FW).

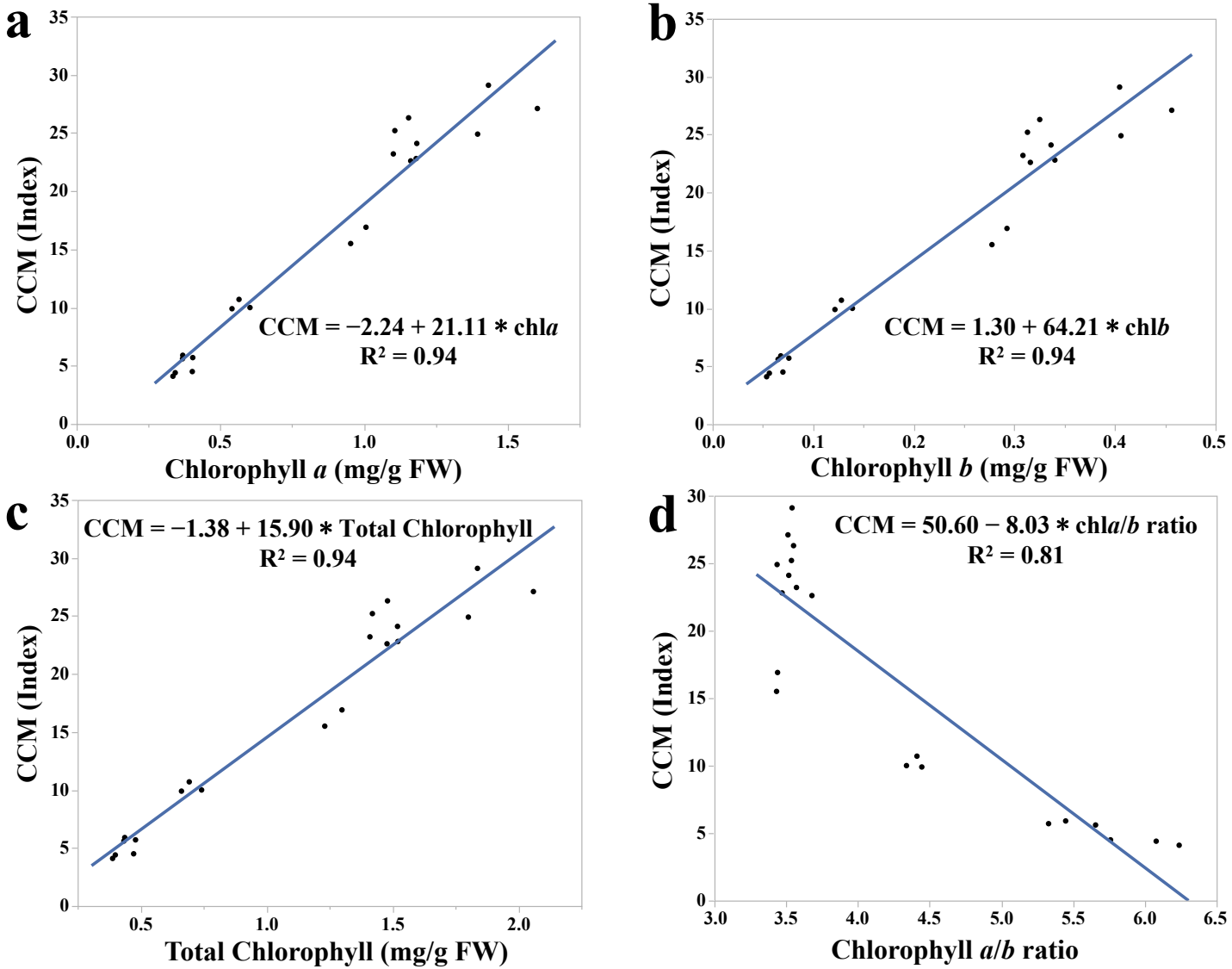

Figure S2. The CCM quantification of the (a) mutant (*Oy1-N1989/oy1*), and (b) wild-type (*oy1/oy1*) siblings in B73, Mo17 x B73, and Mo17 (BC_6 generation) genetic background at 30 days after planting. Data were derived from three randomized replications grown in the field for each cross. CCM was quantified on the top fully-expanded leaf from multiple plants (2-4) for each genotype (mutant and wild-type). Connecting letter report indicates statistical significance determined using ANOVA followed by the mean comparison between all three genotypes with Tukey's HSD (post-hoc test) at $p<0.01$.

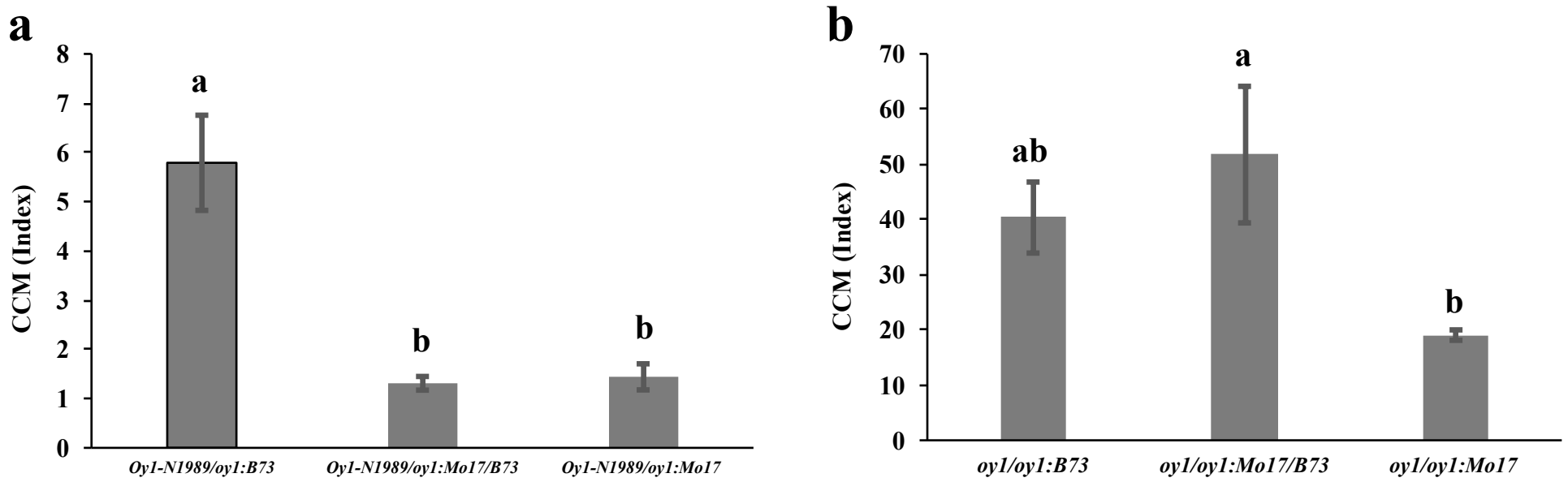

Figure S3. The pairwise scatter plot of primary trait measurements in IBM x *Oy1-N1989/oy1*:B73 F_1 populations.

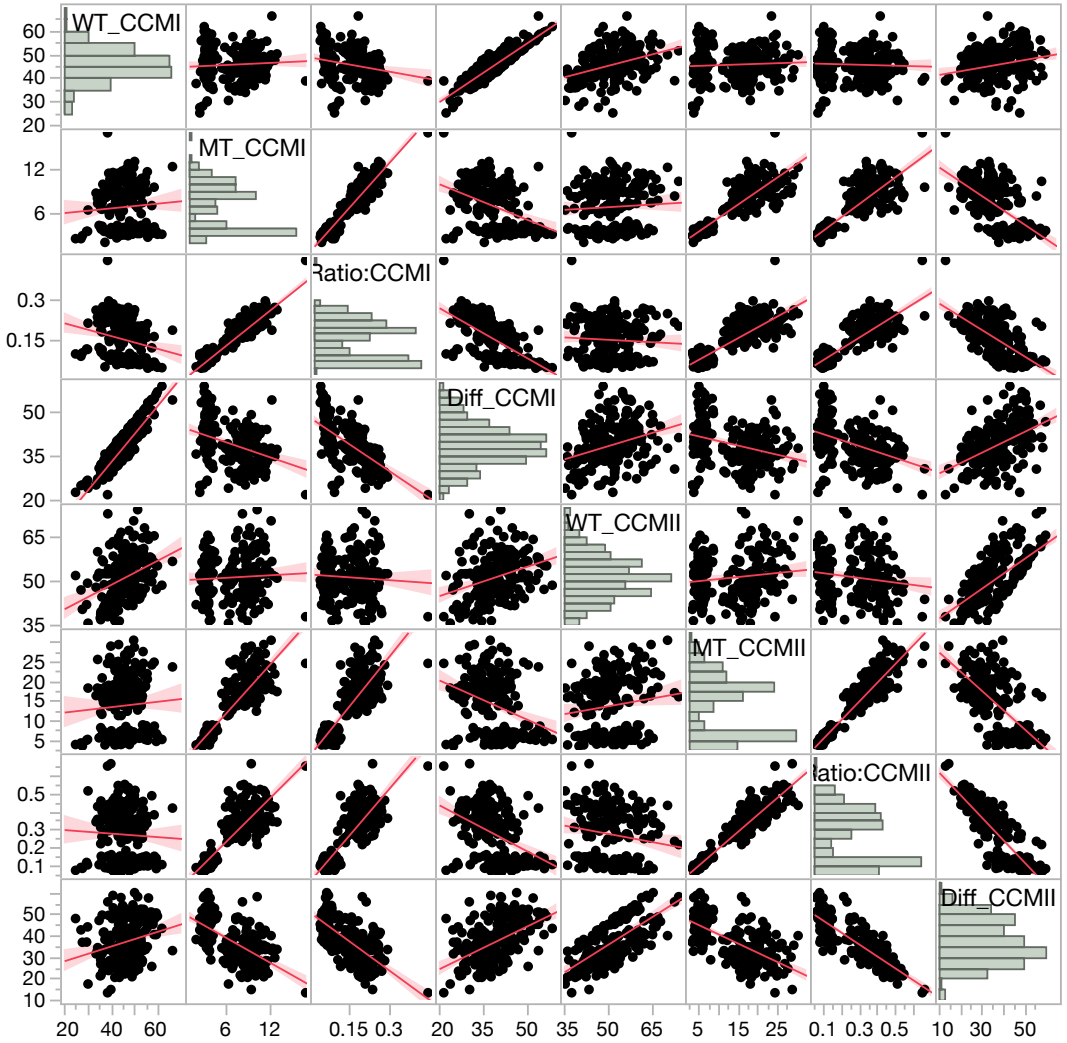

Figure S4. The pairwise scatter plot of primary trait measurements in Syn10 x *Oy1-N1989/oy1*:B73 F_1 populations.

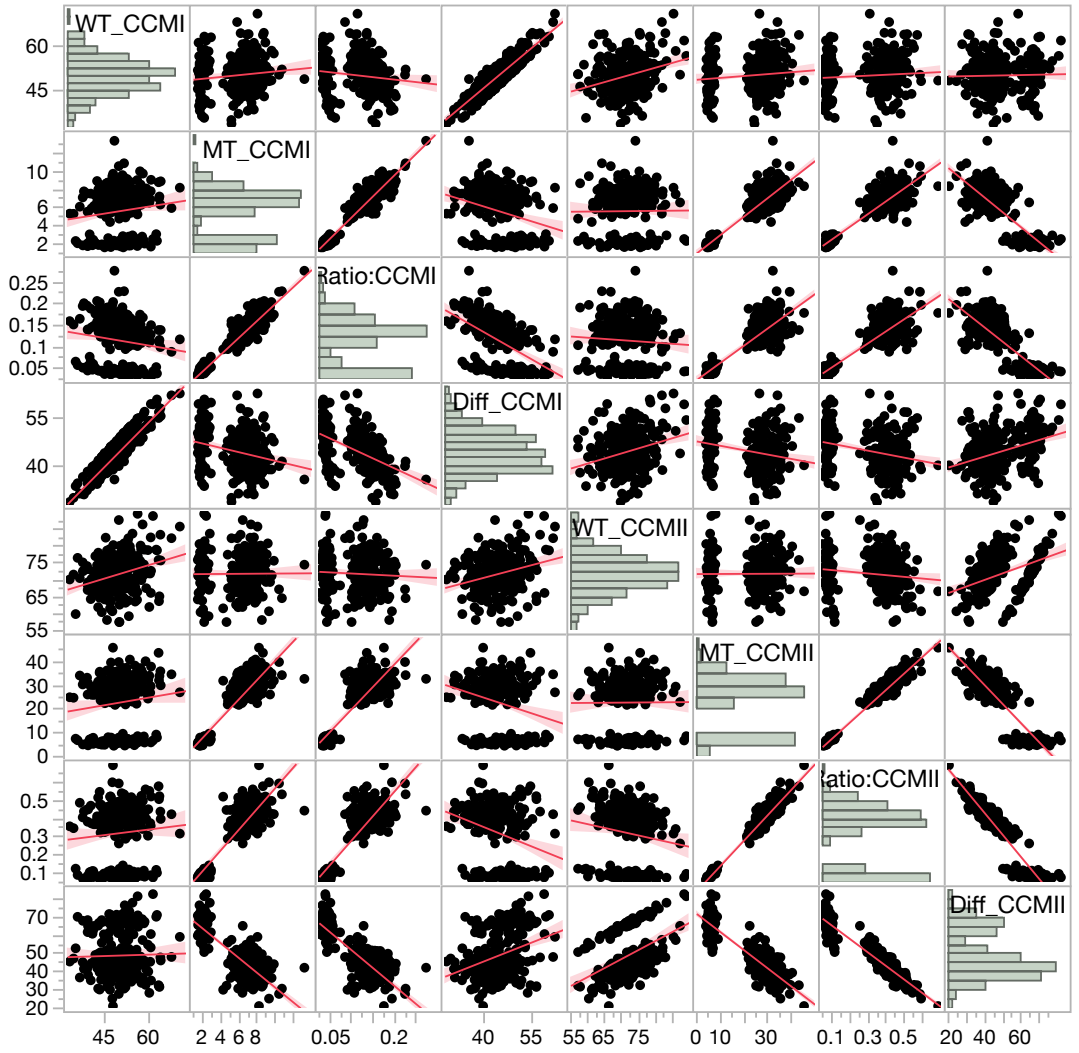

Figure S5. The CCMI and CCMII distribution in the wild-type (WT) and mutant (MT) siblings of (a) IBM x *Oy1-N1989/oy1*:B73 F_1 populations, (b) Syn10 x *Oy1-N1989/oy1*:B73 F_1 populations, and (c) MDL x *Oy1-N1989/oy1*:B73 F_1 populations.

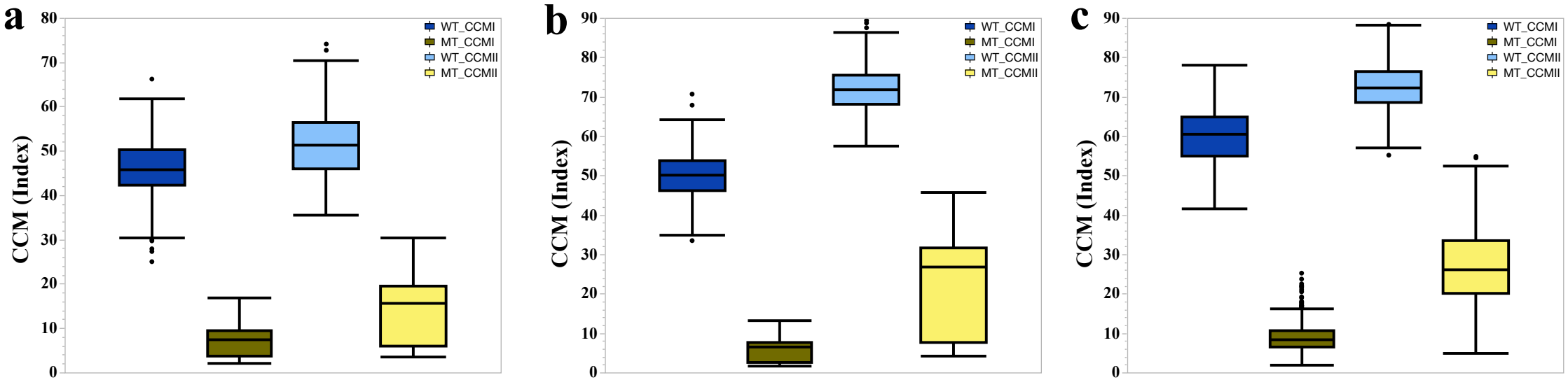

Figure S6. The cartoon showing *vey1* validation in BM-NILs x *Oy1-N1989/oy1*:B73 F_1 populations. The first column shows the female parent of each cross, Colored figure shows the genotypes (B73, Mo17, Heterozygous, and missing colored as blue, golden, grey and white respectively) at a given SNP position (X-axis of the left figure; physical position from B73 RefGen v2); and position of *oy1* locus (between the two SNPs that are highlighted by a black arrow). The average (five replications) of CCM trait values in mutant siblings and their ratios (mutant/wild-type) are shown on the extreme right (last four columns) of the figure. The parental (B73 and Mo17) crosses with *Oy1-N1989/oy1*:B73 that were planted as checks in this experiment are shown in the first two rows for comparison.

Figure S7. The pairwise scatter plot of primary trait measurements in MDL x *Oy1-N1989/oy1*:B73 F_1 populations.

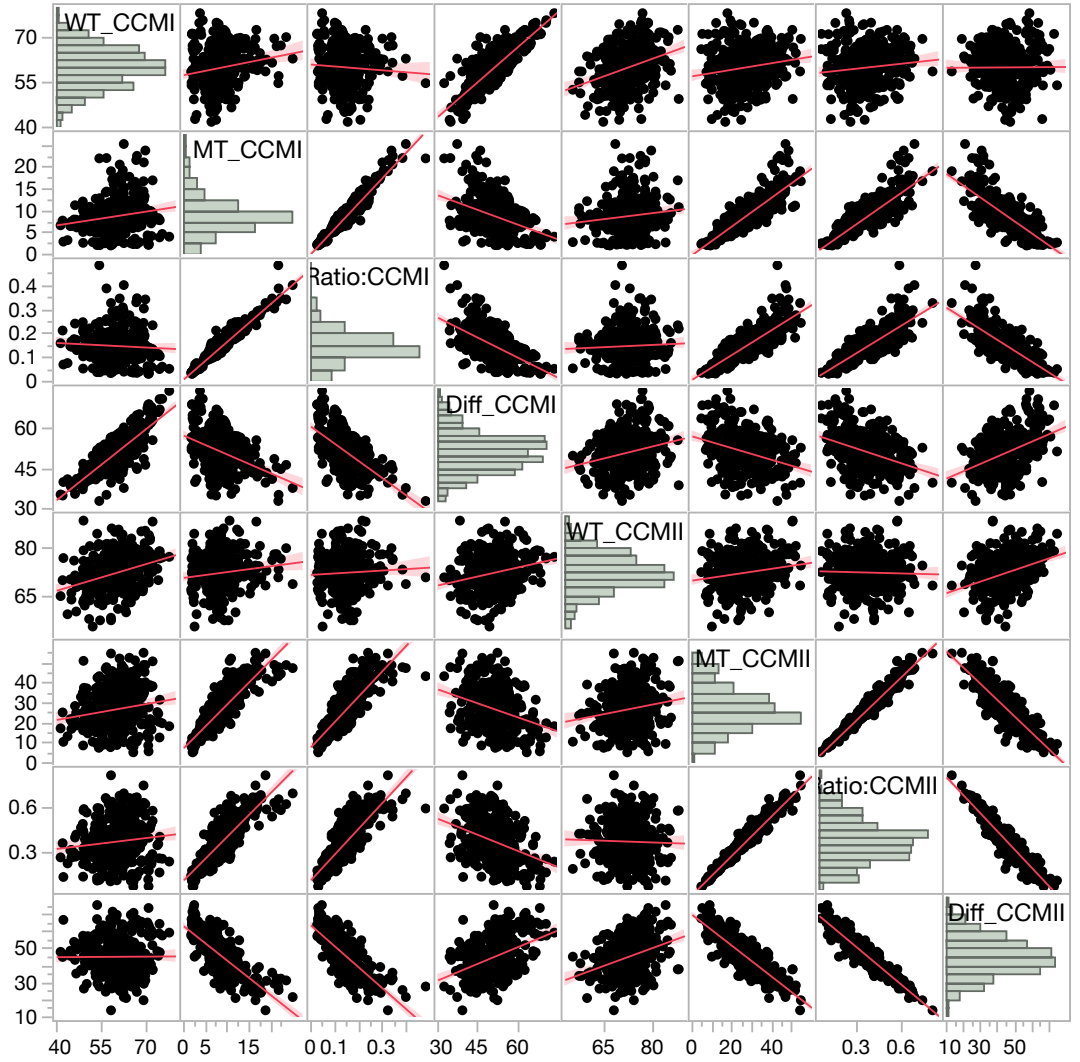

Figure S8. The chlorophyll approximation (using CCM) from the middle of the third leaf in the greenhouse grown F_1 maize seedlings from a cross of B73, Mo17, and PH207 inbred lines (ear-parents) with *Oy1-N1989/oy1*:B73 plants (pollen-parent) at the V3 developmental stage. The CCM values are presented as mean with standard deviation (error bars). The connecting letter report indicates the statistical significance calculated using ANOVA with post-hoc analysis using Tukey's HSD with $p<0.05$ among all genotypes. The sample size (n) for each genotype group varied from five to eight plants. Check supplemental table for details.

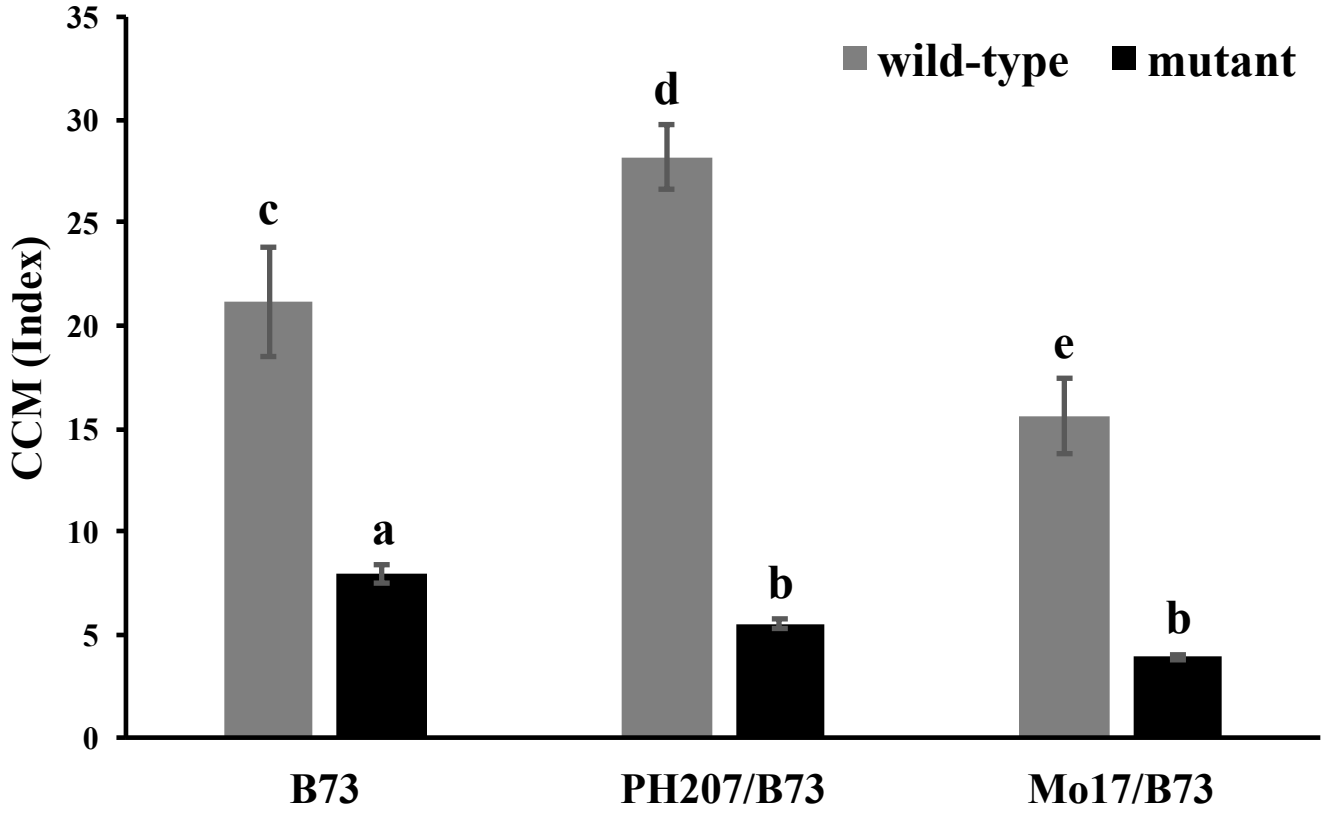

Figure S9. The proposed model for cis-acting regulatory variation as the basis of *vey1*.